

https://dspace.org/

Identification of novel HIV-1 envelope mutations that confer resistance to VRC01

Cohen, Paula

2024
https://hdl.handle.net/10539/37899

Downloaded from a DSpace repository. https://dspace.org/







IDENTIFICATION OF NOVEL HIV-1 ENVELOPE MUTATIONS THAT CONFER RESISTANCE TO VRC01

Paula Cohen

June 2023

Johannesburg

A Dissertation submitted to the Faculty of Health Sciences, University of the Witwatersrand, Johannesburg, in fulfillment of the requirements for the degree of Master of Science in Medicine.

Declaration



PLAGIARISM DECLARATION TO BE SIGNED BY ALL HIGHER DEGREE STUDENTS

SENATE PLAGIARISM POLICY: APPENDIX ONE

I PAULA COHEN (Student number: 1458297) am a student

registered for the degree of MSc (Med) Virology in the academic year 2023.

I hereby declare the following:

- I am aware that plagiarism (the use of someone else's work without their permission and/or without acknowledging the original source) is wrong.
- I confirm that the work submitted for assessment for the above degree is my own unaided work except where I have explicitly indicated otherwise.
- I have followed the required conventions in referencing the thoughts and ideas of others.
- I understand that the University of the Witwatersrand may take disciplinary action against me if there is a belief that this is not my own unaided work or that I have failed to acknowledge the source of the ideas or words in my writing.
- I have included as an appendix a report from "Turnitin" (or other approved plagiarism detection) software indicating the level of plagiarism in my research document.

Signature: _____ Date: 13 June 2023

Presentations

'Defining VRC01 Resistance Mutations in Phenotypically Discordant Envelopes from Multi-lineage HIV Transmissions'. Collaboration for AIDS Vaccine Discovery (CAVD) Africa Regional Meeting in Cape Town, February 2023. Oral and poster presentations.

Acknowledgements

My gratitude goes out to the following people:-

- Prof Penny Moore for whom I have immense respect and admiration as both a scientist and supervisor, and for showing me that I could achieve more than what I believed my limits to be. I am also grateful for the invaluable opportunities Penny afforded me.
- Dr Bronwen Lambson for encouraging me to problem solve and think independently while still guiding and supporting me where necessary.
- My colleagues at the Antibody Immunity Research Unit, whom I can now call friends, for contributing to a happy work environment and for lending a helping hand without hesitation when needed.
- Dr Craig Magaret at Fred Hutchinson Cancer Research Center for his instrumental assistance from afar and for running the many sequences through his machine learning tool.
- Last but not least my family and friends for their encouragement and support throughout my Master's journey.

Funding and support for this project was provided by the National Research Foundation, for which I'm extremely grateful.

Table of Contents

Declaration 2
Presentations 3
Acknowledgements 3
Table of Contents 4
Abstract 6
List of figures 7
List of tables 8
List of Amino Acids 8
List of Abbreviations 9
1. Introduction 10
    1.1. The HIV-1 epidemic 10
    1.2. HIV-1 Structure and Function 11
        1.2.1. The HIV-1 Envelope Protein and Variation 13
    1.3. Antibody Structure and Function 15
        1.3.1. Antibody Response to HIV-1 Infection 17
        1.3.2. Development and Maturation of bNAbs 18
        1.3.3. bNAb Epitope Targets on the HIV-1 Env 19
    1.4. HIV-1 Vaccine Development 21
        1.4.1. Active Vaccination vs Passive Immunization 22
        1.4.2. The Antibody Mediated Prevention Trial 23
    1.5. Mutations associated with VRC01 resistance 26
        1.5.1. Evidence of Selection of VRC01 Resistance Mutations and Viral Fitness 28
    1.6. Transmission of multiple founder variants and discordant profiles 29
    1.7. Project Aim 30
        1.7.1. Objectives 30
2. Materials and Methods 31
    2.1. Sequence analysis, molecular visualization and structural visualization of putative VRC01 resistance mutations 31
    2.2. Introduction of mutations into HIV-1 Env 32
        2.2.1. Primer design 32
        2.2.2. Site Directed Mutagenesis 33
        2.2.3. Construction of chimeras 34
        2.2.4. Transformation of XL10 Gold Ultracompetent cells 37

2.2.5. Plasmid Purification 37
2.2.6. Sanger sequencing 39
2.3. Maintenance and culture of HEK 293T cells and TZM-bl cells 40
2.4. Production of Pseudoviruses by Transfection of 293T cells 41
2.5. TCID50 Assay 42
2.6. TZM-bl Neutralization Assay 44
3. Results 46
3.1. Multi-lineage infections with discordant profiles 46
3.1.1. Identification of potential VRC01 resistance mutations 48
3.2. Assessing the overall neutralization phenotype of mutated viruses 64
3.3. Assessing the neutralization phenotype of mutants against other CD4 binding site mAbs 68
4. Discussion 73
5. Conclusion 77
Appendix A- Sequences of viruses 84
Appendix B- List of primers 85
Appendix D- Ethics clearance certificate 88
Appendix E- Turnitin report 89

Abstract

The Antibody Mediated Prevention Trials showed that passively infused VRC01, a potent and broadly neutralizing antibody, was able to protect individuals against HIV-1 infection if they were exposed to sensitive viruses. However, breakthrough HIV-1 infections occurred when individuals in the VRC01 arms were exposed to viruses either resistant to VRC01 or to sensitive viruses when participants were in a VRC01 serum trough. We identified seven individuals with multi-lineage breakthrough HIV-1 infections, where one variant was resistant to VRC01 but another was VRC01 sensitive. By comparing the Env sequences of the resistant and sensitive clones from each participant, we identified mutations that were predicted to confer differential VRC01 neutralization phenotypes. These mutations were reverted to sensitive residues by site-directed mutagenesis, and the wildtype and mutant envelopes were screened against VRC01 and other CD4 binding site antibodies in TZM-bl neutralization assays. In four of the seven pairs of clones, a single mutation was sufficient to confer sensitivity to VRC01. In each case, the mutations responsible for the differential neutralization phenotypes occurred at different sites across the Env, such as 279 and 280 in loop D, 369 in the CD4 binding-loop and 459 between β23 and the V5 loop. In two cases, the resistant backbones were mutated (through generation of chimeras) to contain either the entire V1V2 region or the β23-V5 loop of their matched sensitive clones. This resulted in the transfer of 8 or 20 amino acid mutations to confer VRC01 neutralization sensitivity. We were unable to identify the mutations conferring VRC01 resistance in one participant, where the resistant and sensitive clones differed by both length and 100 amino acid changes. Interestingly, all VRC01 resistant clones were sensitive to other, clinically relevant, related CD4 binding-site bNAbs, such as VRC07-523 LS and N6, which are being tested in future passive immunization trials. Further studies will investigate the kinetics of VRC01 resistance mutations within the AMP multi-lineage transmissions over time.

List of figures

Figure 1. 1. Schematic showing the various Groups and Subtypes of HIV-1.

Figure 1. 2. HIV-1 mature virion.

Figure 1. 3. Representation of HIV-1 Env.

Figure 1. 4. Structure of an antibody.

Figure 1. 5. Summary describing how viral evolution causes development of HIV-1 breadth.

Figure 1. 6. An HIV-1 viral envelope glycoprotein showing the epitopes of bNAbs.

Figure 1. 7. Initial VRC01 neutralization profiles of HVTN 703 AMP breakthrough cloned Envs.

Figure 1. 8. Major epitope regions of CD4 binding site antibodies on HIV-1 Env.

Figure 2. 1. Representation of introduction of single mutations via SDM.

Figure 2. 2. Representation of production of V1V2 and both CD4 and V5 chimeras.

Figure 2. 3. Representation of introduction of V1V2 and both CD4 and V5 chimeras in desired backbone.

Figure 2. 4. Structural representation of the pSG3Δenv backbone.

Figure 2. 5. Schematic of TCID50 assay plate set-up.

Figure 2. 6. Schematic of Neutralization assay plate set-up for each virus.

Figure 3. 1. Virus clones from each individual with discordant neutralization profiles.

Figure 3. 2. Logoplots of the probabilities of amino acids observed at important positions.

Figure 3.2. 1. Results for PTID 703-0790.

Figure 3.2. 2. Results for PTID 703-1714.

Figure 3.2. 3. Results for PTID 703-2769.

Figure 3.2. 4. Results for PTID 703-0510.

Figure 3.2. 5. Results for PTID 703-1586.

Figure 3.2. 6. Results for PTID 703-2805.

Figure 3.2. 7. Results for PTID 703-0514.

Figure 3.3. 1. Overall neutralization phenotypes of mutated viruses.

Figure 3.3. 2. Overall neutralization curves of mutated viruses.

Figure 3.4. 1. Neutralization results of WT and mutant viruses against VRC01, N6, 3BNC117, VRC07-523 LS, HJ16 and 1-18.

Figure 3.4. 2. Neutralization curves of mutated viruses against other CD4 binding site mAbs.

Figure C1. Important findings.

List of tables

Table 1. 1. HVTN 703 AMP protocol showing the number of Sub-Saharan women (total 1900) who received infusions of different doses at specific time points over a 22 month period.

Table 2. 1. Cycling Parameters for Mutant Strand Synthesis Reaction.

Table 2. 2. Cycling Parameters for Chimeric Strand Synthesis Reaction- Backbone.

Table 2. 3. Cycling Parameters for Chimeric Strand Synthesis Reaction- Insert.

Table 2. 4. Cycling Parameters for Sanger Dideoxy Sequencing.

Table A1. Accession numbers for nucleotide sequences of viruses analysed

Table B1. Primers used to mutate Resistant WT plasmids.

Table B2. Primers used to mutate Sensitive WT plasmids.

Table B3. Primers used to sequence plasmids

List of Amino Acids

Residue:	One letter abbreviation:
Arginine	R
Asparagine	N
Aspartic acid	D
Glutamic acid	E
Glutamine	Q
Glycine	G
Histidine	H
Isoleucine	I
Leucine	L
Lysine	K
Phenylalanine	F
Proline	P
Serine	S
Threonine	T
Valine	V

List of Abbreviations

AIDS: Acquired Immunodeficiency Syndrome

AMP: Antibody Mediated Prevention

ART: Antiretroviral therapy

β-ME: β-mercaptoethanol

BCR: B-cell receptors

bNAb: Broadly neutralizing antibody

bp: base pairs

CDR: Complementarity-determining regions

CRF: Circulating recombinant forms

D: Diversity

DEAE: Diethylaminoethyl

ddH_2O: Double distilled water

ddNTP: Dideoxynucleotide triphosphate

dH_2O: Distilled water

DMEM: Dulbecco's modified eagle media

DNA: Deoxyribonucleic acid

dNTP: Deoxynucleotide triphosphate

Env: Envelope

EtOH: Anhydrous ethanol

Fab: Antigen binding fragment

FBS: Fetal bovine serum

Fc: Fragment crystallizable

FR: Framework regions

HIV-1: Human Immunodeficiency Virus 1

J: Joining

mAbs: Monoclonal antibodies

MPER: Membrane proximal external region

NAbs: Neutralizing antibodies

NaAc: Sodium Acetate

NHP: Non-human primates

PBS: Phosphate-buffered saline

PCR: Polymerase chain reaction

PEImax: Linear polyethylenimine hydrochloride Mw 40, 000

PNGS: Potential N-linked glycosylation sites

PrEP: Pre-exposure prophylaxis

PTID: Participant ID

RLU: Relative luminescence units

SDM: Site-directed mutagenesis

SHIV: Simian-Human Immunodeficiency Virus

SHM: Somatic hypermutation

ssRNA: Single-stranded ribonucleic acid

TF: Transmitted/founder

V: Variable

WT: Wild Type

1. Introduction

1.1. The HIV-1 epidemic

The global Human Immunodeficiency Virus-1 (HIV-1) epidemic is one of the world's major public health challenges, with approximately 38.4 million people living with HIV-1 by the end of 2021 (WHO, 2022). South Africa continues to have the largest HIV epidemic in the world, and it has been estimated that 8.2 million people are living with HIV in South Africa (Statistics South Africa, 2022). The HIV-1 positivity rate is estimated to be 19.5% for adults aged 15-49 years living in South Africa (Statistics South Africa, 2022).

HIV-1 attacks the cells that fight infection (CD4+ T cells) which in turn leaves the infected persons vulnerable and unable to fight off other infections and diseases. The progression of HIV-1, when left untreated, leads to Acquired Immunodeficiency Syndrome (AIDS) 5-10 years after infection, and these people with severely damaged immune systems often acquire opportunistic infections or other illnesses. Young women have higher prevalence and incidence rates compared to males, due to factors such as biological, behavioural and socioeconomic risks which increase their vulnerability to the acquisition of HIV (Ramjee and Daniels, 2013). Although the use of condoms is an effective form of prevention against HIV-1, antiretroviral therapy (ART) is also a prominent form of HIV-1 prevention (Granich *et al*., 2012). ART suppresses viral replication, therefore preventing the progression to AIDS, as well as limits sexual transmission (Cohen *et al*., 2011). Other uses for ART are prevention of mother-to-child transmission using ART administered to pregnant and breastfeeding mothers (Hurst, Appelgren and Kourtis, 2015), and consistent use of antiretrovirals as pre-exposure prophylaxis (PrEP) by uninfected individuals which substantially reduces the risk of becoming infected (Lundgren and Phillips, 2018). However, these preventative methods are dependent on the person's adherence and commitment (Morris and Mkhize, 2017) and therefore come with challenges. Non-adherence to long-term ART is due to factors such as stigma, side effects, travel for both work and socializing, alcohol consumption, treatment fatigue and little education on the importance of continuous ART adherence (Bukenya *et al*., 2019).

Although ART regimens have been successful, with an estimated 62% reduction of HIV-1 infections in South Africa between 2000 and 2019 and a 47% reduction relative to 2010 (Johnson *et al*., 2022), ART does not completely eliminate the virus and therefore does not eradicate the spread of HIV-1 (Rabiu, Willie and Parumasur, 2021). This is why a vaccine against HIV-1 would be an ideal solution, in order to minimize the issue of human responsibility as well as stop the transmission of HIV-1.

1.2. HIV-1 Structure and Function

There are two types of HIV, referred to as HIV-1 and HIV-2, which are more than 55% genetically different from one another. HIV-1 is the predominant virus over HIV-2 and accounts for approximately 95% of all the HIV infections worldwide (Campbell-Yesufu and Gandhi, 2011). HIV-2 is less infectious than HIV-1 and causes AIDS over a longer period of time (Campbell-Yesufu and Gandhi, 2011). HIV-1 is split into four groups. Group M is divided into nine subtypes, represented as letters A-K, which have been identified in different geographical regions (Figure 1.1). The subtypes show how virus has evolved over time and the recombination of two or more subtypes result in circulating recombinant forms (CRFs). Subtype C accounts for almost half of the HIV-1 infections and was the cause of the HIV-1 pandemic in Africa and India (Taylor and Hammer, 2008).

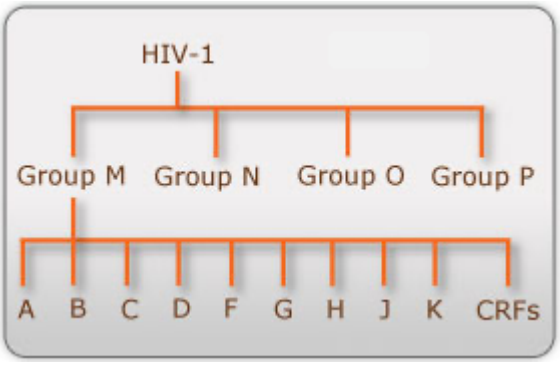

Figure 1.1. Schematic showing the various Groups and Subtypes of HIV-1. Four distinct groups of HIV-1 have been identified thus far. Group M is divided into subtypes and CRFs, where subtype C accounts for almost half of the HIV-1 infections.

HIV-1 is a single-stranded (+ sense) enveloped ribonucleic acid (ssRNA) virus consisting of 9.8 kilobases that encode nine viral genes (Cross, 2011). The genome encodes three major structural genes known as gag, pol and env, which in turn encode structural proteins such as matrix, capsid and nucleocapsid; viral enzymes such as protease, reverse transcriptase and integrase; and envelope (Env) proteins known as gp120 and gp41, respectively (van Heuvel *et al*., 2022). The genome also encodes six regulatory genes known as vif, rev, nef, tat, vpu and vpr, which control viral replication (van Heuvel *et al*., 2022) (Figure 1.2).

The infection of the host cell begins with binding of the Env protein to the host cell receptor CD4 and co-receptors CCR5 and CXCR4, whereafter a conformational change occurs and the virion releases its interior into the cytoplasm of the host cell. Upon entry, reverse transcriptase converts the ssRNA into double stranded deoxyribonucleic acid (DNA). The viral DNA then enters the nucleus and integrase is responsible for genome integration, where the HIV-1 DNA becomes part of the infected host cell. After successful integration of the provirus, the host transcription machinery is utilized to produce HIV-1 proteins. The HIV-1 viral RNA and proteins assemble into immature HIV-1 particles, which bud from the cell membrane. The immature HIV-1 particles are released from the host cell. Lastly, maturation occurs when protease cleaves precursor proteins into their intended subunits. The mature HIV-1 virion is ready to infect the next host cell, which commences a new replication cycle.

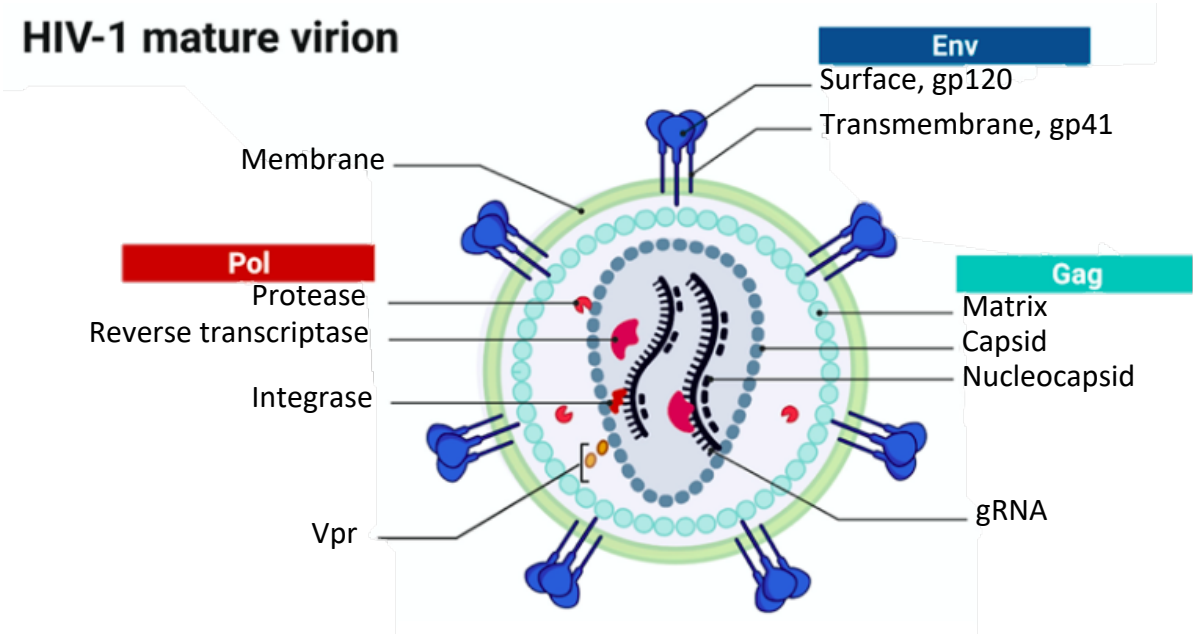

Figure 1.2. HIV-1 mature virion. Structural representation of a mature HIV-1 virion. The Env, made up of the gp120 and gp41 subunits, is embedded in the membrane. The protease and capsid are found in the matrix. The capsid contains the integrase, reverse transcriptase, viral genome and nucleocapsid. (Adapted from van Heuvel *et al*., 2022).

1.2.1. The HIV-1 Envelope Protein and Variation

The Env glycoprotein is the structural protein found on the surface of the HIV-1 virion surface and exists as a trimer. During the HIV-1 replication cycle, the precursor protein gp160 is expressed which is then cleaved by a cellular protease called furin into two proteins gp120 and gp41 (Blumenthal, Durell and Viard, 2012). The Env is composed of three gp120 Env glycoproteins attached to three gp41 transmembrane molecules (Pancera *et al*., 2010). A high degree of variability has been seen in the gp120 (Checkley, Luttge and Freed, 2012). The gp120 consists of five variable domains (V1-V5) and five relatively constant domains (C1-C5), interspersed along the gp160 (Checkley, Luttge and Freed, 2012). The gp41 subunit is organized into three domains: the extracellular domain, the transmembrane domain and the C-terminal cytoplasmic tail (Checkley, Luttge and Freed, 2012). Within the gp41, both the fusion peptide and the conserved membrane proximal external region (MPER) are found in the extracellular domain (Checkley, Luttge and Freed, 2012) (Figure 1.3).

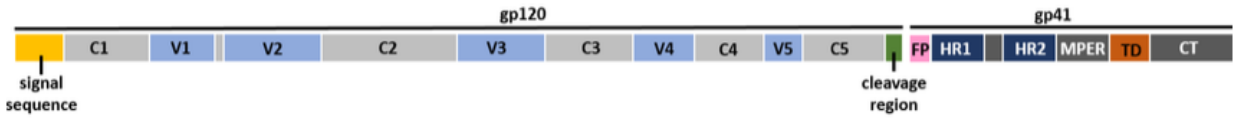

Figure 1.3. Representation of HIV-1 Env. Linear representation shows gp120 and gp41, separated by the cleavage region. The gp120 contains five constant (C1-C5) and five variable (V1-V5) regions. The gp41 subunit is organized into three domains: the extracellular domain, the transmembrane domain and the C-terminal cytoplasmic tail. Within the gp41, both the fusion peptide and the conserved MPER are found in the extracellular domain. Two heptad regions (HR1 and HR2) are also found in the gp41.

There is a large amount of genetic variation within HIV-1 subtypes, which can be as much as 15%-20% (Araújo and Almeida, 2013). The variation is due to the rapid reproductive rate of HIV-1 and the error prone reverse transcriptase (Araújo and Almeida, 2013). This results in mutations/polymorphisms that can alter the viral protein's structure (Araújo and Almeida, 2013). The immune response and immune pressure also leads to HIV-1 variation as escape mutations develop during infection in order to become resistant to the immune response (Batorsky, Sergeev and Rouzine, 2014). Although the HIV-1 Env is a complex protein, the amino acid substitutions, insertions/deletions and glycan shifting occurs mostly in the variable regions, it has been shown that there are conserved regions across the Env that can be the target for antibody neutralization (Wibmer, Moore and Morris, 2015).

1.3. Antibody Structure and Function

Antibodies play a critical role in the adaptive immune response by serving as barriers to infection (Murin, Wilson and Ward, 2019). Antibodies recognise invading pathogens and interfere with their life cycle, by functions such as binding to the foreign antigen and neutralizing it as well as eliciting fragment crystallisable (Fc) effector functions against the infected cells (Forthal, 2014). Antibodies consist of two identical heavy chains and two identical light chains. Both heavy and light chains consist of constant and variable regions. The antigen binding fragment (Fab) region of both the heavy and light chains contain highly variable portions, and these determine the specificity of the antibody to the corresponding antigen, and the fragment crystallizable (Fc) region is the constant region that mediates function by interacting with cell surface receptors (Janeway *et al*., 2020). Complementarity-determining regions (CDRs) contribute to the variable portion of the antibodies and are responsible for diverse antigen specificity which help the antibodies bind to their corresponding antigen (Sela-Culang, Kunik and Ofran, 2013). The CDRs are separated by conserved regions called framework regions (FRs). The FRs, which make up 85% of the variable region, support the CDRs and are important in determining the structure of the variable domain (Gąciarz and Ruddock, 2017) (Figure 1.4).

During B cell maturation, the cells undergo variable (V), diversity (D) and joining (J) recombination, which is a mechanism by which gene segments are rearranged to produce diverse antigen receptors in mammals (Roth, 2015). These receptors are secreted as soluble proteins bound to the membrane of B-cells, known as B-cell receptors (BCR). Naïve BCRs are exceptionally diverse due to V(D)J recombination. This leads to the likelihood of a naïve antibody being present which is able to bind to a new antigen, although possibly very weakly, initially (Van Beek, Nussenzweig and Chakraborty, 2022). If the BCR can bind strongly enough to the antigen, intracellular signaling occurs and activates gene transcription (Van Beek, Nussenzweig and Chakraborty, 2022). The antibodies that have bound to an antigen, undergo affinity maturation mediated by somatic hypermutation (SHM) (Van Beek, Nussenzweig and Chakraborty, 2022). SHM is a change that introduces somatic mutations in the variable part of the Fab region of an

antibody, which leads to a change in the affinity of the antibody to the antigen and thereafter these BCRs are selected for within germinal centers.

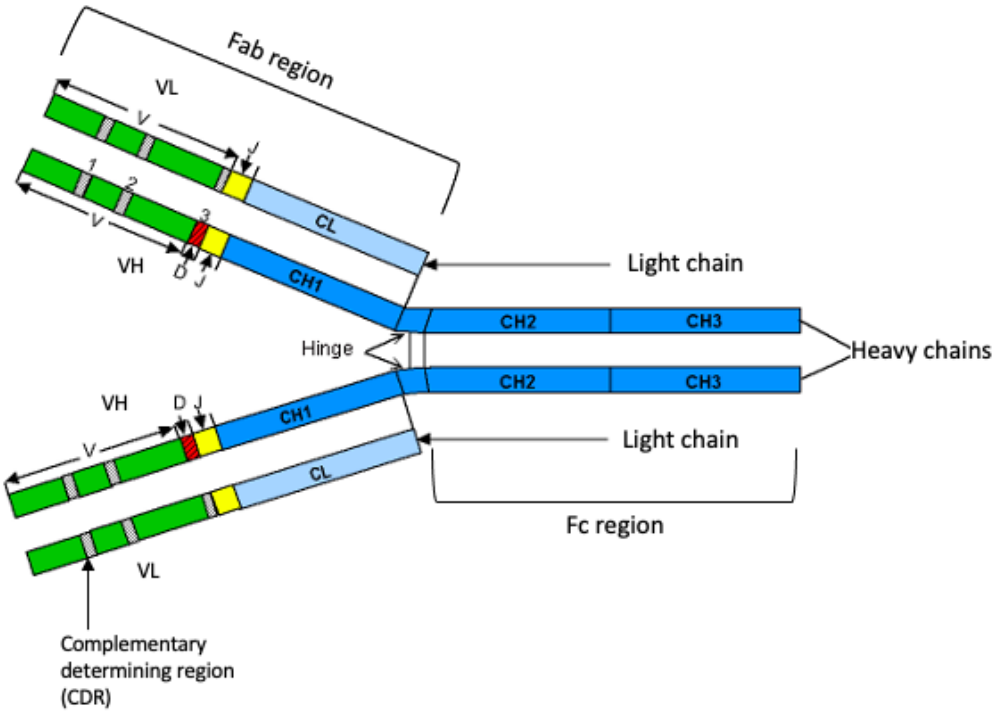

Figure 1.4. Structure of an antibody. Schematic representation showing the antibody consists of two heavy chains and two light chains. The constant regions for the heavy (CH1, CH2 and CH3) and light chains (CL) are shown in dark blue and light blue respectively, while the variable regions of the heavy (VH) and light (VL) chains, shown in green. The CDR found in the variable regions are seen by grey bars. The Fab region, consisting of the light chain, heavy chain variable region and one heavy chain constant region (CH1) and Fc region consisting of two heavy chain variable regions (CH2 & CH3) are indicated. (Adapted from Lefranc and Lefranc, 2020).

1.3.1. Antibody Response to HIV-1 Infection

When a person becomes infected with HIV-1, a robust immune response is elicited by means of cell-mediated and humoral pathways. The humoral antibody response is directed towards the Env protein, which, as mentioned above, is the only antigen target of neutralizing antibodies on the HIV-1 surface. The antibodies bind to the Env protein and therefore obstruct viral entry into host cells.

Within a year of infection, all HIV-1 infected individuals develop a potent immune response against the autologous/infecting virus. These are strain-specific neutralizing antibodies (NAbs) that target the variable regions of the Env (Moore *et al*., 2009). These variable regions have many differences between virus strains and therefore the strain specific NAbs are only able to recognize the virus that the individual was infected with (Moore, Williamson and Morris, 2015). There is rapid evolution of HIV-1 Env over the course of infection which leads to the continual escape of antibody-mediated neutralization by the virus (Richman *et al*., 2003). The NAbs exert a level of selective pressure on the virus and in turn, the virus mutates and hides its epitopes in order to escape and therefore leaving the strain-specific NAbs unable to recognise and neutralize the viral Env (Richman *et al*., 2003).

Certain individuals develop antibodies with some level of cross-reactivity after several years of being infected with HIV-1. These antibodies are able to recognize the conserved epitopes on many circulating HIV-1 strains (Burton and Hangartner, 2016). Approximately 20% of infected individuals develop broadly neutralizing antibodies (bNAbs), which are able to neutralize 80-90% of viral particles from many strains of HIV-1, despite the Env diversity (Landais and Moore, 2018).

1.3.2. Development and Maturation of bNAbs

During infection, bNAbs undergo incremental development before they become broadly neutralizing, suggesting that both the bNAbs and HIV-1 epitope variants co-evolve in order to achieve their breadth (Landais and Moore, 2018). Multiple factors contribute to the complex interaction that occurs to develop high levels of neutralization breadth in order for antibodies to become bNAbs (Moore, Williamson and Morris, 2015) (Figure 1.5). These factors include: early viral diversity; duration of infection; formation of bNAb epitopes due to viral escape from strain-specific antibodies; viral escape mutations causing exposure of bNAb epitopes; addition and deletion of shielding glycan molecules; and finally, exposure to varying immunotypes lead to affinity maturation of NAb lineages (Moore, Williamson and Morris, 2015). bNAbs often have unusual immunological features which include high levels of SHM and unusually long or short CDRs (Burton and Hangartner, 2016).

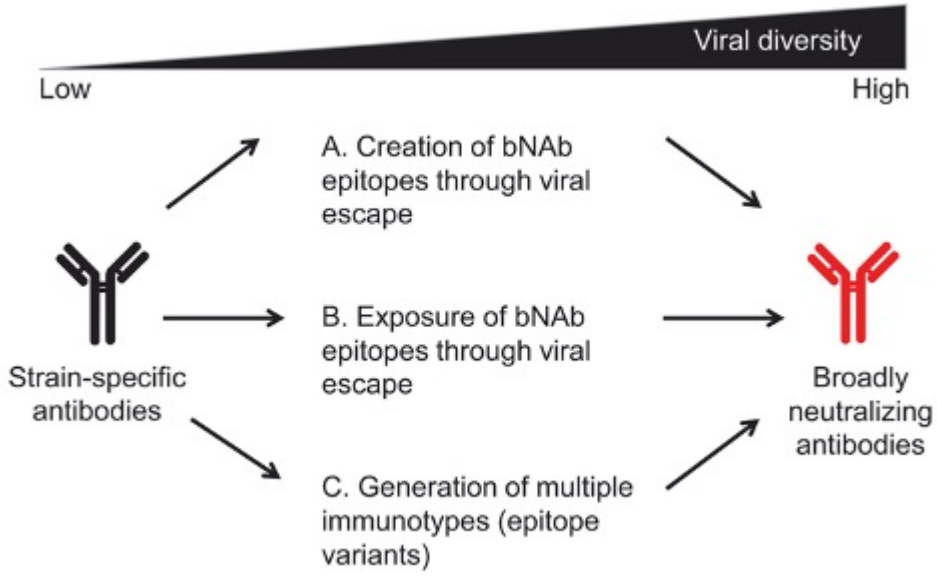

Figure 1.5. Summary describing how viral evolution causes development of HIV-1 breadth. Development of HIV-1 breadth occurs as a result of (A) creating bNAb epitopes due to viral escape from strain-specific antibodies, (B) exposure of bNAb epitope resulting from viral escape, and (C) exposure to multiple immunotypes results in affinity maturation of neutralizing antibodies. (Adapted from Moore, Williamson and Morris, 2015).

1.3.3. bNAb Epitope Targets on the HIV-1 Env

Due to the advancement of new technologies, there has been a surge in the number of bNAbs isolated from individuals (Moore, Williamson and Morris, 2015). Many of these isolated bNAbs have shown remarkable breadth and potency, which in turn has led to the identification of six conserved regions on the viral Env: the V2-apex, N332 supersite in the V3 region, CD4 binding site, gp120-gp41 interface, fusion peptide and the MPER (Magaret *et al*., 2019) (Figure 1.6A and B). The V2-apex is densely packed with glycans which are utilized for viral protection against the antibody response (Tian *et al*., 2016). However, some of the most potent bNAbs are able to penetrate this site, namely CAP256, PG9 and PG16 (Tian *et al*., 2016). Due to the MPER's high level of conservation, very broad bNAbs, known as 10E8 and 4E10, have developed towards the MPER epitope, although they do lack potency (Huang *et al*., 2012). The N332 supersite or the V3-glycan site is targeted by bNAbs, PGT121 and PGT128, whose epitopes are positioned on the glycan N332 (Deshpande *et al*., 2016). To date, more than two dozen CD4 binding site antibodies have been isolated (Zhou *et al*., 2019). Clinically relevant CD4 binding site targeting bNAbs include VRC01-class N6, 3BNC117, VRC07 and non-VRC01-class HJ16 and 1-18 (Figure 1.6A).

VRC01, the bNAb which is the focus of this study, is a bNAb that was isolated from a subtype B infected individual and neutralizes a panel of diverse pseudotyped viruses (Zhou *et al*., 2019). Although the CD4 binding site is present on all HIV-1 viruses, VRC01 is able to target the CD4 binding site in ~70% of HIV-1 isolates and is therefore able to neutralize them (Morris and Mkhize, 2017). CD4 binding site bNAbs that have recently been isolated show similar or enhanced breadth and potency when compared to VRC01 (Zhou *et al.*, 2019). The CD4 binding site is large and complex and spans several portions of the Env. Major components of the CD4 binding site include the CD4 binding loop, loop D and V5 (Zhou *et al*., 2019). Although the CD4 binding site it protected by glycans, VRC01-class bNAbs that target this site do not usually interact with the glycans but rather mimic binding to the CD4 by interacting with conserved residues on the gp120 CD4 binding loop (Huang *et al*., 2018). CD4 binding site directed, VRC01-class bNAbs develop over a long period of time due to high levels of SHM but this leads to a better combination of breadth and potency (Moore, Williamson and Morris, 2015).

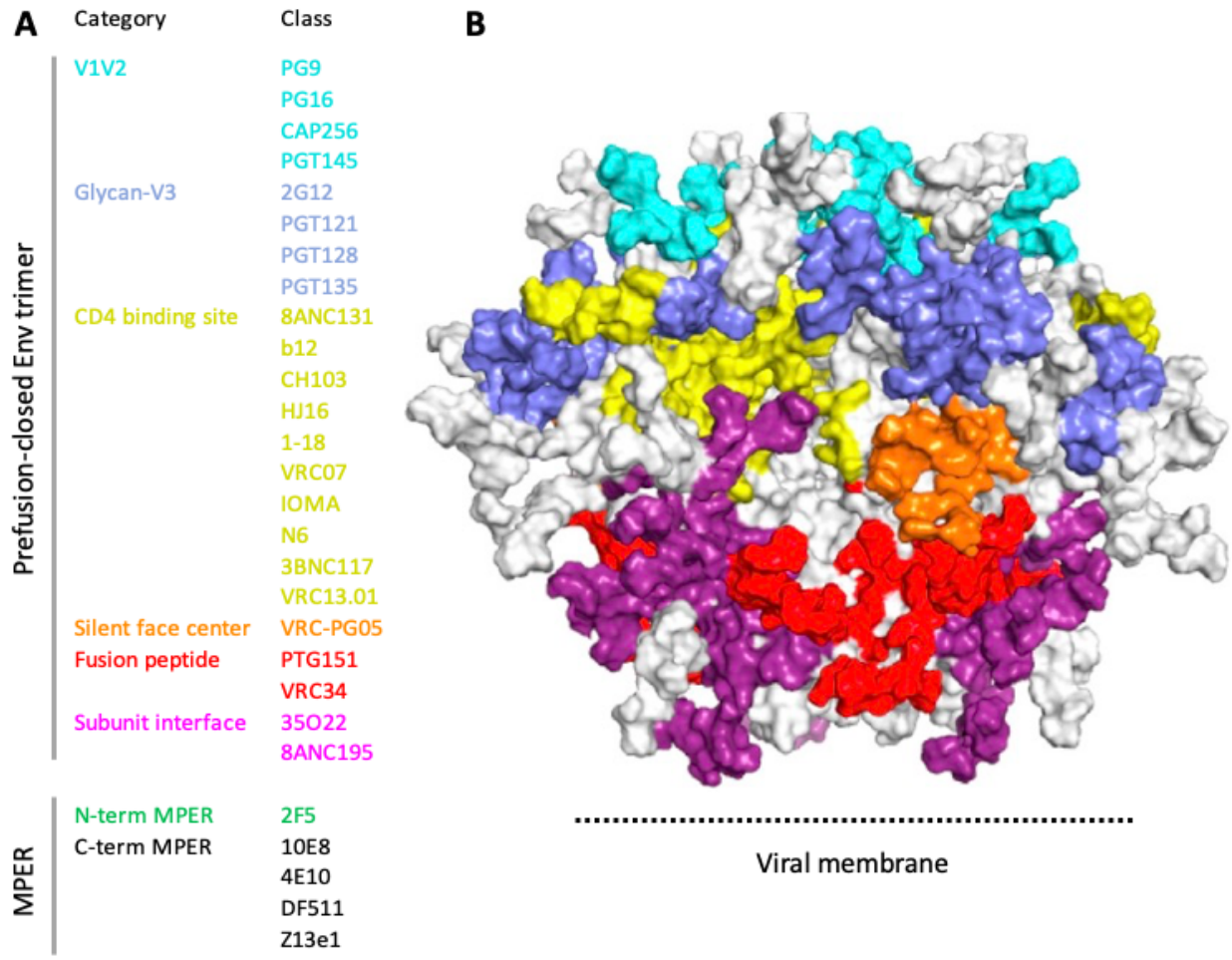

Figure 1.6. An HIV-1 viral envelope glycoprotein showing the epitopes of bNAbs. (A) The category defines the region of the Env glycoprotein that is recognised by the bNAb, and the class shows specific bNAbs coloured by epitope. (B) A visualization of the specific epitopes, corresponding to the colours seen in A, on the molecular surface of the virus. (Adapted from Kwong and Mascola, 2018).

1.4. HIV-1 Vaccine Development

Researchers have dedicated a substantial amount of time and money to develop a vaccine that will induce protective immunity against the virus. There have been a number of attempts at vaccines over the years since HIV was discovered to be the cause of AIDS in 1984. Unfortunately, these vaccines have thus far proved to be ineffective against the transmission of HIV-1. An example is a trial called AIDSVAX, which was terminated in America due to it having no effect on transmission (Vaccari *et al.*, 2010). The vaccine was then tested on a group of at-risk Thai individuals but, in 2000, this trial was terminated due to it not being able to prevent or decrease the risk of infection of HIV in the participants in the study (Harris, 2003). To date, the most successful vaccine candidate has been from the RV144 vaccine trial that was carried out in Thailand. The RV144 vaccine trial is the only trial that has shown any efficacy, having a 31% preventative effect in low-risk participants (Rerks-Ngarm *et al*., 2017). This trial used a combination of two vaccines which was based on the specific strains of HIV that were circulating in Thailand at the time (Rerks-Ngarm *et al*., 2017). A wide response against HIV-1 was elicited by this vaccine, including antibodies directed to Env and antibody-directed cell-mediated cytotoxicity (Kim, Excler and Michael, 2015). However, there was no neutralizing antibody response elicited by the vaccine. The HVTN 702 clinical trial was based on RV144 and adapted to subtype C viruses prevalent in Southern Africa but was terminated in early 2020 due to lack of efficacy (Zolla-Pazner et al., 2021). Most recently, the HVTN 706 or Mosaico phase 3 clinical trial, which was carried out in the Americas and Europe, was discontinued in early 2023 (Anklesaria & Russell, 2023). The vaccine regimen included subtype C and mosaic gp140 Env proteins expressed by an adenovirus vector, which were intended to trigger a broader immune response, but did not demonstrate protective efficacy against the acquisition of HIV infection (Anklesaria & Russell, 2023). These attempts and failures at a HIV-1 vaccine have resulted in a concerted effort to understand the immune correlates of protection. However, the low efficacy of this vaccine means the field is exploring other avenues such as eliciting bNAbs as a preventative vaccine candidate based on the advancement of research on bNAb development during HIV-1 infection. There are currently multiple vaccines in small-scale clinical trials with the main aim to elicit bNAb responses.

1.4.1. Active Vaccination vs Passive Immunization

An active vaccination to induce bNAbs would be an ideal preventative vaccine that would be given to individuals who have not been infected with HIV-1. Ideally, the vaccine would stimulate the immune system to produce bNAbs that would recognize and neutralize any strain of HIV-1 that the individual may be infected by. Unfortunately, all attempts to elicit bNAbs in humans have failed thus far (Ahmed, Tian and Gao, 2017).

Although the vaccine development process has not shown successful results in preventing HIV-1 transmission, isolated bNAbs have reinvigorated the vaccine field by suggesting the use of cloned monoclonal antibodies (mAbs) for passive immunization in order to prevent the transmission of HIV. The above-mentioned anti-HIV-1 bNAbs isolated from elite neutralizers were used for passive immunization in animal models, such as non- human primates (NHP), in order to determine whether a single or combination of mAbs are able to target simian-human immunodeficiency virus (SHIV) Env epitopes and block infection (Walsh and Seaman, 2021). These experiments were successful and varying degrees of protection were seen in the NHP (Julg and Barouch, 2019). An example shows that potent anti-HIV antibodies PGT121 and VRC01 could protect against SHIV at relatively low concentrations of antibody which suggested that modest levels of antibody could lead to protection in humans. (Saunders *et al*., 2015).

1.4.2. The Antibody Mediated Prevention Trial

This concept of using bNAbs for prevention was recently tested in humans for the first time in the HVTN Antibody Mediated Prevention (AMP) trials, HVTN703/HPTN081 and HVTN704/HPTN085 (Walsh and Seaman, 2021). This was done to determine whether passively infused VRC01 was able to prevent HIV- 1 infection in adults at high risk of being infected. A total of 1900 high-risk uninfected women in Sub-Saharan Africa, were enrolled in the HVTN 703 trial. These women were split up into three groups where two received different doses of the bNAb infusions and the third a placebo (Table 1.1). This was done in order to determine how efficient this preventative method is by comparing how many individuals in the two VRC01 infusion groups were infected compared to in the placebo group, as well as to determine the titre at which the antibody will protect them from infection (Morris and Mkhize, 2017). Breakthrough HIV-1 infections in the women in the active arms would likely be mediated by subtype C viruses resistant to the antibody due to naturally occurring mutations in the HIV- 1 Env glycoprotein, or as a result of a selective pressure resulting in the evolution of resistance after transmission. The infection of breakthrough viruses may have occurred when VRC01 serum levels decreased below the threshold known to protect against infection (Reeves *et al*., 2020). These troughs in the levels of VRC01 were seen just before each transfusion.

Table 1.1. HVTN 703 AMP protocol showing the number of Sub-Saharan women (total 1900) who received infusions of different doses at specific time points over a 22 month period.

Number of women	Regimen	Number of infusions	Time
633	VRC01 10 mg/kg	10	Every 8 weeks
633	VRC01 30 mg/kg	10	Every 8 weeks
634	Control/Placebo	10	Every 8 weeks

The results of the AMP trial showed that VRC01 at either dose was not associated with significantly lower HIV-1 transmission (Corey *et al*., 2021). However, breakthrough isolates from VRC01 recipients were more resistant to VRC01 than those acquired from placebo recipients (Corey *et al*., 2021). Furthermore, when the analysis focused on highly sensitive viruses, the women in sub-Saharan Africa that received VRC01 had 75% protection over the trial period. The fact that only 30% of the viruses circulating in the trial area were highly sensitive was the reason that no overall protection was seen (Corey *et al*., 2021).

The next challenge that will need to be overcome in vaccine development with passively infused bNAbs will be identifying the required protective dose as well as the combination of bNAbs, targeting different epitopes.

The Antibody Immunity Research Unit (AIRU) at National Institute for Communicable Diseases (NICD), the laboratory in which I conducted my research, is an endpoint laboratory for the AMP HVTN 703 trial. The lab therefore has access to Env sequences from the breakthrough infections that were isolated from the women in the trial. To examine the genetic barrier to resistance, the HVTN collaborators at University of Cape Town (UCT) used a novel PacBio deep sequencing approach to generate hundreds of viral Env sequences per individual, at two timepoints. A subset of these sequences were cloned and the AIRU evaluated their neutralization sensitivity to a panel of bnAbs using a pseudovirus assay (Figure 1.7). The neutralization profiles are based on the viruses' IC80 values, the 80% maximal inhibitory concentration. The higher the titre of VRC01 required to neutralize 80% of the virus, the more resistant the virus is to the bNAb.

Clone Name	IC80	Clone Name	IC80	Clone Name	IC80	Clone Name	IC80
H703_0015_110s	>100	V703_1586_210_RE_pblib002_s	33.85	V703_0279_110_RE_pblib002_s	4.62	H703_2631_150_RE_e2F8s	1.83
H703_0132_200s_10H3	>100	H703_1689_110_RE_e4E6s	31.36	H703_0322_130s_M1I	4.62	H703_0309_100s	1.78
H703_0157_090s	>100	H703_1104_100_RE_e10G5s	30.74	V703_1240_201_RE_pblib003_s	4.52	H703_0636_200Es	1.63
H703_0217_050e_2A3	>100	H703_0944_180s	29.83	H703_0109_210s	4.46	V703_1383_240_RE_pblib002_s	1.60
H703_0455_160_RE_cs	>100	V703_1240_201_RE_sga3D1_s	25.60	V703_0629_150_RE_pblib002_s	4.39	V703_0309_100_RE_pblib002_s	1.54
H703_0482_250Es	>100	H703_2934_110_RE_cs	23.96	H703_2539_070_RE_e6F6s	4.25	H703_1758_260_RE_cs	1.43
H703_0514_150Es_F4_V03_024	>100	V703_1034_190_RE_pblib002_s	22.80	V703_1848_190_RE_pblib002_s	4.22	H703_1675_080s	1.37
H703_0514_150s_6C1	>100	V703_1104_100_RE_pblib001_s	22.07	H703_1848_190_RE_e6D1s	4.15	H703_1675_080s_G613S	1.34
H703_0865_070s	>100	H703_0406_240_RE_e12B2s	18.10	H703_1407_090s_4G4	3.99	V703_0712_250_RE_pblib002_s	1.32
H703_0902_140_RE_p01s	>100	V703_0203_081_RE_pblib002_s	17.25	H703_0279_110s	3.94	H703_2805_080Es	1.29
H703_1446_040s	>100	H703_1104_100_RE_e10A5s	16.45	V703_0597_190_RE_pblib002_s	3.84	H703_1383_240_RE_e5D3s	1.20
H703_1515_120Es	>100	H703_1034_190_RE_e5D5s	16.06	V703_0629_150_RE_pblib003_s	3.79	H703_0967_040s	1.11
H703_1670_220_RE_cs	>100	V703_0510_260_RE_pblib002_s	15.93	H703_1026_120Es_A5	3.75	H703_1828_220Es	1.08
H703_1798_170_RE_p01s	>100	H703_1357_230Es_H1	15.84	H703_1945_090s_2A3	3.64	H703_1714_080c	1.03
H703_1889_100Es	>100	H703_0646_051sN	15.78	V703_1407_090_RE_pblib003_s	3.63	V703_1383_240_RE_pblib003_s	1.00
H703_2038_260_RE_e5C3s	>100	H703_0203_081_RE_e8A5s	15.28	V703_0629_150_RE_pblib004_s	3.31	H703_0805_770_RE_e10F8s	0.99
V703_0015_110_RE_pblib002_s	>100	V703_0510_260_RE_pblib001_s	13.82	V703_2372_170_RE_con_s	3.28	H703_1551_143s_2G8	0.82
V703_0132_200_RE_pblib002_s	>100	V703_1453_240_RE_pblib002_s	13.13	H703_1687_100Es	3.18	H703_0805_770_RE_e10C9s	0.81
V703_0217_050_RE_pblib002_s	>100	H703_0790_190_RE_e5G1s	13.02	V703_3000_090_RE_pblib002_s	3.04	H703_1764_250_RE_cs	0.80
V703_0510_260_RE_pblib003_s	>100	V703_0566_160_RE_pblib002_s	10.61	V703_2141_160_RE_sga3D6_s	2.89	H703_0578_130_RE_cs	0.69
V703_0514_150_RE_pblib004_s	>100	H703_0013_090Es	9.21	H703_1750_140Es	2.85	H703_2149_060_RE_eB10s	0.65
V703_1255_260_RE_pblib003_s	>100	V703_0712_250_RE_pblib001_s	7.69	H703_2018_240_RE_e6A1s	2.84	H703_2117_110_RE_e2A10s	0.64
V703_1298_080_RE_pblib002_s	>100	V703_1034_190_RE_pblib003_s	7.65	H703_2788_030Es_B1	2.72	H703_2304_150_RE_cs	0.54
V703_1515_120_RE_pblib002_s	>100	H703_1453_240_RE_e9B7s	7.04	V703_0597_190_RE_pblib003_s	2.71	H703_1471_190s	0.52
V703_1586_210_RE_sga3E8_s	>100	V703_1194_150_RE_pblib002_s	6.93	H703_0860_150Es	2.63	H703_0739_110s	0.46
V703_1714_080_RE_pblib002_s	>100	V703_1855_162_RE_pblib003_s	6.83	H703_0629_150_RE_e5A2s	2.52	H703_0520_030Es	0.43
V703_2805_080_RE_pblib002_s	>100	H703_1060_080s	6.27	H703_1313_040s	2.47	V703_2769_050_RE_pblib002_s	0.41
H703_1789_230_RE_e3A3s	>100	H703_1807_240_RE_cs	5.71	H703_0597_190_RE_e5A1s	2.39	H703_0537_110s_4H1	0.26
H703_0842_200Es	>100	H703_0948_170_RE_e4D2s	5.32	V703_1915_250_RE_sgaA3_s	2.26	V703_3000_090_RE_pblib001_s	0.25
V703_0790_190_RE_pblib002_s	>100	H703_0566_160s	5.21	H703_0993_110_RE_cs	2.21	V703_0537_110_RE_pblib003_s	0.19
H703_2769_050_RE_p01s	77.56	H703_1194_150_RE_cs	4.84	H703_1945_090s_2F1	2.10	H703_0514_150Es_A4_V02_028	0.14
H703_0406_240_RE_e11E4s	47.69	H703_0795_040s	4.77	H703_1783_170Es	2.06	V703_0458_260_RE_sga6H5_s	0.09
H703_0926_070s_2H2	35.60	V703_1240_201_RE_sga4F1_s	4.76	H703_1945_090s_3D5	1.95	H703_0472_030s	0.07
						H703_0537_110s_2B5	0.07

Figure 1.7. Initial VRC01 neutralization profiles of HVTN 703 AMP breakthrough cloned Envs. IC80 profile of breakthrough clones, against VRC01. IC80 profiles highlighted in blue represent the viruses most resistant to VRC01. As the colours change to yellow (IC80 10->99 µg/ml), orange (1-9 µg/ml) and red (0.01-0.99 µg/ml), the more sensitive the viruses to VRC01. The values represent the concentration of antibody needed to neutralize 80% of the virus, measured in ug/ml.

Once the neutralization profile of each pseudovirus was obtained, it was possible to compare the sequences of the resistant and sensitive viruses isolated from the AMP HVTN 703 trial. These results could lead to further understanding of the genetic differences that cause VRC01 resistance in subtype C HIV-1 viruses.

1.5. Mutations associated with VRC01 resistance

The development of mutations in both the CD4 binding site as well as the VRC01 contact sites facilitate resistance to the neutralization by this bNAb. Resistance mutations are studied in order to determine how breakthrough viruses arise by changing the binding affinity of the antibodies. There are many mutations that are associated with VRC01 resistance. Single point mutations or combinations of Env mutations change the charge and conformation of the epitope, which confers resistance to the antibody (Zhou *et al*., 2019). There are 35 contact sites between VRC01 and gp120 of the HIV-1 Env and 22 of these are found in the CD4 binding site (Zhou *et al*., 2010). Mutations that are responsible for VRC01-class antibody resistance can be found between residues 278 and 283 of Loop D, and at potential N-linked glycosylation sites between residues 458 and 467 of the V5 region (Zhou *et al*., 2019). Residues that have been previously identified to have a variable importance in influencing VRC01's neutralization ability are: P124, N156, L179, D279, N280, S365, H374, N425, Q428, R456, D457, G458, G459, E466, R469, G471, T569, and D589 (Magaret *et al*., 2019). There are antigenic differences in subtype B and C Envs which translate into differences in the bNAb activity against the gp160 of these subtypes (Binley *et al.*, 2008), and may mean that, in some cases, escape mutations in subtype C differ from those in subtype B.

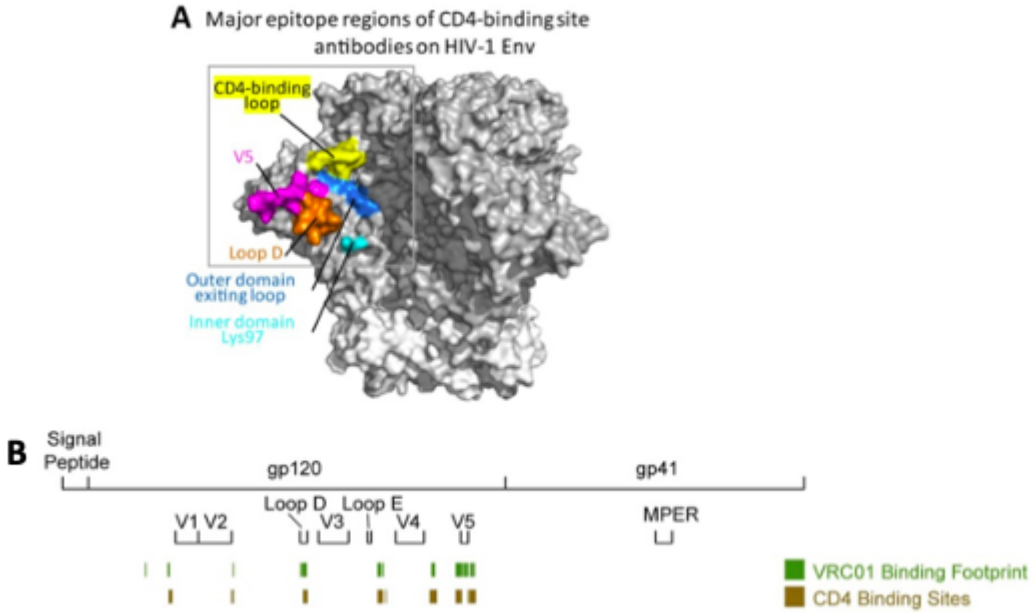

Figure 1.8. Major epitope regions of CD4 binding site antibodies on HIV-1 Env. (A) The major components of the CD4 binding site include the CD4 binding loop, loop D and V5 (Adapted from Zhou *et al*., 2019). (B) The CD4 binding sites and VRC01 binding footprint are represented in order to visualize binding patterns.

In addition to sequence variation, regions of the HIV Env undergo additional modifications in order to prevent the neutralization by antibodies. An example of these modifications is epitope masking (Zolla-Pazner and Cardozo, 2010). During epitope masking, glycans move in order to hide epitopes that can be recognized and targeted by the antibody. This mechanism is dependent on glycan density which has an effect on antibody activity (Zolla-Pazner and Cardozo, 2010). The variability of glycosylation is due to the variation in the glycan type and the positions at which they are expressed on the Env protein (Raska *et al*., 2014). Another example of epitope masking suggests that the 3D structure of the epitope is able to undergo conformational changes so the antibody is unable to recognize it (Zolla-Pazner and Cardozo, 2010). This explains why the conserved regions that are unable to undergo fewer modifications are targets of bNAbs.

1.5.1. Evidence of Selection of VRC01 Resistance Mutations and Viral Fitness

The evidence of selection of VRC01 resistance mutations was described by Lynch *et al*., where they mapped the VRC01-induced escape pathway of Envs from donor 45, from whom VRC01 was isolated. Several of the archival proviral Envs derived from donor 45 were sensitive to VRC01, while the majority of plasma-derived Envs isolated at a later stage were VRC01 resistant. When analyzing the viruses that developed over time (at three time points) in donor 45, they saw VRC01-sensitive, -intermediate, and -resistant Envs. The first amino acid change observed was at position 278, which resulted in a change from lysine to either serine or threonine, which subsequently inserted an N-linked glycosylation sequon at position 276 in the intermediate Envs. Introduction of the D279E mutation into the intermediate Env left it completely resistant to VRC01. The sensitive Envs became more resistant with the addition of a glycan at position 276 and/or a D279E mutation. When the glycan was removed from 276, VRC01 sensitivity increased substantially. Overall, the VRC01 escape pathway seen in donor 45 indicated that the addition of the glycan at 276 followed by the D279E mutation in loop D, resulted in VRC01 resistance. This describes the basis of the escape pathways seen in breakthrough viruses.

Furthermore, due to bNAbs closely mimicking CD4 in the interaction between the gp120, escape from the bNAbs could lead to impaired viral function and/or replication. It was seen that mutations in loop D or β23-loop V5 confer resistance to VRC01 and impact viral replication. This fitness cost is due to the less efficient CD4 receptor containing resistance mutations, especially when multiple resistance mutations were present. Mutations in loop D and β23 and V5 loop associated with VRC01 resistance are not highly observed in nature suggesting that these mutations have an unfavourable impact on viral fitness. These observations have not yet been widely interrogated in subtype C viruses. If VRC01 selects for less pathogenic viruses, individuals who become infected with VRC01 resistant viruses may have lower viral loads and show clinical relevance going forward.

However, it has been seen that the acquisition of compensatory mutations and full replicative fitness sometimes follows. Longitudinal sequence analysis of donor 45 Envs showed that changes

at position 279 mostly occurred concurrently with changes at position 281. It is believed that this change was compensatory as when A281H was introduced with the glycan at 276 and D279E, viral replication was restored to wildtype (WT) viral replication levels.

1.6. Transmission of multiple founder variants and discordant profiles

During initial HIV-1 infection at mucosal surfaces, the individual is infected with transmitted/founder (TF) viruses selected from the quasispecies of the chronically infected donor. HIV-1 transmission is associated with a severe bottleneck, where a limited number of variants establish infection, from a pool of genetically diverse quasispecies (Macharia *et al*., 2020). This shows that there is a selective pressure acting on the virus in the transmission fluid and in the recipient tissues (Joseph *et al*., 2015). However, the transmission bottleneck can be overcome as it is possible for an individual to be infected with concomitant or sequential infection by two to five TF HIV-1 strains (Keele *et al.*, 2008; Powell, Kinge and Nyambi, 2010). There is evidence of mutations selected for cytotoxic-T-lymphocyte or antibody escape and a high prevalence of recombination in individuals infected with multiple variants (Abrahams *et al*., 2009). This contrasts what was previously shown where only 20% of infections were caused by multiple variants.

A high proportion of multi-lineage infections were identified in the HVTN 703 and HVTN 704 trials and although genetically different, it was determined that in some cases, the viruses differed phenotypically as they had differential VRC01 profiles. It is possible that the individual could have been infected with phenotypically different TF viruses with discordant neutralization profiles. However, in the case of a single-lineage infection, evolution of resistance post-infection, due to VRC01 pressure, can lead to discordant VRC01 profiles of viruses within individuals.

Understanding the pathway of VRC01 resistance will be important to inform strategies that need to restrict bNAb escape pathways in subtype C viruses.

1.7. Project Aim

The overall aim of this project was to identify which mutations in the gp160 of VRC01 resistant viral Envs confer escape as well as to assess the effect of these mutations on other CD4 binding site antibodies.

1.7.1. Objectives

- To identify putative and novel escape mutations in the gp160 of subtype C VRC01 resistant viral Envs that confer escape.
  -Env sequences were analyzed and 3D modeling tools were utilized.

- To revert putative escape mutations that were suspected to cause VRC01 resistance.
  -Reversion was done by using site-directed mutagenesis and the production of chimeras.

- To test whether these mutations confer sensitivity of pseudoviruses to VRC01.
  -Neutralization assays were performed.

- To determine whether the subtype C resistance mutations affect recognition by other CD4 binding site bNAbs.
  -Neutralization assays were performed.

2. Materials and Methods

2.1. Sequence analysis, molecular visualization and structural visualization of putative VRC01 resistance mutations

We utilized six sets of Envs with discordant neutralization phenotypes identified from the AMP HVTN 703 trial (Figure 1.7) (Ethics clearance M210406). In order to identify the mutations that result in VRC01 resistance, the sequences of the resistant viral Envs were compared to the sequence (or sequences) of the sensitive virus from the same individual, sensitive subtype C AMP viruses as well as the sequence of HXB2 (Appendix A) using the HIVAlign tool (https://www.hiv.lanl.gov). Once the nucleotide sequences were aligned using HIVAlign, they were transferred to AliView (Larsson, 2014), the nucleotide sequences were translated into amino acid sequences and were compared to determine the differences between them. HXB2, a subtype B virus, was added to the alignment as the standard amino acid numbering across gp160 is based on the HXB2 sequence. By comparing the amino acid sequences of the isolated virus of interest to the sensitive virus's amino acid sequence, using the database tool CATNAP (Yoon et al., 2015), it was possible to identify putative escape mutations in sites of interest, such as the CD4 binding site epitope, which enabled the virus to become resistant to VRC01. In order to identify VRC01 resistance mutations in HIV-1 subtype C viruses, both the regions of the Envs that are known to form part of the CD4 epitope (loop D, V5 region and the CD4 binding site) as well as the VRC01 binding footprint were focused on. CATNAP integrates neutralization and sequence data from published studies. By using this tool, it is possible to obtain information about viruses of all subtypes that are resistant to VRC01, and in this case, particularly subtype C viruses were studied.

After identifying possible escape mutations, a molecular modeling tool, PyMOL (The PyMOL Molecular Graphics System, Version 2.0 Schrödinger, LLC), was utilized for 3D visualization of the HIV-1 viral Envs as well as the interaction and co-localisation between the WT and mutant HIV-1 viral Envs and VRC01. The resistant Env protein structure was analyzed in order to determine

how the CD4 binding site undergoes change in charge as well as change in hydrophobicity, which may enable escape.

2.2. Introduction of mutations into HIV-1 Env

2.2.1. Primer design

In order to revert the putative escape mutations to the conserved region sequence on the HIV-1 Env, primers were designed such that the nucleotide reversion sequence should be able to produce the same amino acid sequence as in known sensitive viruses of the desired region (Appendix B, Tables B1 and B2). Forward and reverse mutagenesis primers were designed that contained the point mutations needed to produce the nucleotide sequence required at specific sites. Once the position of the point mutation was identified, the primer was extended by 15-20 nucleotides in both directions, homologous to the template, to ensure the mutation was in the middle of the primer sequence. The GC content and melting temperatures were calculated (http://biotools.nubic.northwestern.edu/OligoCalc.html). All the primers were synthesized by Inqaba Biotec.

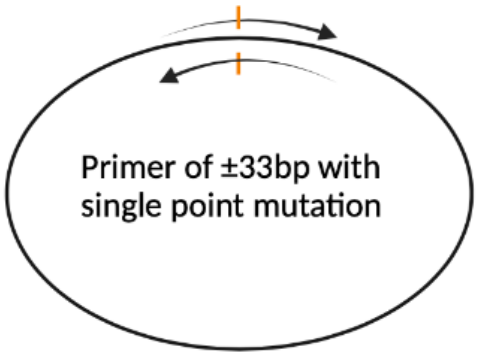

Figure 2.1. Representation of introduction of single mutations via SDM.

In some cases, chimeras were needed as there were too many differences between the resistant and sensitive sequences in the region of interest. This was performed according to Gibson's NEBuilder HiFi DNA assembly Cloning Kit (NEB #5520S version 1.3). In one case, to make V1V2 chimeras with an average of 68aa in length to be transferred, forward and reverse primers were

designed to amplify the chimera insert of the desired V1V2. The primers were designed to be 25 base pairs (bp) in length and the insert had to contain 200 bp for optimal cloning efficiency. Other forward and reverse primers, also 25bp, were designed to amplify the rest of the gp160 backbone (Figure 2.2). To make CD4bs or V5 chimeras, which are approximately 18aa in length, it was possible to design overlapping primers that contained the entire chimera and was then able to amplify the rest of the gp160 that would eventually contain the chimera (Figure 2.2). The primers were ~41 bp with an overlap of 10-16 bp to include the chimera. The GC content was calculated and the Tm was aimed to be equal to or greater than 48°C, according to manufacturer's instructions. All the primers (Appendix B, Tables B1 and B2) were synthesized by Inqaba Biotec.

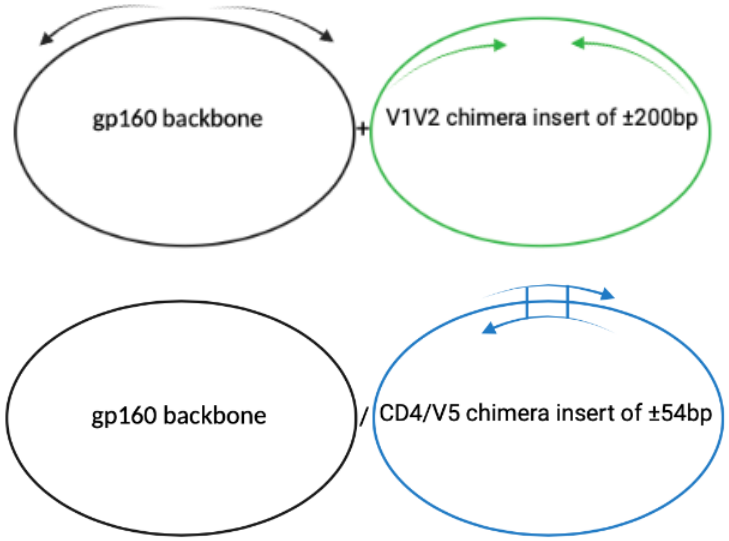

Figure 2.2. Representation of production of V1V2 and both CD4 and V5 chimeras.

2.2.2. Site Directed Mutagenesis

Site-directed mutagenesis (SDM) was performed using the QuikChange Lightning Multi Site-Directed Mutagenesis Kit (Agilent Technologies) as per the manufacturer's instructions. Primers were designed to be as close to 78°C as possible (Tables A1 and A2), which is recommended by the QuikChange Lightning Multi Site-Directed Mutagenesis Kit. During polymerase chain reaction (PCR), the double stranded deoxyribonucleic acid (DNA) template was denatured, the mutagenic

primers hybridized to the homologous section of the Env in the plasmid during the annealing step and, finally, the DNA polymerase extended the newly synthesized sequence to match the rest of the original plasmid. The mutant strand synthesis PCR reaction components include: 2.5 µl 10x QuikChange Lightning Multi reaction buffer, 18 µl double-distilled water (ddH_2O), 0.5 µl QuikSolution, 1 µl (100 ng) cloned WT plasmid ds-DNA template, 1 µl mutagenic primers each, 1 µl deoxynucleotide triphosphate (dNTP) mix and 1 µl QuikChange Lightning Multi enzyme blend which were added together in order and mixed gently. The cycling parameters from the instruction manual were followed (Table 2.1). All PCR reactions were carried out in the Perkin Elmer PE 9700 Thermal Cycler. Once complete, the reaction was placed on ice for 2 minutes.

Table 2.1. Cycling Parameters for Mutant Strand Synthesis Reaction.

	Cycles	Temperature °C	Time
Initial denaturation	1	95	2 minutes
Denaturation	30	95	20 seconds
Annealing		55	30 seconds
Extension		65	4 minutes (30 seconds/kb of plasmid length)
Final extension	1	95	5 minutes

Once the PCR products were amplified, they underwent DpnI digestion at 37°C for 1 hour. This occurred by the addition of 2 µl (units not specified in manual) DpnI restriction enzyme, which is an endonuclease that cleaves specific recognition sites on the original methylated parental (non-mutated) DNA template of the cloned WT plasmid. This was the selection process for the mutated single stranded DNA.

2.2.3. Construction of chimeras

The following steps were carried out in order to prepare for the introduction of chimeras. For the V1V2 chimeras, two PCR reactions were set up in order to amplify the required gp160 backbone and insert before assembly (Tables 2.2 and 2.3). For the CD4bs and V5 chimeras, one PCR reaction was set up in order to amplify the required gp160 with the included chimera (Table 2.2). The chimeric strand synthesis PCR reaction components included: 10.5 µl double-distilled water (ddH_2O), 0.5 µl forward primer (25 µM), 0.5 µl reverse primer (25 µM), 5 ng/µl cloned WT plasmid ds-DNA template and 12.5 µl Q5 Hot start master mix (NEB #M0491), a high-fidelity DNA polymerase, which were added together in order and mixed gently. The cycling parameters from the instruction manual were followed (Tables 2.2 and 2.3).

Table 2.2. Cycling Parameters for Chimeric Strand Synthesis Reaction- Backbone.

	Cycles	Temperature °C	Time
Initial denaturation	1	98	30 seconds
Denaturation	25	98	10 seconds
Annealing		55	20 seconds
Extension		72	4.5 minutes (30 seconds/kb of plasmid length)
Final extension	1	72	2 minutes

Table 2.3. Cycling Parameters for Chimeric Strand Synthesis Reaction- Insert.

	Cycles	Temperature °C	Time
Initial denaturation	1	98	30 seconds
Denaturation	25	98	10 seconds
Annealing		55	20 seconds
Extension		72	1 minute (30 seconds/kb of plasmid length)
Final extension	1	72	2 minutes

Once the PCR reactions were complete, the products were visualized on a 1% agarose gel in order to confirm that the amplicons were the desired size when compared to a DNA ladder. UltraPure™ Agarose (Invitrogen) was dissolved in 1X Tris Acetate electrophoresis buffer (40 mM Tris, 20 mM acetic acid, 1 mM EDTA) (Thermo Fisher Scientific), supplemented with 0.5 µL/mL ethidium bromide. The chamber was filled with 1X TAE buffer covering the entire gel and wells. In the first lane 4 µL of Marker VIII (Promega) was loaded followed by the PCR product with loading dye. The 1 % gels were resolved at 80V. An image of the gel was taken using UV light in the ChemiDoc™ XRS+ imager.

A DpnI digest was recommended in order to destroy the methylated plasmid template before setting up the assembly reaction. In a 10 µl reaction, 8 µl of PCR product was mixed with 1 µl 10x CutSmart™ buffer and 1 µl of DpnI (NEB #R0176, 20 units). The reaction was incubated at 37°C for 30 minutes and then 80°C for 20 minutes to heat inactivate the DpnI.

Assembly of chimeras was performed according to the NEBuilder HiFi DNA Assembly Cloning Kit (New England Biolabs® Inc) as per the manufacturer's instructions. For the V1V2 chimeras, a DNA molar ratio vector:insert of 1:2, estimated from bands on a 1% agarose gel prepared as above, was adjusted for. In a 20 µl reaction, 1 µl and 2 µl vector and insert, respectively, were added to 7 µl ddH_2O and 10 µl NEBuilder HiFi DNA Assembly Master Mix. For the CD4bs and V5 chimeras, 2 µl PCR product was added to 8 µl ddH_2O and 10 µl NEBuilder HiFi DNA Assembly Master Mix. The samples were incubated at 50°C for 15 minutes in the thermocycler. This is done to produce closed circular DNA plasmids in order to be transformed.

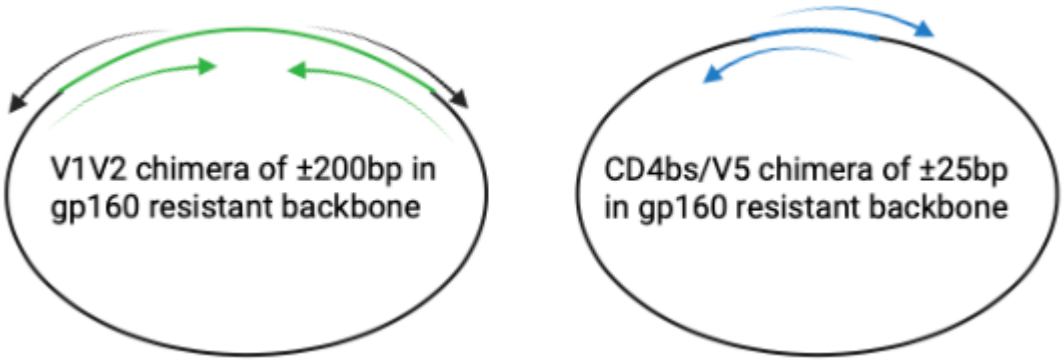

Figure 2.3. Representation of introduction of V1V2 and both CD4 and V5 chimeras in desired backbone.

2.2.4. Transformation of XL10 Gold Ultracompetent cells

Transformation was done by adding 2 µl β-mercaptoethanol (β-ME), a compound that denatures surface nucleases of cells and therefore improves their transformation efficiency, to 45 µl of XL10-Gold ultracompetent cells (Agilent) and incubated on ice for 10 minutes. Then, 2 µl of the DpnI-treated DNA from each SDM reaction was transferred to separate aliquots of the ultracompetent cells and incubated on ice for 30 minutes. The tubes were heat-pulsed at 42°C for 30 seconds, 300 µl S.O.C broth (Super Optimal broth with Catabolite repression: 20 mM Glucose, 10 mM Magnesium chloride, 10 mM Magnesium sulfate, 2.5 mM Potassium chloride, 10 mM Sodium chloride, 20 g/L Tryptone, 5 g/L Yeast extract) was added to each tube and they then were incubated at 37°C for 1 hour while shaking at 250 rpm. Once the transformation reactions were complete, 100 µl of each were plated on separate agar plates containing Carbenicillin (100 µg/ml) as a selection marker. This ensures that only the bacteria with plasmids containing the antibiotic resistant gene grow. The transformation plates were incubated at 37°C for 16 hours.

2.2.5. Plasmid Purification

A total of four colonies from each plate were picked with a pipette tip and separate aliquots of 15 ml Luria-Bertani broth (10g Select Peptone 140, 5g Select Yeast Extract and 5g Sodium Chloride) containing Carbenicillin, were inoculated and incubated at 37oC for 16 hours while shaking. The cells were harvested by centrifugation at 5000 rpm at 4°C for 10 minutes in the Centrifuge Universal 320R (Labotec). The supernatant was discarded and plasmid DNA in the pellet was purified using the QIAprep Spin Miniprep Kit (QIAGEN) as per the manufacturer's instructions. The procedure of the kit consists of steps including the preparation and clearing of cell lysate; adsorption of DNA onto the membrane; and washing and eluting the plasmid DNA. These steps are based on alkaline lysis of the cells, neutralization of the lysate, followed by the adsorption of plasmid DNA onto silica membrane in the presence of high-salt buffer, and finally elution in the presence of a low-salt buffer (QIAprep Miniprep Handbook). The required buffers were prepared before the protocol began, by adding a vial of RNase to resuspension Buffer P1, adding ethanol (96-100%) to wash Buffer PE and finally adding a vial of LyseBlue reagent to Buffer P1. LyseBlue was added to provide visual identification of correct buffer mixing. The pelleted bacterial cells were resuspended completely in 250 µl Buffer P1. The suspension was transferred to a microcentrifuge tube and 250 µl Buffer P2 was added and the tube was mixed well by inversion. Following these steps, 350 µl Buffer N3 was added and mixed immediately and thoroughly by inversion. The tubes were centrifuged at 13000 rpm for 10 minutes in a table-top microcentrifuge. The supernatants were transferred to QIAprep spin columns by decanting and centrifuged at 13000 rpm for 60 seconds. The flow-through was discarded. The spin column was washed by adding 750 µl Buffer PE and centrifuging again at 13000 rpm for 60 seconds. The flow-through was discarded and the spin columns were centrifuged at 13000 rpm for another 60 seconds to remove residual buffer. For the elution of DNA, the QIAprep column was placed in a clean microcentrifuge tube, 40 µl Buffer EB was added to the middle of the spin column, left to stand for 1 minute and then centrifuged at 13000 rpm for 2 minutes. A Nanodrop® ND-1000 Spectrophotometer (Thermo Fisher Scientific, USA) was used to measure the DNA concentration from each plasmid purification procedure at a wavelength of 260nm.

2.2.6. Sanger sequencing

Sanger sequencing was carried out to determine if the SDM and introduction of chimera reactions were successful. The Sanger dideoxy sequencing reaction mixture contains both dNTPs and fluorescently labeled dideoxynucleotide triphosphates (ddNTPs). As ddNTPs lack a hydroxyl group, and therefore unable to form a phosphodiester bond with the next nucleotide, they terminate the strand elongation and produce different lengths of DNA strands. This reaction uses the principle of a PCR reaction as the DNA is denatured, a DNA primer is hybridized to a homologous section of the template strand and DNA polymerase elongates it by adding on dNTPs and ddNTPs at different positions during elongation. After the reaction is complete, a laser excites the ddNTP at the ends of the different length strands and the wavelength of the emission is able to establish which base is at the specific position. The sequencing results can be visualized as a chromatogram.

The ABI PRISM BigDye Terminator Cycle Sequencing Ready Reaction kit (Applied Biosystems) was used to sequence the HIV-1 viral Env plasmid. The sequencing reaction components include: 1 µl Ready reaction mix, 1.5 µl ABI buffer, 2.5 µl dH_2O, 2 µl (300 ng) template DNA and 3 µl each 2 µM primer in separate wells, which bind to and sequence different portions of the DNA template. The eight primers used were EnvB, A589, A589 rev, EnvA, E55, Mf, Nr and Nf in order to sequence the whole Env (Appendix B, Table B3). The cycling parameters from the instruction manual were followed (Table 2.4).

Table 2.4. Cycling Parameters for Sanger Dideoxy Sequencing.

	Cycles	Temperature °C	Time
Denaturation	25	96	10 seconds
Annealing		50	5 seconds
Extension		60	4 minutes
Hold	1	4	∞

Once the reaction was complete, the Sodium Acetate (NaAc) sequencing reactions clean-up was performed. Anhydrous ethanol (EtOH) and NaAc (3M pH 4.6), 8 ml and 320 µl respectively, were mixed together and 50 µl was aliquoted into each well that contained a sequencing reaction and mixed well by pipetting. The plate was centrifuged at 2000 x g for 30 minutes. The plate was then inverted and centrifuged inverted at 150 x g for 1 minute. The pellet was rinsed with 100 µl cold 70% ethanol (EtOH) and centrifuged at 2000 x g for 5 minutes. Finally, the plate was inverted and centrifuged inverted at 150 x g for 1 minute and heated at 65°C for 3 minutes in order for the wells to dry. The cleaned up sequencing products were resolved on an automatic genetic analyser (Applied Biosystems™ 3500xL Genetic Analyser) and the chromatograms and nucleotide base sequences were analyzed and interpreted using the Sequencher® software (Version 5.4.6 DNA sequence analysis software, Gene Codes Corporation, Ann Arbor, MI USA, http://www.genecodes.com)). The obtained sequences were compared to the WT reference sequences and mutagenesis primers, using Sequencher®, to determine whether the single nucleotide base was changed. Sequencher® was then also used to determine whether the point mutation led to an amino acid change, as well as to ensure that there were no other changes in the entire Env sequence.

2.3. Maintenance and culture of HEK 293T cells and TZM-bl cells

HEK 293T cells were obtained from Dr. George Shaw (University of Alabama, Birmingham, AL) and were used for pseudovirus production. TZM-bl cells are a HeLa cell line expressing high levels of CD4 and CCR5 and transduced with a luciferase gene under the control of the HIV promoter. These were obtained from the AIDS Reagent Program (Division of AIDS, NIAID, NIH developed by Dr. John C. Kappes, and Dr. Xiaoyun Wu).

To produce the required growth media, 65 ml was removed from 500ml Dulbecco's modified eagle media (DMEM) (Gibco™, Thermo Fisher Scientific) and replaced with 50 ml fetal bovine serum (FBS, heat-inactivated, qualified) (Thermo Fisher Scientific), 12.5 ml 25 mM 4-(2-hydroxyethyl)-1-piperazineethanesulfonic acid (HEPES buffer) and 2.5 ml 50 µg/ml gentamicin (Sigma-Aldrich, South Africa)

HEK 293T cells: To passage cells, the media was removed from the T75 flask of previously seeded cells, the cells were washed by the addition of 5 ml PBS, which was spread over the cells and removed. The cells were covered by 2.5 ml Trypsin, which was removed immediately. The cells were then incubated at room temperature for 2 minutes and examined to see whether trypsinization was complete. In order to count cells, 10 ml complete DMEM was added to the cells and mixed well. A 1:10 dilution was made by taking out 10 µl of cells and mixing them with 90 µl trypan blue, 12 µl of the mixture was transferred to a counting chamber and four squares were counted through the Celestron Labs CB2000C Compound Binocular Microscope. The cell density was calculated by ((cells counted x dilution factor)/number of quadrants) x 10^4. Three million cells in a total of 15 ml GM were seeded and incubated for 48 hours.

TZM-bl: To passage cells, the media was removed from the flask of three million previously seeded cells, the cells were washed by the addition of 5 ml PBS, which was spread over the cells and removed. The monolayer of cells was covered by 2.5 ml Trypsin/EDTA (0.25%) (Thermo Fisher Scientific) and incubated at room temperature for 30 seconds. The trypsin was then removed and the flask was incubated at 37°C for 4 minutes in a 5% CO_2 incubator. After the incubation the cells were examined to see whether trypsinization was complete. In order to count cells, 10 ml complete DMEM was added to the cells and mixed well. The cells were counted, the density was calculated and seeded as for HEK 293T cells.

2.4. Production of Pseudoviruses by Transfection of 293T cells

The pseudoviruses were produced according to the Montefiori pseudovirus preparation protocol (Montefiori, 2004). The transfection process began by seeding HEK 293T cells at 2×10^6 cells/10 ml GM into 100mm x 200mm Nunclon Delta Dishes and incubated at 37°C for 24 hours in a 5% CO_2 incubator. The following day, 24 µl linear polyethylenimine hydrochloride (PEI Max Mw 40, 000), the transfection reagent made up to 1 mg/ml, was added to 500 µl Dulbecco's modified eagle media in sterile cryotubes. Then 4 µg of either WT or mutated HIV-1 Env plasmid DNA and 4 µg of backbone plasmid DNA (pSG3Δenv), an Env-deficient HIV-1 backbone vector useful for generating Env pseudotyped infectious virions, were added and left to incubate at room

temperature for 45 minutes. The transfection complex was added to a prepared 100mm x 200mm Nunclon Delta dish of the seeded HEK 293T cells and incubated at 37°C for 48 hours in a 5% CO_2 incubator. The supernatants that contained the pseudoviruses were harvested by filtering the culture fluid through a luer lock syringe and 0.45 µm filter. The FBS concentration was adjusted to 10% and mixed well and 1 ml aliquots were distributed to cryotubes that were labeled. The virus containing aliquots were stored at -80°C.

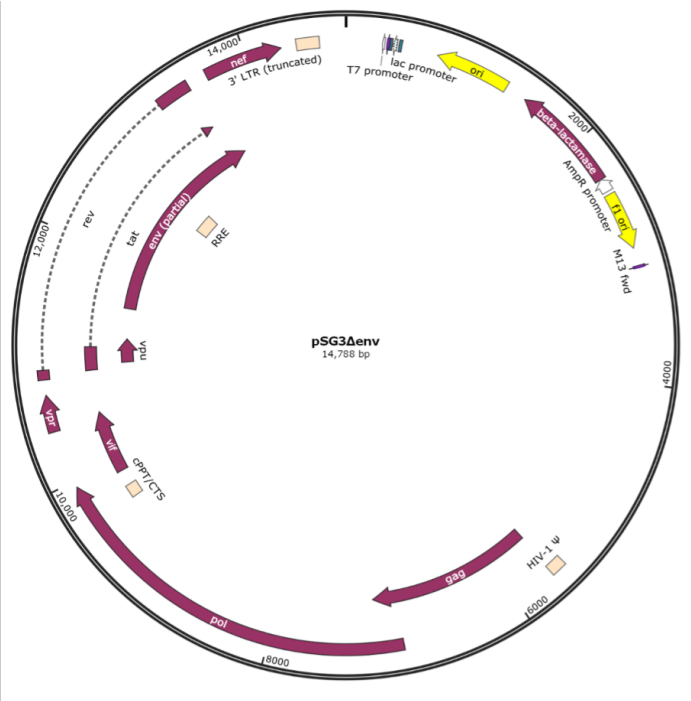

Figure 2.4. Structural representation of the pSG3Δenv backbone. It is derived from pSG3.1 (cat# 2003) through *SpeI* partial digestion, Klenow filling of the 3' recessed ends and religation. This introduced a four-nucleotide insertion mutation (CTAG) in Env and a translation stop codon after amino acid residue 142. It is useful for generating Env pseudotyped infectious virions and facilitates the analysis of immunologic and pharmacologic inhibitors that target the HIV-1 Env glycoprotein.

2.5. TCID50 Assay

Viral titers were determined as follows- In 96-well flat bottom treated culture plates (Corning®), 100 µl growth media was added to each well. The wells in column 1 served as cell controls. Each row received 25 µl of virus in duplicate. A serial 5-fold dilution was performed by transferring 25 µl of mixed virus to the next row and repeated through row H. After the final transfer and mixing

was complete, 25 µl was discarded from row H. The TZM-bl cells were prepared as above and counted. A cell suspension of 0.5×10^6 cells/ml was produced by adding 3 ml cells to 7 ml growth media and then mixed with 40 µl diethylaminoethyl (DEAE) dextran made up to 5 mg/ml per plate, which enhances viral infectivity. The solution was mixed thoroughly and 100 µl was dispensed into all wells. The plates were covered and incubated at 37°C for 48 hours in a 5% CO_2 incubator. To read the plates, 100 µl of the media was removed from the wells, 100 µl Bright-Glo® Luciferase substrate (Promega) was added to each well and incubated at room temperature for 2 minutes (the Bio-Safety Cabinet light remained off as Luciferase is light sensitive). The remaining contents of the wells were mixed thoroughly and 150 µl was transferred to a black plate (Corning®). The plates were read using a VICTOR XLight Luminometer (PerkinElmer) and analyzed to determine if the viruses grew and were able to infect the cells by reading the relative luminescence units (RLU).

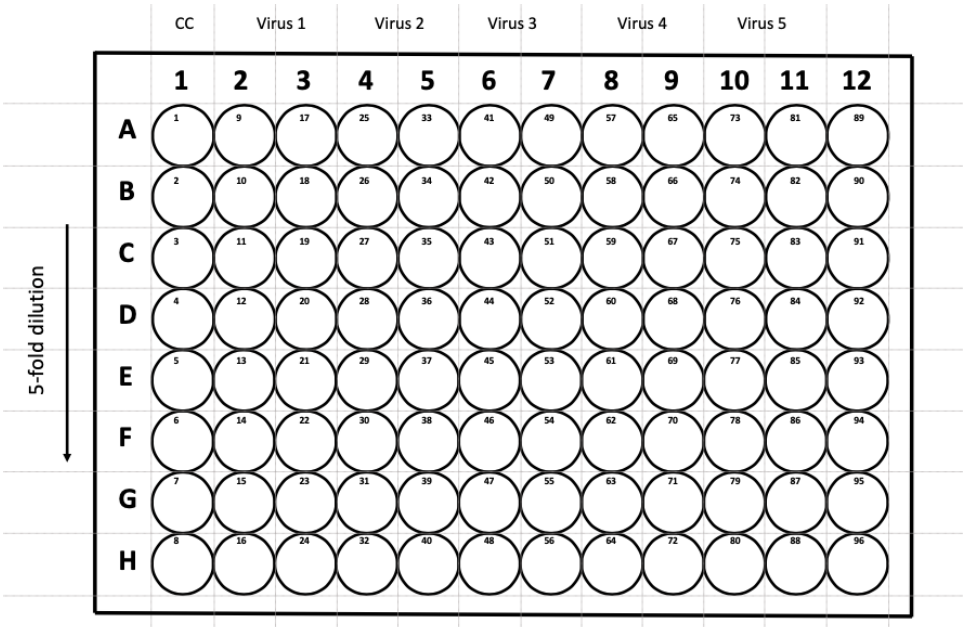

Figure 2.5. Schematic of TCID50 assay plate set-up. Column 1 is the cell control. The viruses are added in duplicate from column 2-11 along row A. A 5-fold serial dilution was made for each column from row A-H.

2.6. TZM-bl Neutralization Assay

Neutralization assays were performed as described by Montefiori (2004). In 96-well flat bottom culture plates, 25 µl growth media was added to each well and an additional 25 µl was added into column one which served as a cell control. Another 12.5 µl of growth media was added to row H. VRC01, CD4 binding site mAbs (3BNC117, N6, VRC07-523LS, HJ16 and 1-18) as well as control bNAbs (10e8, PGT121 and PG9), which are all made in the NICD lab, were added to their appropriate wells at 25 µg/ml and a 3-fold serial dilution was made by transferring 12.5 µl to the next row, mixed and repeated through row A. A virus control column was included which did not contain antibody. After the final transfer and mixing was complete, 12.5 µl was discarded from row A. The dilution of the selected pseudoviruses were determined by the TCID50 assay and the viruses were thawed in room temperature water. The virus and growth media were mixed and 25 µl was dispensed into each well except the cell control. The plates were covered and incubated at 37°C for 60 minutes in a 5% CO_2 incubator. The TZM-bl cells were prepared as above and counted. A cell suspension of 0.5×10^6 cells/ml was produced by adding 2 ml cells to 8 ml growth media and then mixed with 140 µl DEAE dextran made up to 5 mg/ml, which enhances viral infectivity. The cell suspension was mixed thoroughly and 20 µl added to all wells and the plates were incubated at 37°C for 24 hours in a 5% CO_2 incubator. The cells were then topped up with 130 µl growth media and incubated at 37°C for 24 hours in a 5% CO_2 incubator. After a further 24 hours, 100 µl of the media was removed from the wells and 100 µl of Luciferase substrate (Bright Glo) was added to each well and incubated at room temperature for 2 minutes. The contents of the wells were mixed thoroughly and 150 µl was transferred to a black plate. The plates were read using a VICTOR XLight Luminometer (PerkinElmer) as above and the results were analyzed using a macro template in order to determine whether the antibody was able to bind to and neutralize the viral entry into the cell or whether the virus was resistant to the neutralizations by the antibodies.

These experiments were done in duplicates and all fell within 3-fold, therefore statistically significant results were obtained.

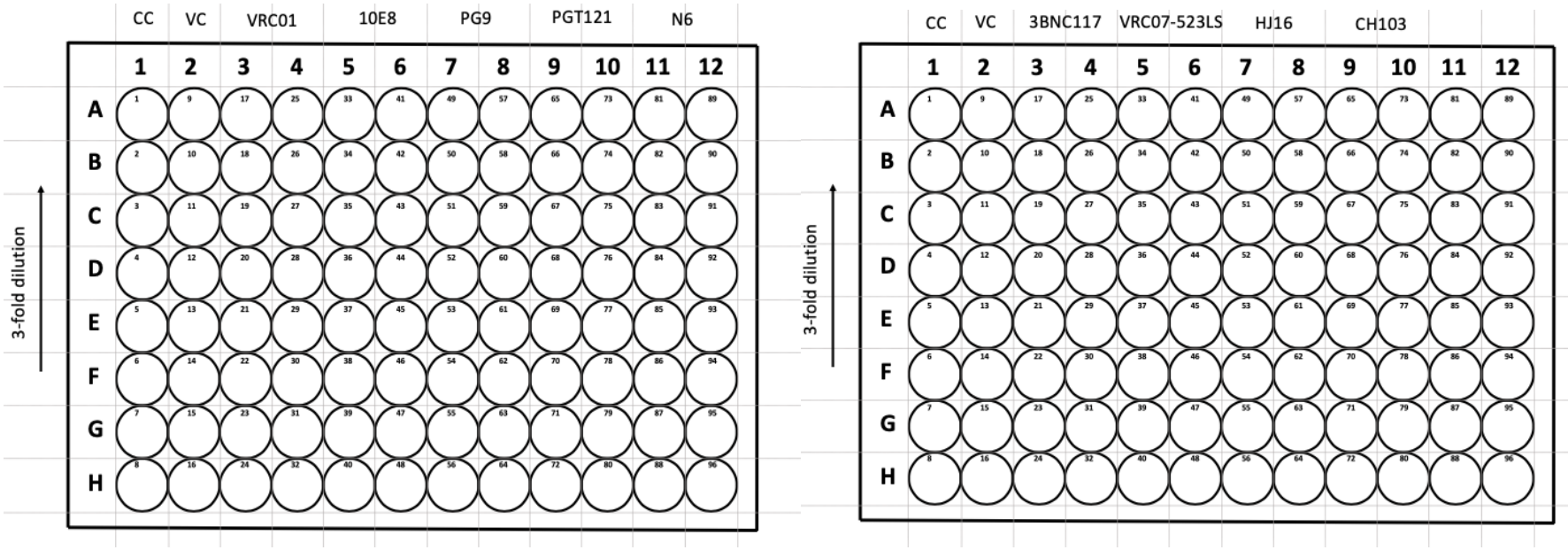

Figure 2.6. Schematic of Neutralization assay plate set-up for each virus. Cell control in column 1, virus control in column 2 and mAbs added in duplicate in row H. A 3-fold dilution was made for each column from H-A. Both plates used to test every virus.

3. Results

3.1. Multi-lineage infections with discordant profiles

Based on the analysis of the initial AMP breakthrough viruses, several cases of multi-lineage transmission had been identified and in some cases, multiple Env clones were generated and tested for their sensitivity to VRC01 (Figure 1.7). Comparison of the IC80 values of cloned viruses from within donors revealed differential sensitivity profiles to VRC01 (Figure 3.1).

The IC80 is able to provide us with a measure of potency of a bNAb against a specific virus. An IC80 of >100 indicates that the virus is highly resistant to VRC01 and 100 μg/ml is unable to neutralize 80% of the virus while an IC80 <1 tells us that the virus is highly sensitive to VRC01 as a low amount of VRC01 is able to neutralize 80% of the virus. For example, when comparing the sensitivity of clones from Participant ID (PTID) 703-0510, two clones were observed to be sensitive to VRC01, with IC80s of 17.58 μg/ml and 14.02 μg/ml, whereas the third clone, 703_0510_260_RE_pblib003_s, showed resistance to VRC01 with an IC80 of >100 μg/ml. Similarly, three Envs sequenced from PTID 703-0514 were highly resistant to VRC01 with IC80 >100. In contrast, a fourth Env had an IC80 of 0.25, showing high level sensitivity. In the other five PTID sets, only one resistant and one sensitive virus were cloned. Although viruses in PTID sets 703-0790 and 703-2769 have IC80s of 88.69 and 74.88 respectively, they are still considered resistant as they are at the higher end of the 10-99 μg/ml range. IC80s of >100 μg/ml are completely resistant, between 10-99 μg/ml are intermediately resistant, 1-9 μg/ml are sensitive and <0.01-0.9 μg/ml are hyper-sensitive.

PTID	Virus clone name	IC80
703-0790	V703_0790_190_RE_pblib002_s	88.69
	H703_0790_190_RE_e5G1s	13.19
703-1714	V703_1714_080_RE_pblib002_s	>100
	H703_1714_080c	0.89
703-2769	H703_2769_050_RE_p01s	74.88
	V703_2769_050_RE_pblib002_s	0.26
703-0510	V703_0510_260_RE_pblib003_s	>100
	V703_0510_260_RE_pblib001_s	14.02
	V703_0510_260_RE_pblib002_s	17.58
703-1586	V703_1586_210_RE_sga3E8_s	>100
	V703_1586_210_RE_pblib002_s	34.03
703-2805	V703_2805_080_RE_pblib002_s	>100
	H703_2805_080Es	1.04
703-0514	H703_0514_150Es_F4_V03_024	>100
	V703_0514_150_RE_pblib004_s	>100
	H703_0514_150s_6C1	>100
	H703_0514_150Es_A4_V02_028	0.25

Figure 3.1. Virus clones from each individual with discordant neutralization profiles. Each Participant ID (PTID) and the respective IC80 profiles of each VRC01 resistant and sensitive breakthrough clone. IC80 profiles in blue represent the viruses most resistant to VRC01 (>100 µg/ml), intermediate in yellow (IC80 10->99 µg/ml), sensitive in orange (1-9 µg/ml) and hyper-sensitive red (0.01-0.9 µg/ml).

3.1.1. Identification of potential VRC01 resistance mutations

The following overall approach, which will be described in more detail below, was followed to identify the potential mutations that confer resistance to VRC01. We visually inspected each sequence to identify mutations that distinguished resistant and sensitive Envs and ran the WT and mutant sequences, through a machine learning VRC01 sensitivity prediction tool. Based on the analyses of these two sets of results, we chose mutants that we wanted to test, carried out SDM (both to make sensitive clones resistant, and to make resistant clones sensitive) and tested the mutants against VRC01 to confirm whether the identified mutations were the cause of the resistance. These are described below in more detail.

We collaborated with Dr Craig Magaret, a Bioinformatician from Fred Hutchinson Cancer Research Center in Seattle, Washington, who has developed a software which uses a machine learning tool that is able to analyse HIV-1 Env sequences and predict a virus's probability of sensitivity to VRC01 and its IC80 (unpublished data). This was done by using machine learning to compile a database of 611 HIV-1 Env pseudoviruses, with known data on how well VRC01 neutralizes each pseudovirus. This sieve analysis uses the probability of different amino acid variations at specific sieve sites across the Env to predict whether sequences with these mutations cause sensitivity (Figure 3.2A) or resistance (Figure 3.2B) to VRC01.

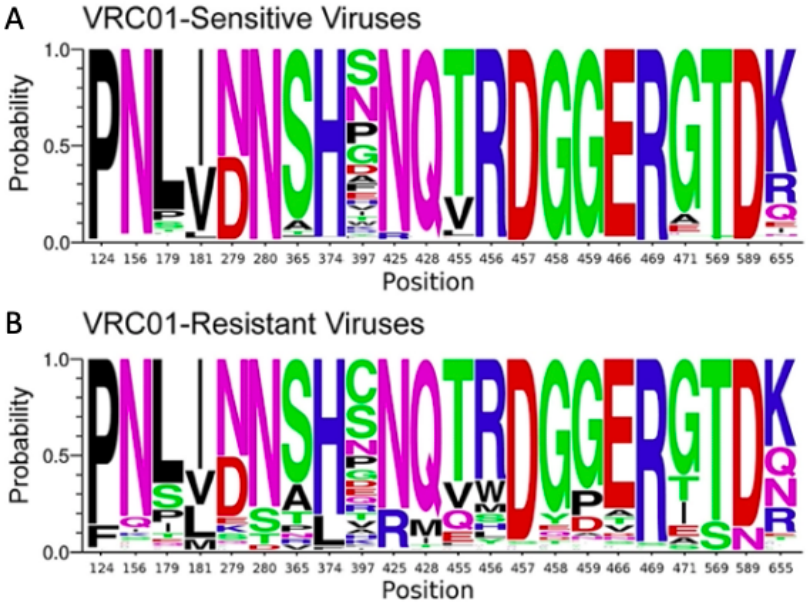

Figure 3.2. Logoplots of the probabilities of amino acids observed at important positions, in (A) VRC01-sensitive pseudoviruses and (B) VRC01-resistant pseudoviruses. (Adapted from Magaret *et al*., 2019).

The WT sequences from discordant clones were aligned to identify residues which might account for varying phenotypes. Particular attention was paid to mutations within the CD4 binding site as well as features such as length of V1V2 and V5; and number and position of potential N-linked glycosylation sites (PNGS) (Magaret *et al*., 2019).

We constructed a series of approximately 200 theoretical sequences, all aligned to HXB2, including the WT resistant virus, the WT sensitive virus, and mutants that contained amino acid changes at positions likely to be involved in VRC01 resistance for each discordant virus set. These theoretical sequences contained individual mutations, chimeras and a combination of all likely VRC01 resistance mutations (focusing on the conserved regions and sites likely to be implicated in resistance). The machine learning tool was used to predict which mutations caused the sequences' predicted probability of sensitivity to VRC01 to increase and predicted IC80 to decrease when compared to the resistant WT sequence values. We would then modify the VRC01 resistant plasmids to contain the reversion mutations of interest individually or in groups that are shown to confer sensitivity to VRC01.

As there is no threshold for the software predictions, to identify which sequences the software predicted to become more sensitive to VRC01 we analyzed the trend within each set of sequences where their respective mutants had a higher predicted probability of sensitivity to VRC01 and a lower IC80 either towards the values of the sensitive virus or away from the resistant virus.

Based on this analysis, we made a consolidated list of mutants that fit our criteria, and proceeded with the reversion of the suspected mutations by SDM or creation of chimeras. We introduced mutations in the resistant viruses to determine if the mutations, away from the WT, at the identified positions conferred sensitivity to VRC01, and then reversed the process by inserting

the amino acid suspected to cause resistance into the sensitive WT to confirm whether resistance to VRC01 was conferred. Below, each of the discordant pairs is described in more detail.

PTID 703-0790

We first assessed PTID 703-0790 where comparison of the sequences showed that there was a single amino acid difference between the two discordant clones. The more resistant virus with an IC80 of 88.69 µg/ml contains a Serine (S) at position 280 in loop D whereas the sensitive virus (IC80 of 13.19 µg/ml) contains an Asparagine (N) at position 280 (Figure 3.2.1). We therefore concluded that mutation N280S was responsible for conferring resistance to VRC01 and did not need to asses these clones in neutralization assays.

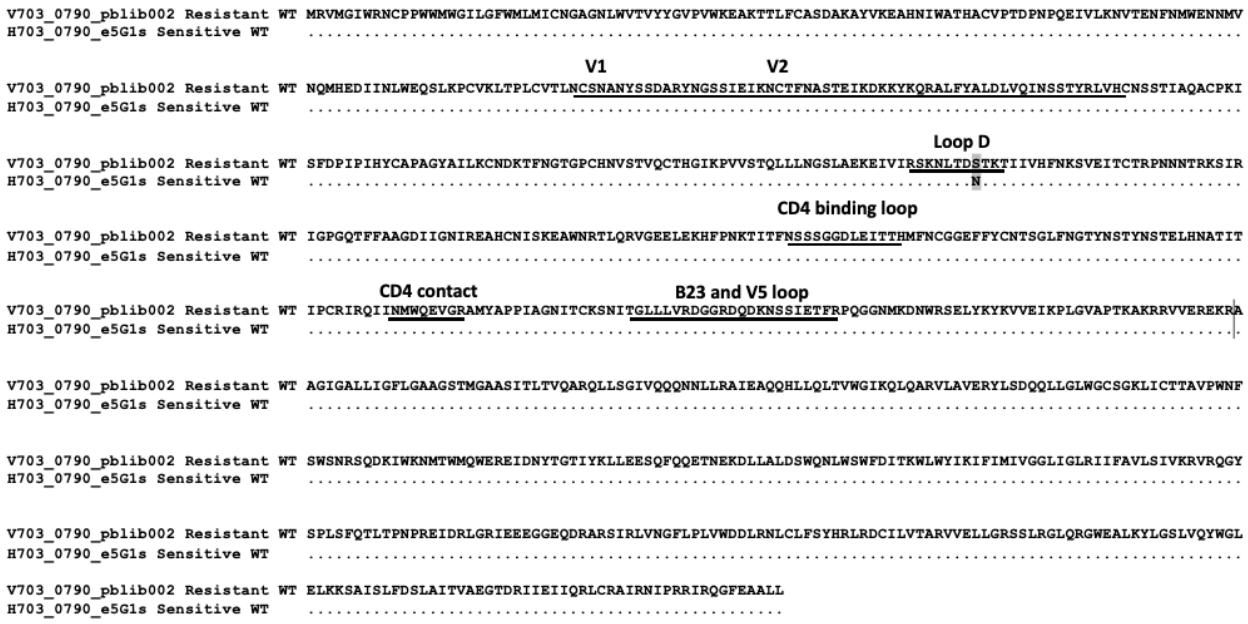

Figure 3.2.1. Results for PTID 703-0790. Sequence alignment of Envs cloned from PTID 0790. Resistant WT (top) and sensitive WT (below). Regions of interest V1V2, Loop D, CD4 binding loop, CD4 contact and β23 V5 loops are underlined in black. Black dots in the sensitive sequence represent an amino acid match to the resistant sequence. Amino acids highlighted in grey represent a single mutation site. The vertical grey line represents the end of gp120 and the start of gp41.

PTID 703-1714

Although we observed multiple differences between Envs cloned from PTID 703-1714, we again focused on mutations within the CD4 binding site region. Sequence alignment of viruses cloned from PTID 703-1714 showed two differences between the β23 and V5 loop of resistant and sensitive viruses. Mutations D459G and E462D were identified, where either one of the single mutations or the double mutation could be responsible for conferring resistance to VRC01 (Figure 3.2.2A). Although there were four amino acid differences in the V1V2 region there was no indication on CATNAP that these would play a role in conferring resistance to VRC01 so these were not pursued.

For the set of sequences for PTID 703-1714, the machine learning predictions showed that V703_1714_pblib002 D459G as well as the double mutant V703_1714_pblib002 D459G E462D would become sensitive to VRC01, having a higher probability of sensitivity and lower IC80 than the H703_1714_080s sensitive WT, whereas V703_1714_pblib002 E462D single mutant remains as resistant as the WT resistant sequence (Figure 3.2.2B).

We therefore used SDM to introduce each mutation, and a combination of both into the resistant WT Env, and assayed these in neutralization assay against VRC01 (Figure 3.2.2C). The neutralization curve verifies that the D459G mutation causes complete sensitivity to VRC01 and E462D has no effect on the virus's neutralization profile with IC50s of 1.87 μg/ml and >25 μg/ml respectively. The double mutant had an IC50 of 1 μg/ml suggesting the D459G mutation is responsible for the shift in IC50. When the experiment was reversed and H703_1714_080s was mutated to contain both G459D and D462E as single mutations and in combination, it was confirmed that the G459D mutation lead to the sensitive WT virus becoming resistant to VRC01, with an IC50 changing from 0.32 to >25 μg/ml while the D462E mutant remained sensitive (0.38 μg/ml) (Figure 3.2.2D). The laboratory results also confirm the machine learning prediction, that V703_1714_pblib002 mutants become more sensitive to VRC01 than the H703_1714_080s sensitive WT.

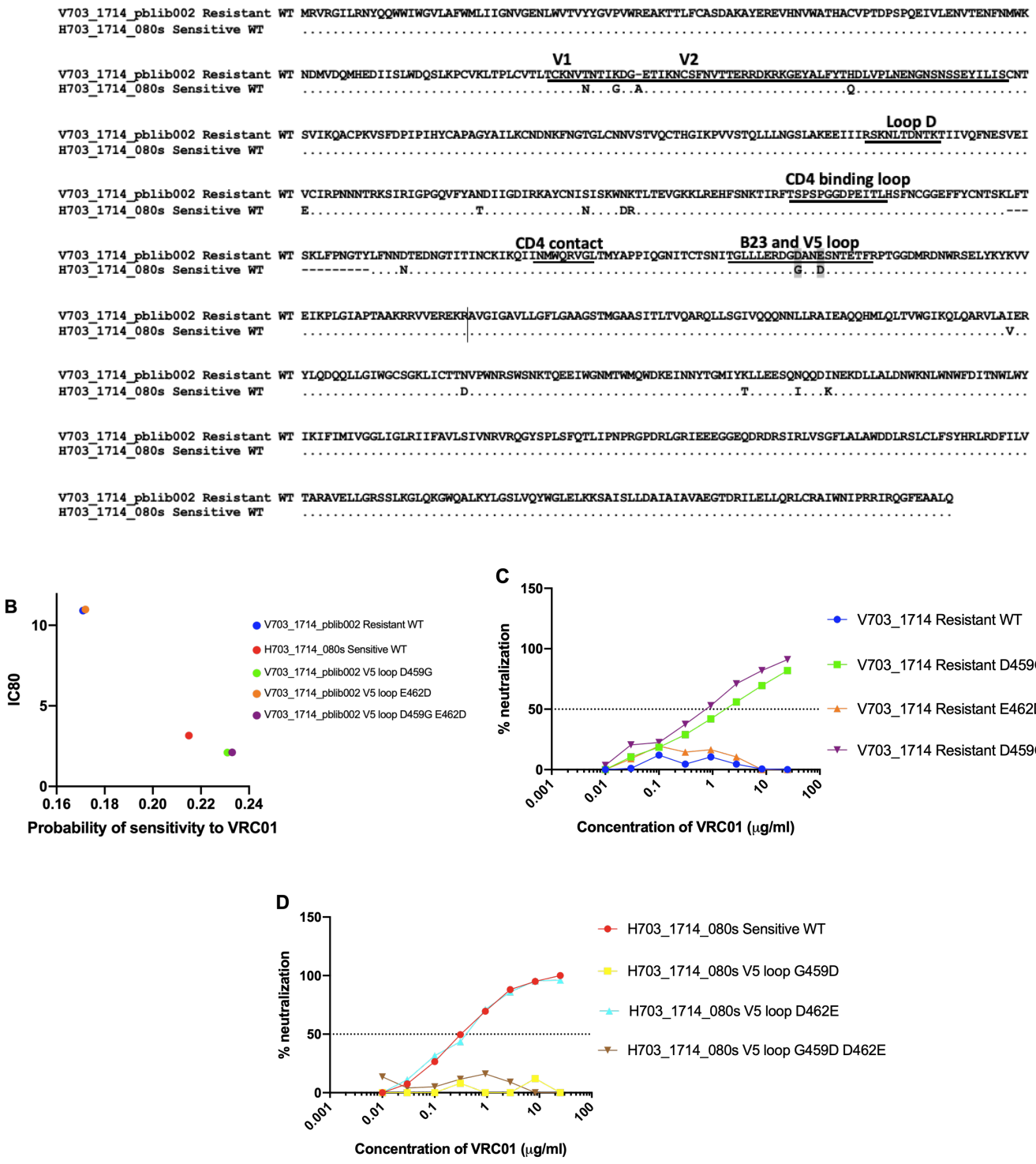

Figure 3.2.2. Results for PTID 703-1714. (A) Sequence alignment of Envs cloned from PTID 1714. Resistant WT (top) and sensitive WT (below). Regions of interest V1V2, Loop D, CD4 binding loop, CD4 contact and β23 V5 loops are underlined in black. Black dots in the sensitive sequence represent an amino acid match to the resistant sequence. Dashes show a deletion in the sequence. Amino acids highlighted in grey represent mutation sites in regions responsible for

conferring resistance to VRC01. The vertical grey line represents the end of gp120 and the start of gp41. (B) Correlation plots representing the machine learning-based predicted IC80 vs the predicted probability of sensitivity to VRC01 for the WTs and mutants in each set. The resistant WT is represented in blue, the sensitive WT is represented in red and the mutants are represented in the remaining colours. (C) Neutralization curves of the resistant WT and mutant viruses representing the concentration of VRC01 needed to neutralize 50% of the virus. (D) Neutralization curve of the sensitive WT and mutant viruses to confirm the effect of the mutations against VRC01.

PTID 703-2769

PTID 703-2769 had striking differences between the resistant and sensitive sequences in all the major CD4 binding site regions (Figure 3.2.3A). They had many differences between the V1V2 regions, although not a major length change, a N279D mutation in loop D from the sensitive WT to resistant WT, four amino acid changes in the CD4 binding loop, a single Q432R mutation in the CD4 contact and finally a four amino acid deletion and three amino acid deviation in β23 and V5 loop of the sensitive virus (Figure 3.2.3A).

We constructed a series of six theoretical sequences for PTID 703-2769 and tested these on the machine learning prediction tool. We found that only two of the four mutants had increased probability of sensitivity to VRC01 and decreased IC80 values, namely the R432Q mutant and the sequence that contained the sensitive clone's V5 loop chimera (Figure 3.2.3B), and therefore performed mutagenesis and produced pseudoviruses. Interestingly, the H703_2769_050_RE_p01s D279N mutant was predicted to be substantially more resistant to VRC01 than the resistant WT sequence.

In neutralization assays, the H703_2769_050_RE_p01s resistant WT virus and the R432Q mutant had similar neutralization curves and IC50s of >25 µg/ml needed to neutralize 50% of the viruses, the sensitive β23 and V5 loop chimera caused the resistant virus to become sensitive to VRC01 with an IC50 of 6.82 µg/ml (Figure 3.2.3C). Similarly, V703_2769_050_RE_pblib002 sensitive WT virus and the Q432R mutant were sensitive to VRC01 with IC50s of 0,14 and 0.15 µg/ml, respectively, therefore confirming that mutations at position 432 do not have a role in conferring resistant to VRC01. While V703_2769_050_RE_pblib002 sensitive virus containing the β23 and

V5 loop chimera of the resistant virus remained sensitive, the higher IC50 of 2.97 µg/ml indicates that more VRC01 was needed to neutralize 50% of the virus and it became more resistant to VRC01 than the WT (Figure 3.2.3D). The change in IC50s may be due to an individual mutation within the chimera or the change in length of the β23 and V5 loop.

```
H703_2769_050_RE_p01s Resistant WT     MRVRGMLRNCPPWWIWSILGLWMVIMGNEEKDLWVTVYYGVPVWREAKTTLFCASDAKSYEKEAHNIWATHACVPTDPNPQEVFLDNVTE
V703_2769_050_RE_pblib002 Sensitive WT ...........................................................................V.K....
                                                                                V1                  V2
H703_2769_050_RE_p01s Resistant WT     NFNMWKNDMVDQMHEDIISLWDESLKPCVKLTPLCVTLNCSDVTVSQNETTKY--STINANQTEQMKNCSFNTTTVIRDKKKQEYALFYK
V703_2769_050_RE_pblib002 Sensitive WT ........................................K.N.NDTQIAEIRKGIV.TS...E.......A.A.LKN...K.......

H703_2769_050_RE_p01s Resistant WT     LDIEALPKNKNSNNSDSNSNDSNEYILINCNTSTIAQACPKITFEPIPIHYCAPAGYAILKCNNNTFNGTGPCNNVSTVQCTHGIKPVVS
V703_2769_050_RE_pblib002 Sensitive WT ....P.H..G...D.--------K.........A.............................DKE.......................
                                                  Loop D
H703_2769_050_RE_p01s Resistant WT     TQLLLNGSLVEGKDIIIRSENITDNVKTIIVHLNESVEINCTRPGNNTRKSVRIGPGQTFYATGAIIGDIRQAHCNISRAKWNITLERVK
V703_2769_050_RE_pblib002 Sensitive WT .........A.-DG.........N..........K..G.............I......A.....D.............ETE..A......
                                                CD4 binding loop                                  CD4 contact
H703_2769_050_RE_p01s Resistant WT     TKLGEYFSNSTIVFKPPVPGGDPEITTHSFNCGGEFFYCNTTDLFSANATTNSSATGTITLQCRIKQIINMWQQVGRAIYAPPIAGNITC
V703_2769_050_RE_pblib002 Sensitive WT E...Q....K.TISFE.AS.....VI................K...---S.H.AVN.....P.K............Q.............
                                                B23 and V5 loop
H703_2769_050_RE_p01s Resistant WT     NSTITGLLLTRDGGETNKTNNSTEEIFRPGGGDMRDNWRSELYKYKVVEIKPLGVAPTRAKRRVVEREKRAVGIGAMFLGFLAAAGSTMG
V703_2769_050_RE_pblib002 Sensitive WT ..N...........---NV....-.T...............................G.R..........L..V.I...G.......

H703_2769_050_RE_p01s Resistant WT     AASITLTVQARQLLSGIVQQQSNLLRAIEAQQHLLQLTVWGIKQLQTRVLALERYLKDQQLLGIWGCSGKLICTTSVPWNNSWSNKSLGD
V703_2769_050_RE_pblib002 Sensitive WT ........................................V..............T..................N..............

H703_2769_050_RE_p01s Resistant WT     IWENMTWMQWDREVSNYTNTIYMLLEKSQIQQEQNEKDLLSLNSWGSLWNWFSITQWLWYIKIFIMIVGGLIGLRIIVAVISTVNRVRQG
V703_2769_050_RE_pblib002 Sensitive WT ..D...................R...E..N.........................R...............................

H703_2769_050_RE_p01s Resistant WT     YSPLSFQTLYPSPGGPDRLGRIEEEGGEQDKNRSVRLVNGFLPLVWDDLRSLCLFCYHRLRDCILIATRAVEILGRSSLRGLQRGWETLK
V703_2769_050_RE_pblib002 Sensitive WT .........I.......................K.........A...................F................K..........

H703_2769_050_RE_p01s Resistant WT     YLGNLVLYWVLELKKSAISLLDTLAITVAEGTDRIIELGQRICRAIISIPRRIRQGFEAALQ
V703_2769_050_RE_pblib002 Sensitive WT ...S.....G..........I.....A..............T....RN..............
```

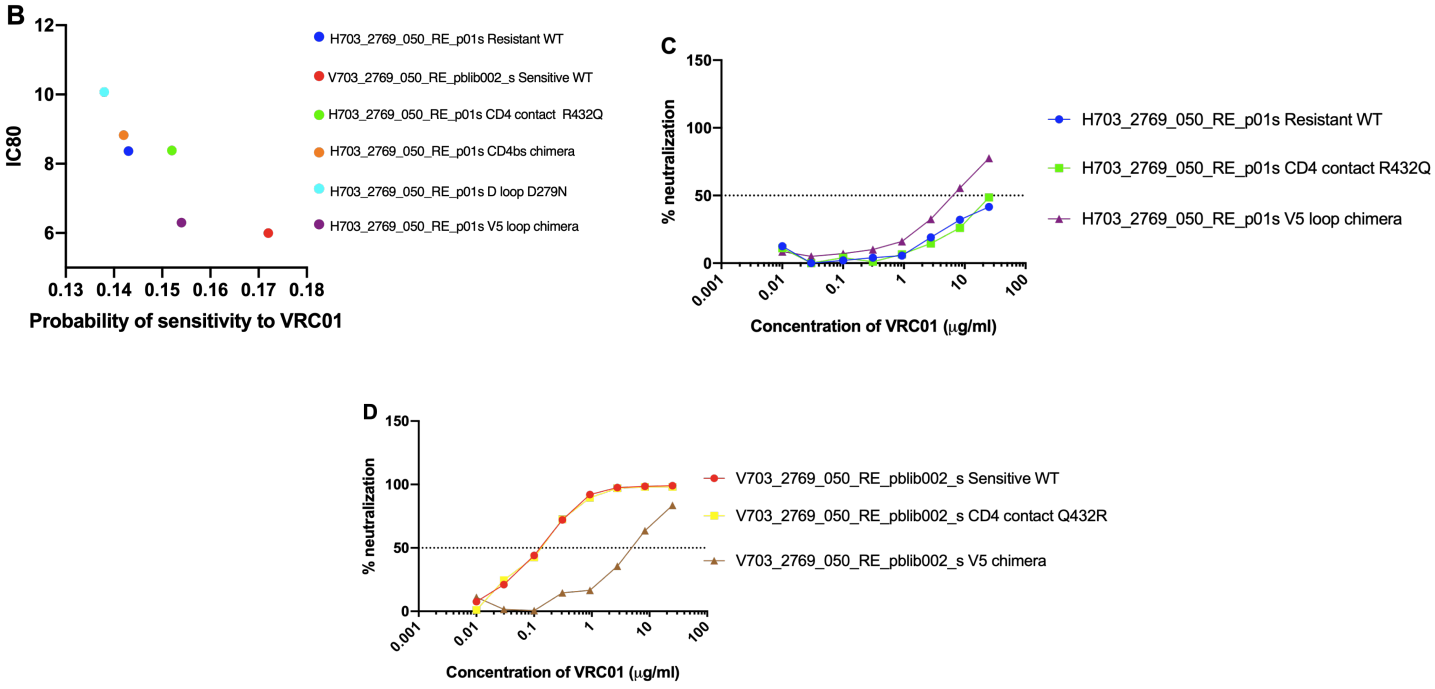

Figure 3.2.3. Results for PTID 703-2769. (A) Sequence alignment of Envs cloned from PTID 2769. Resistant WT (top) and sensitive WT (below). Regions of interest V1V2, Loop D, CD4 binding loop, CD4 contact and β23 V5 loops are underlined in black. Black dots in the sensitive sequence

represent an amino acid match to the resistant sequence. Dashes show a deletion in the sequence. Amino acids highlighted in grey represent mutation sites in regions responsible for conferring resistance to VRC01. The vertical grey line represents the end of gp120 and the start of gp41. (B) Correlation plots representing the machine learning-based predicted IC80 vs the predicted probability of sensitivity to VRC01 for the WTs and mutants in each set. The resistant WT is represented in blue, the sensitive WT is represented in red and the mutants are represented in the remaining colours. (C) Neutralization curves of the resistant WT and mutant viruses representing the concentration of VRC01 needed to neutralize 50% of the virus. (D) Neutralization curve of the sensitive WT and mutant viruses to confirm the effect of the mutations against VRC01.

PTID 703-0510

In participant PTID 703-0510 the CD4 binding loop of the resistant virus contained two mutations away from both the sensitive viruses. This common observation suggested that L369P and V371I, either alone or in combination, confer resistance to VRC01 (Figure 3.2.4A). Although V703_0510_pblib002 contained many mutations within the V1V2 region away from both the resistant virus and V703_0510_pblib001, the two sensitive viruses had similar IC80s of 17.58 µg/ml and 14.02 µg/ml, which suggest that the mutations in the V1V2 region do not play a part in conferring resistance to VRC01.

Machine learning predictions of mutations in the CD4 binding loop of PTID 703-0510 resistant WT showed that V703_0510_pblib003 P369L would slightly confer sensitivity to VRC01 (Figure 3.2.4B). Although the single I371V and double mutant sequences have a higher predicted IC80s than the resistant WT sequence, we hypothesized that these predictions may be inconsistent with the laboratory results. As seen above, Figure 3.1 shows a significant difference in IC80s between the resistant and sensitive WTs which is not seen in these predictions. We proceeded with mutagenesis and ran neutralization assays for each mutant to determine if the predictions were correct.

The neutralization curve verified that P369L mutation caused complete sensitivity to VRC01 and I371V had no effect on the neutralization profile with IC50s of 1.89 µg/ml and >25 µg/ml respectively. The double mutant had an IC50 of 2.67 µg/ml suggesting the P369L mutation is

responsible for the shift in IC50 (Figure 3.2.4C). When the experiment was reversed and V703_0510_pblib002 was mutated to contain both L369P and V371I as single mutations and in combination, it was confirmed that the L369P mutation lead to the sensitive WT virus becoming resistant to VRC01, with an IC50 changing from 5.73 to >25 µg/ml while the V371I mutant remained sensitive (8.08 µg/ml) (Figure 3.2.4D).

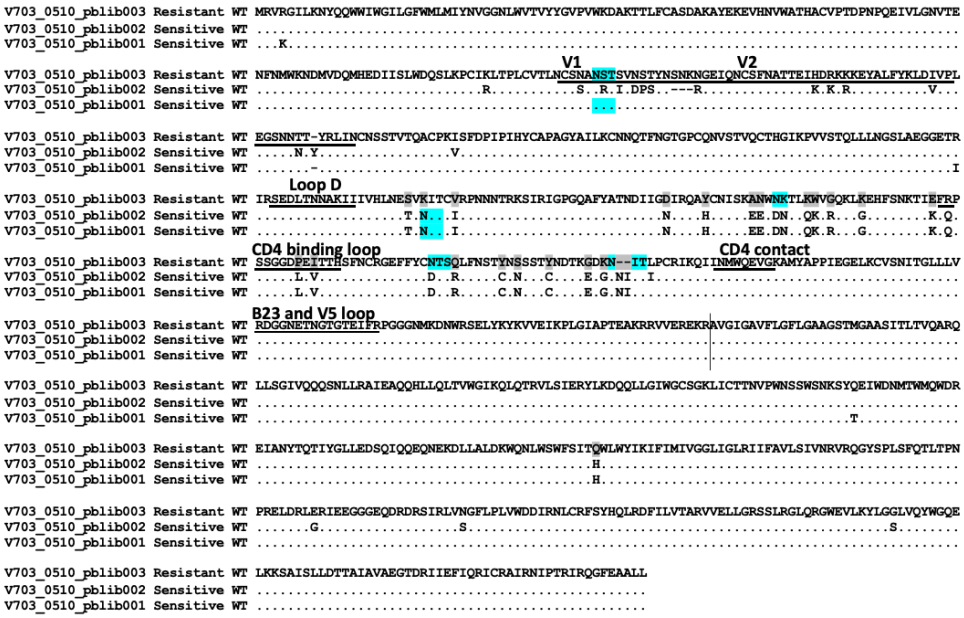

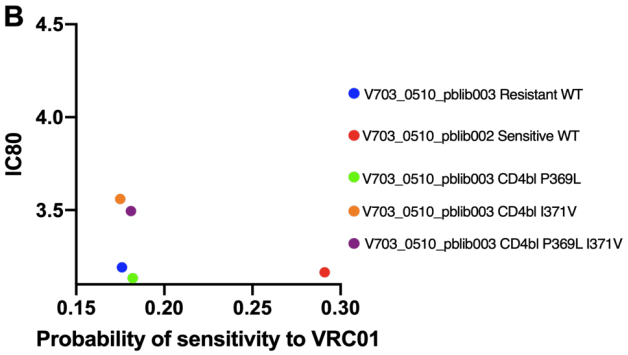

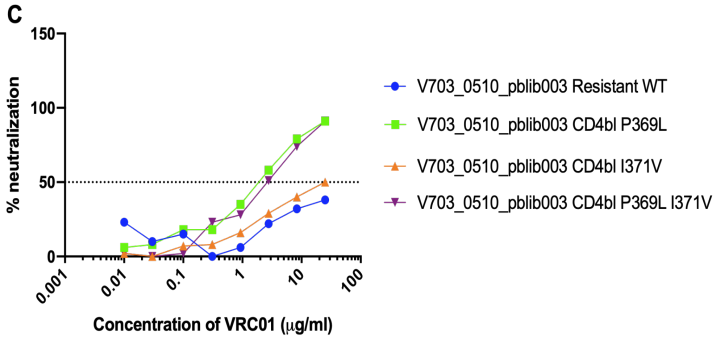

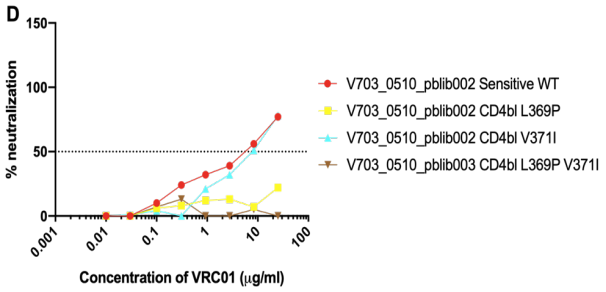

Figure 3.2.4. Results for PTID 703-0510. (A) Sequence alignment of Envs cloned from PTID 0510. Resistant WT (top) and sensitive WT (bottom 2). Regions of interest V1V2, Loop D, CD4 binding loop, CD4 contact and β23 V5 loops are underlined in black. Black dots in the sensitive sequence represent an amino acid match to the resistant sequence. Dashes show a deletion in the sequence. Amino acids highlighted in grey represent mutation sites unique to resistant virus and amino acids highlighted in blue represent the PNGS that differ between viruses. The vertical grey line represents the end of gp120 and the start of gp41. (B) Correlation plots representing the machine learning-based predicted IC80 vs the predicted probability of sensitivity to VRC01 for the WTs and mutants in each set. The resistant WT is represented in blue, the sensitive WT is represented in red and the mutants are represented in the remaining colours. (C) Neutralization curves of the resistant WT and mutant viruses representing the concentration of VRC01 needed to neutralize 50% of the virus. (D) Neutralization curve of the sensitive WT and mutant viruses to confirm the effect of the mutations against VRC01.

PTID 703-1586

We next looked at the sequences of PTID 703-1586, where the IC80s of the resistant and sensitive viruses were >100 μg/ml and 34.03 μg/ml, respectively. We identified several discrepancies across the gp160 which distinguished the resistant and sensitive clones (Figure 3.2.5). These included six differences between the sequences and a four amino acid insertion in the sensitive clone's sequence between the CD4 binding loop and CD4 contact of the gp120 as well as another eight mutations in the gp41. However we focused on the single mutation at position 279 which is in loop D of the CD4 binding site.

When analyzing the predictions, the WT sensitive sequence was seen to have a lower probability of sensitivity to VRC01 and higher IC80 than the WT resistant sequence (Figure 3.2.5B), although it was shown that this was not the case when the clones were initially tested for sensitivity against VRC01, IC80s shown in figure 3.1 above. However, V703_1586_sga3E8 N279D has a lower predicted IC80 and higher predicted probability of sensitivity to VRC01 than what was predicted to be the sensitive sequence (Figure 3.2.5B). We therefore wanted to confirm that D279N was responsible for the difference in the neutralization profile of the resistant and sensitive viruses. The results show that V703_1586_sga3E8 N279D became sensitive to VRC01 (IC50 from >25 to 13.4 μg/ml) and therefore the 279N amino acid is responsible for resistance to VRC01 (Figure 3.2.5C). This was confirmed by mutating V703_1586_pblib002 sensitive sequence to contain a D279N which conferred resistance to VRC01 (IC50 from 11.8 to >25 μg/ml) (Figure 3.2.5D).

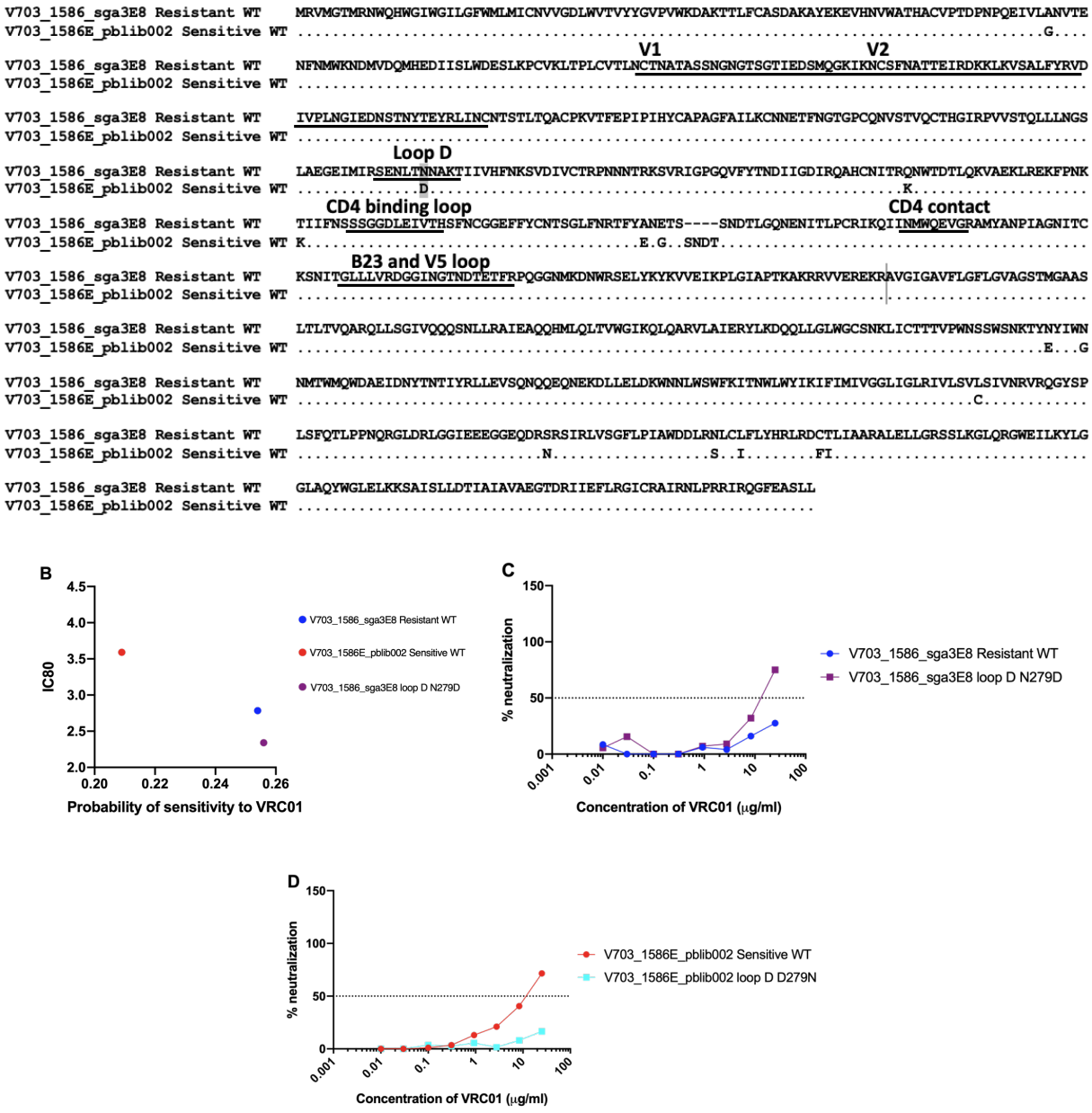

Figure 3.2.5. Results for PTID 703-1586. (A) Sequence alignment of Envs cloned from PTID 1586. Resistant WT (top) and sensitive WT (below). Regions of interest V1V2, Loop D, CD4 binding loop, CD4 contact and β23 V5 loops are underlined in black. Black dots in the sensitive sequence represent an amino acid match to the resistant sequence. Dashes show a deletion in the sequence. Amino acids highlighted in grey represent the mutation site of interest in regions responsible for conferring resistance to VRC01. The vertical grey line represents the end of gp120 and the start of gp41. (B) Correlation plots representing the machine learning-based predicted IC80 vs the predicted probability of sensitivity to VRC01 for the WTs and mutants in each set. The resistant WT is represented in blue, the sensitive WT is represented in red and the mutants are represented in the remaining colours.(C) Neutralization curves of the resistant WT and mutant viruses representing the concentration of VRC01 needed to neutralize 50% of the virus. (D)

Neutralization curve of the sensitive WT and mutant viruses to confirm the effect of the mutations against VRC01.

PTID 703-2805

The V1V2 region of PTID 703-2805 sensitive virus is significantly shorter than the resistant virus as two large stretches were deleted, a single A281T was seen in loop D, five amino acids did not match in the CD4 binding loop, the sensitive virus contained a Lysine (K) whereas the resistant virus contained an arginine (R) at position 432, and finally, the β23 and V5 loop had the highest amount of variation in any of the regions focused on (Figure 3.2.6A). A contrast in the positions and numbers of the PNGS in the V1V2 region and the β23 and V5 loop were also noted. PTID 703-2805 had differences between the resistant and sensitive WT sequences in all CD4 binding site regions and therefore five resistant sequences with all mutations/chimeras were constructed. The two V703_2805_080_pblib002_s sequences that contained the V1V2 and V5 chimeras of the WT sensitive clones, respectively, were predicted to become more sensitive to VRC01 than the resistant WT while the other mutants that remained resistant had very similar IC80s and probability of sensitivity as the resistant WT sequence (Figure 3.2.6B).

Once the resistant plasmids were mutated to contain the sensitive chimeras, we sequenced them to confirm the incorporation of the respective chimeras and proceeded to grow them as pseudoviruses in order to do the laboratory tests. Unfortunately, the β23 and V5 loop chimera mutant did not grow as a pseudovirus in this case, despite several transfections, likely a consequence of structural incompatibility in these regions.

The V703_2805_080_pblib002_s mutant containing the V1V2 chimera from the sensitive virus became more sensitive to VRC01 with an IC50 of 3.9 µg/ml whereas the WT remained resistant with an IC50 0f >25 µg/ml (Figure 3.2.6C). When reversed, the resistant chimera in the WT sensitive backbone did not have an effect on the neutralization profile and the WT and mutant had IC50s of 0.64 and 0.39 µg/ml, respectively (Figure 3.2.6D).

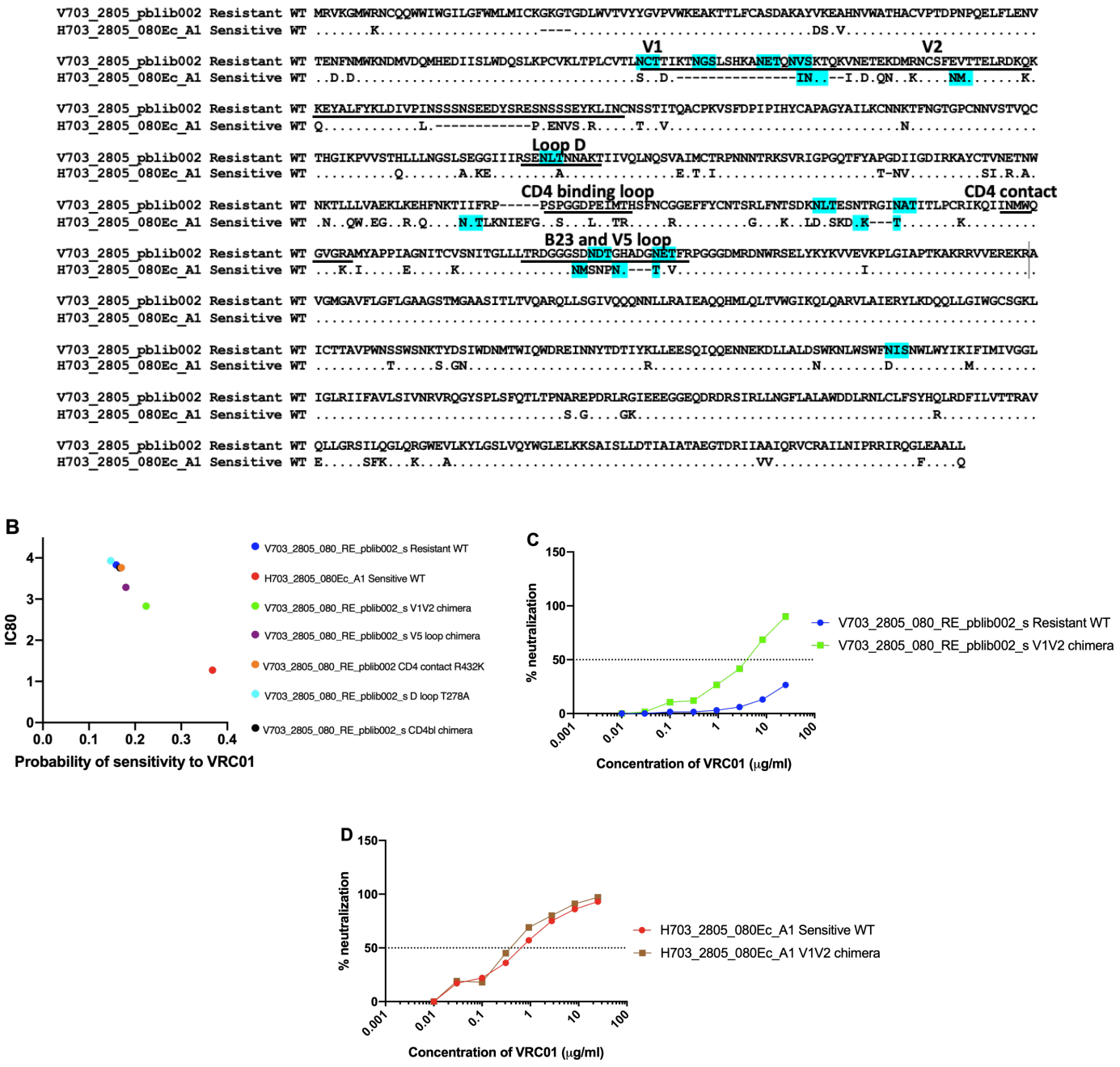

Figure 3.2.6. Results for PTID 703-2805. (A) Sequence alignment of Envs cloned from PTID 2805. Resistant WT (top) and sensitive WT (below). Regions of interest V1V2, Loop D, CD4 binding loop, CD4 contact and β23 V5 loops are underlined in black. Black dots in the sensitive sequence represent an amino acid match to the resistant sequence. Dashes show a deletion in the sequence. Amino acids highlighted in blue represent PNGS that differ between sensitive and resistant viruses. The vertical grey line represents the end of gp120 and the start of gp41. (B) Correlation plots representing the machine learning-based predicted IC80 vs the predicted probability of sensitivity to VRC01 for the WTs and mutants in each set. The resistant WT is represented in blue, the sensitive WT is represented in red and the mutants are represented in

the remaining colours. (C) Neutralization curves of the resistant WT and mutant viruses representing the concentration of VRC01 needed to neutralize 50% of the virus. (D) Neutralization curve of the sensitive WT and mutant viruses to confirm the effect of the mutations against VRC01.

PTID 703-0154

Lastly, the three resistant sequences from PTID 703-0514, all with an IC80 of >100 μg/ml, were compared and then compared to the single sensitive sequence. H703_0514_F4_V03 contains many unique amino acids compared to the other two resistant viruses, whereas only one difference between the second and third resistant viruses is seen. The PNGS pattern remains the same for all three resistant viruses despite the first sequence being slightly different. Interestingly, the CD4 binding loop, CD4 contact and β23 and V5 loop remain constant between all three resistant viruses. The V1V2 region of the sensitive virus is both marginally different and shorter than the resistant virus, two mutations were seen in loop D at positions 279 and 281, four differences seen in the CD4 binding loop, a single E429G mutation in the CD4 contact and finally, a stretch of seven amino acids containing six differences between the resistant and sensitive β23 and V5 loop as well as a differential PNGS position was seen (Figure 3.2.7A).

There were no sequences from the set of PTID 703-0514 that predicted any movement on the graph towards the sensitive WT sequence (Figure 3.2.7B). The change in predicted IC80 and probability of sensitivity to VRC01 from the resistant WT sequence to the sensitive WT sequence was not significant and four mutants remained around the point of the resistant WT sequence. H703_0514_150s_F4_V03_024 that contained the V1V2 chimera of the sensitive WT sequence and the mutant that contained the mutation in loop D had higher predicted IC80s as well as lower probabilities of sensitivity to VRC01 than the resistant WT sequence as well as the other mutants, deeming them more resistant to VRC01 with the changes made.

Both the H703_0514_150s_F4_V03_024 that contained the CD4 binding loop chimera and the β23 and V5 loop chimera of the sensitive WT did not grow as pseudoviruses, leaving only the T281S and G429E mutants being tested against VRC01 (Figure 3.2.7C). The mutants remained

completely resistant to VRC01 together with the resistant WT, all having an IC50 of >25 µg/ml. The same pattern was seen when the experiment was reversed and the sensitive WT containing the S281T and E429G mutations remained sensitive to VRC01 with IC50s between 0.02 and 0.04 µg/ml (Figure 3.2.7D). These results match the predictions where each mutant had similar predictions to the resistant WT virus.

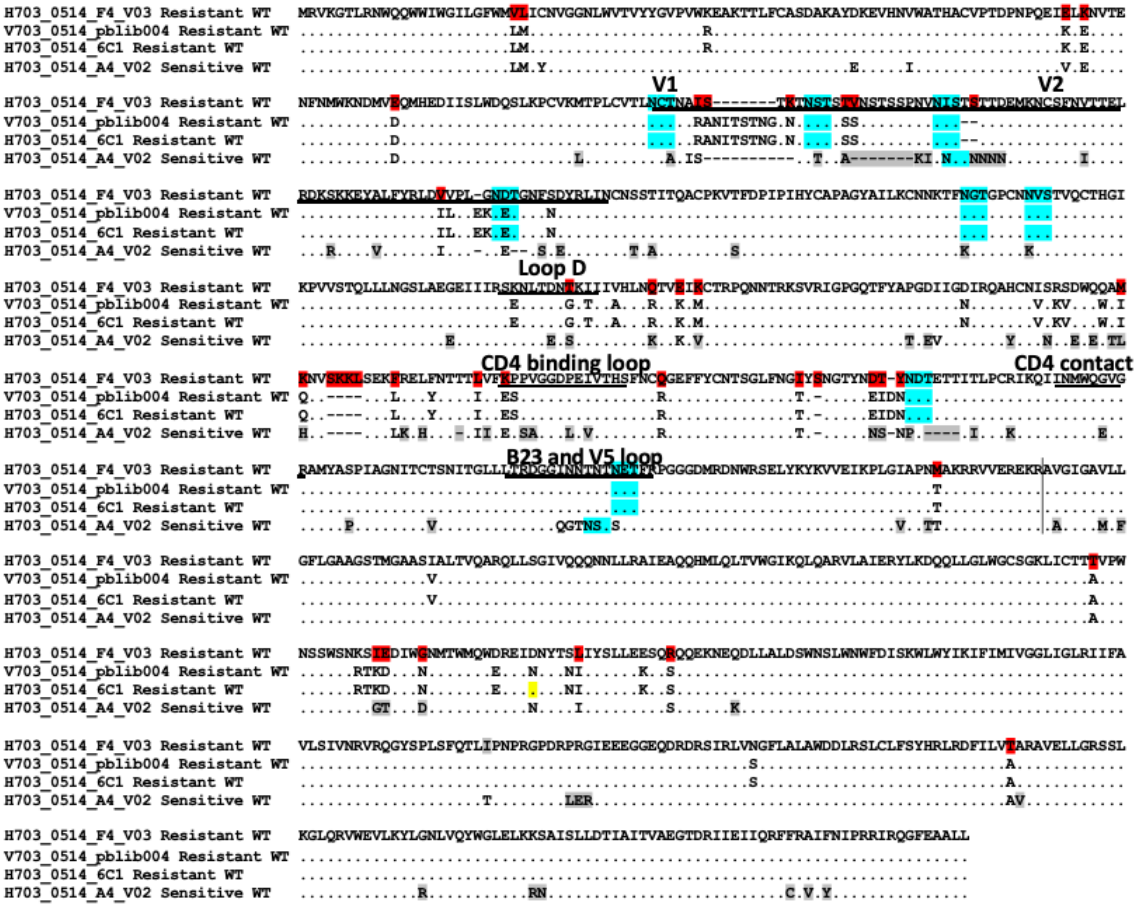

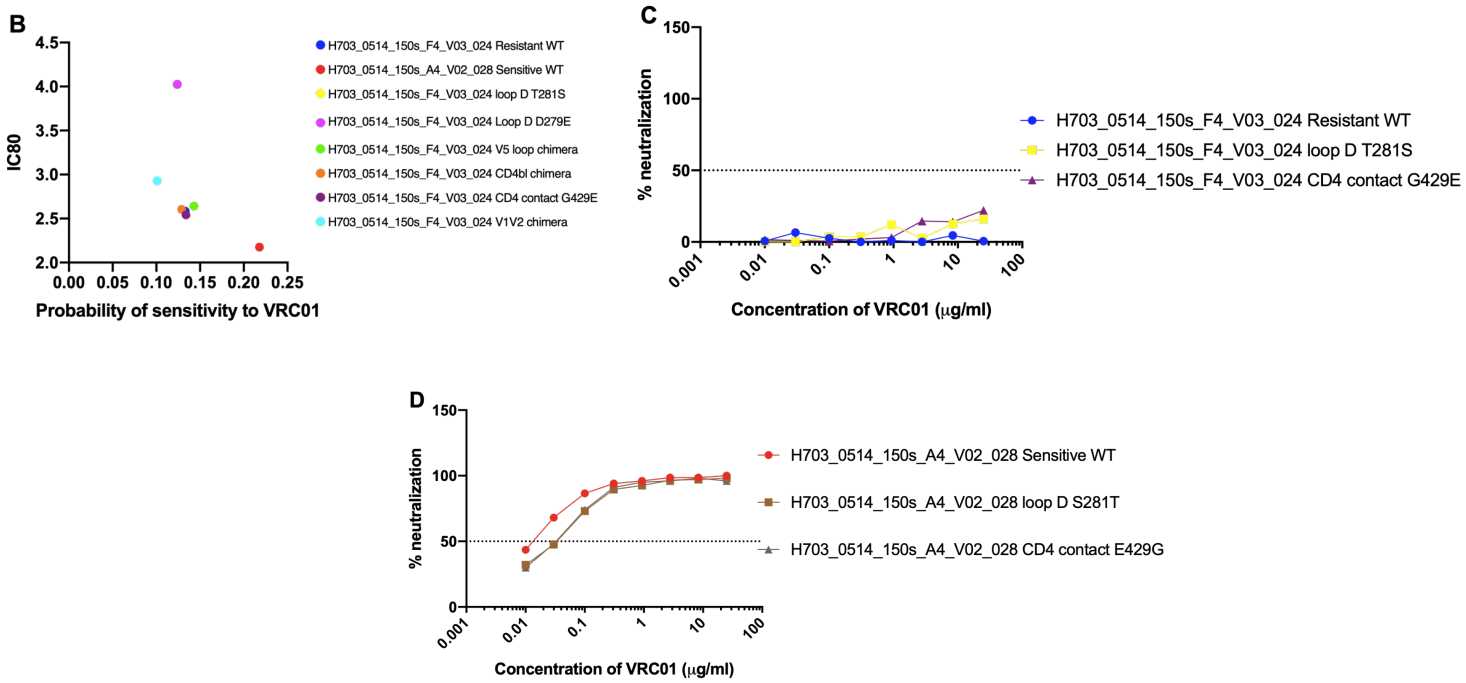

Figure 3.2.7. Results for PTID 703-0514. (A) Sequence alignment of Envs cloned from PTID 0514. Resistant WT (top 3) and sensitive WT (bottom). Regions of interest V1V2, Loop D, CD4 binding loop, CD4 contact and β23 V5 loops are underlined in black. Black dots in the sensitive sequence represent an amino acid match to the resistant sequence. Dashes show a deletion in the sequence. Amino acids highlighted in grey represent mutations unique to sensitive viruses; amino acids highlighted in red represent mutations unique to top resistant virus; amino acids highlighted in yellow represent single difference between the 2nd and 3rd virus; and amino acids highlighted in blue represent PNGS that differ between sensitive and resistant viruses. The vertical grey line represents the end of gp120 and the start of gp41. (B) Correlation plots representing the machine learning-based predicted IC80 vs the predicted probability of sensitivity to VRC01 for the WTs and mutants in each set. The resistant WT is represented in blue, the sensitive WT is represented in red and the mutants are represented in the remaining colours. (C) Neutralization curves of the resistant WT and mutant viruses representing the concentration of VRC01 needed to neutralize 50% of the virus. (D) Neutralization curve of the sensitive WT and mutant viruses to confirm the effect of the mutations against VRC01.

The important findings show that the experimental IC50 results for the WT clones were concordant with the initial IC80 neutralization profiles. Experimentally, we were able to identify five important mutations that conferred sensitivity to WT resistant viruses, while only three were confirmed by reversing the experiment and caused resistance in WT sensitive viruses (Appendix C).

3.2. Assessing the overall neutralization phenotype of mutated viruses

When performing SDM and transferring chimeras into an Env plasmid, there is a risk that they could become structurally compromised and alter their global phenotypes. To confirm that mutated viruses retain their native neutralization phenotype, we tested each virus against three control mAbs. A V1V2 directed antibody, PG9, a V3-glycan directed antibody, PGT121 and a MPER directed antibody, 10E8, were used to determine whether the mutations made in the WT viruses conferred a global structural change in the viruses (Figure 3.3).

In five of the six cases, namely PTID 703-1714, PTID 703-2769, PTID 703-0510, PTID 703-1586, PTID 703-0514, when mutations were made in Loop D, the CD4 binding loop and β23-V5 loop, these Envs had almost identical neutralization phenotypes to their respective WT resistant viruses, with very low IC50 fold differences between the resistant WTs and the mutants (Figure 3.3.1 and Figure 3.3.2 A-Q and U-X). The phenotype discrepancies between the sensitive and resistant WTs are due to mutations seen between the sequences in regions that the respective mAbs bind, but had no effect on the overall structure and function of the viruses (Figure 3.3.1). This was seen in PTID 703-1714 and PTID 703-2769 where the WT sensitive viruses were completely resistant to PGT121 but the resistant WT and mutants were sensitive to PGT121 (Figure 3.3.2A and F). H703_0514_A4_V02 sensitive WT was significantly more sensitive to both PGT121 and PG9 than the resistant WT and mutants (Figure 3.3.2U-X).

When analyzing PTID 703-2805, a difference was seen in the neutralization patterns between the resistant WT and the mutant that contained the V1V2 region of the sensitive WT (Figure 3.3.1 and Figure 3.3.2S and T). It is possible that the transfer of the V1V2 region gave the mutant a similar phenotype to the WT sensitive virus. As both the sensitive and resistant WTs are resistant to PGT121 and the mutant containing the chimera becomes sensitive, it shows the transfer of the V1V2 region may have altered the structure of the virus, leading it to have an IC50 of <0.01 µg/ml (Figure 3.3.1). These results show that the mutant pseudoviruses were not altered and the results represent the specific neutralization profiles of VRC01 and other CD4 binding site mAbs.

	IC50		
	10E8	PG9	PGT121
H703_1714_080s Sensitive WT	0.39	2.36	>25
V703_1714_pblib002 Resistant WT	0.37	0.67	0.39
V703_1714_pblib002 D459G	0.37	1.47	0.44
V703_1714_pblib002 E462D	0.37	2.31	0.34
V703_1714_pblib002 D459G E462D	0.77	4.6	0.87
H703_1714_080s G459D	0.18	2.56	>25
H703_1714_080s D462E	0.43	4.53	>25
H703_1714_080s G459D D462E	0.28	1.63	>25
V703_2769_050_RE_pblib002 Sensitive WT	3.09	<0.01	>25
H703_2769_050_RE_p01s Resistant WT	0.86	0.8	5.8
H703_2769_050_RE_p01s R432Q	0.19	0.68	7.79
H703_2769_050_RE_p01s V5 chimera	1.04	0.7	10.58
V703_2769_050_RE_pblib002 Q432R	1.03	<0.01	5.26
V703_2769_050_RE_pblib002 V5 chimera	2.75	<0.01	>25
V703_0510_pblib002 Sensitive WT	0.03	<0.01	<0.01
V703_0510_pblib003 Resistant WT	0.02	<0.01	<0.01
V703_0510_pblib003 P369L	0.03	<0.01	<0.01
V703_0510_pblib003 I371V	0.08	0.02	<0.01
V703_0510_pblib003 P369L I371V	0.24	<0.01	<0.01
V703_0510_pblib002 L369P	0.03	<0.01	<0.01
V703_0510_pblib002 V371I	0.04	<0.01	<0.01
V703_0510_pblib002 L369P V371I	0.03	<0.01	<0.01
V703_1586_pblib002 Sensitive WT	6.88	0.09	4.57
V703_1586_sga3E8 Resistant WT	5.61	0.05	7.78
V703_1586_sga3E8 N279D	7.26	0.35	15
V703_1586_pblib002 D279N	8.84	0.07	7.6
H703_2805_080Ec_A1 Sensitive WT	1.45	0.12	>25
V703_2805_080_pblib002 Resistant WT	8.93	>25	>25
V703_2805_080_pblib002 V1V2 chimera	0.03	0.34	<0.01
H703_2805_080Ec_A1 V1V2 chimera	1.17	0.01	10.77
H703_0514_150s_A4_V02_028 Sensitive WT	2.28	<0.01	<0.01
H703_0514_150s_F4_V03_024 Resistant WT	10.14	1.99	0.1
H703_0514_150s_F4_V03_024 T281S	8.28	1.61	0.09
H703_0514_150s_F4_V03_024 G429E	8.81	1.53	0.11
H703_0514_150s_A4_V02_028 S281T	2.34	<0.01	<0.01
H703_0514_150s_A4_V02_028 E429G	1.65	<0.01	<0.01

Figure 3.3.1. Overall neutralization phenotypes of mutated viruses. PTID 703-1714, PTID 703-2769, PTID 703-0510, PTID 703-1586, PTID 703-2805 and PTID 703-0514 sensitive and resistant WTs, and their respective mutants against mAbs, 10E8, PG9 and PGT121, showing the concentration of antibody needed to neutralize 50% of the virus. IC50 profiles in blue represent the viruses most resistant to antibodies (>25 µg/ml), orange (IC50 1-24 µg/ml), and red (<0.1-0.9 µg/ml).

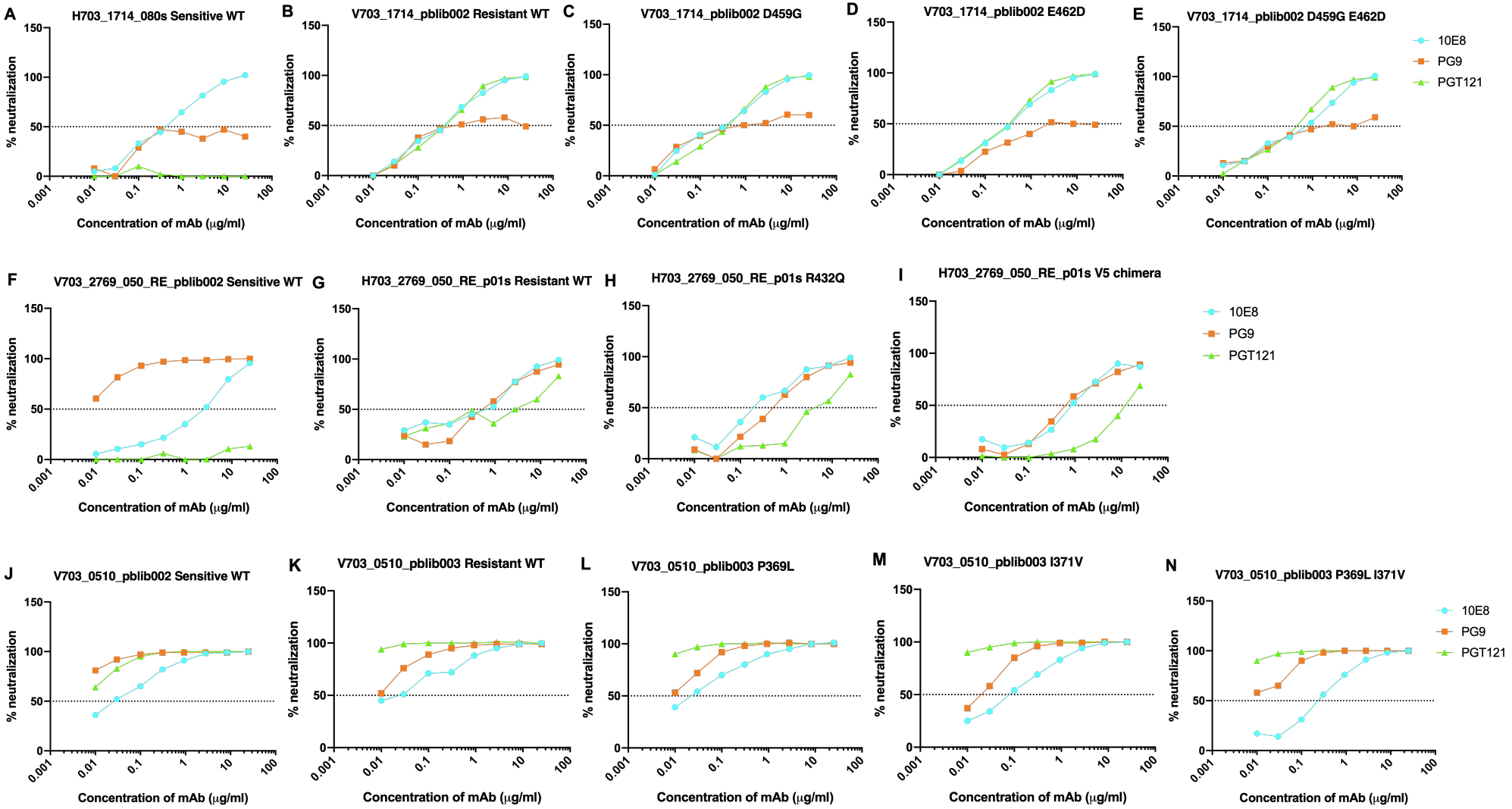
A
H703_1714_080s Sensitive WT
B
V703_1714_pblib002 Resistant WT
C
V703_1714_pblib002 D459G
D
V703_1714_pblib002 E462D
E
V703_1714_pblib002 D459G E462D
F
V703_2769_050_RE_pblib002 Sensitive WT
G
H703_2769_050_RE_p01s Resistant WT
H
H703_2769_050_RE_p01s R432Q
I
H703_2769_050_RE_p01s V5 chimera
J
V703_0510_pblib002 Sensitive WT
K
V703_0510_pblib003 Resistant WT
L
V703_0510_pblib003 P369L
M
V703_0510_pblib003 I371V
N
V703_0510_pblib003 P369L I371V
% neutralization
Concentration of mAb (μg/ml)
10E8
PG9
PGT121

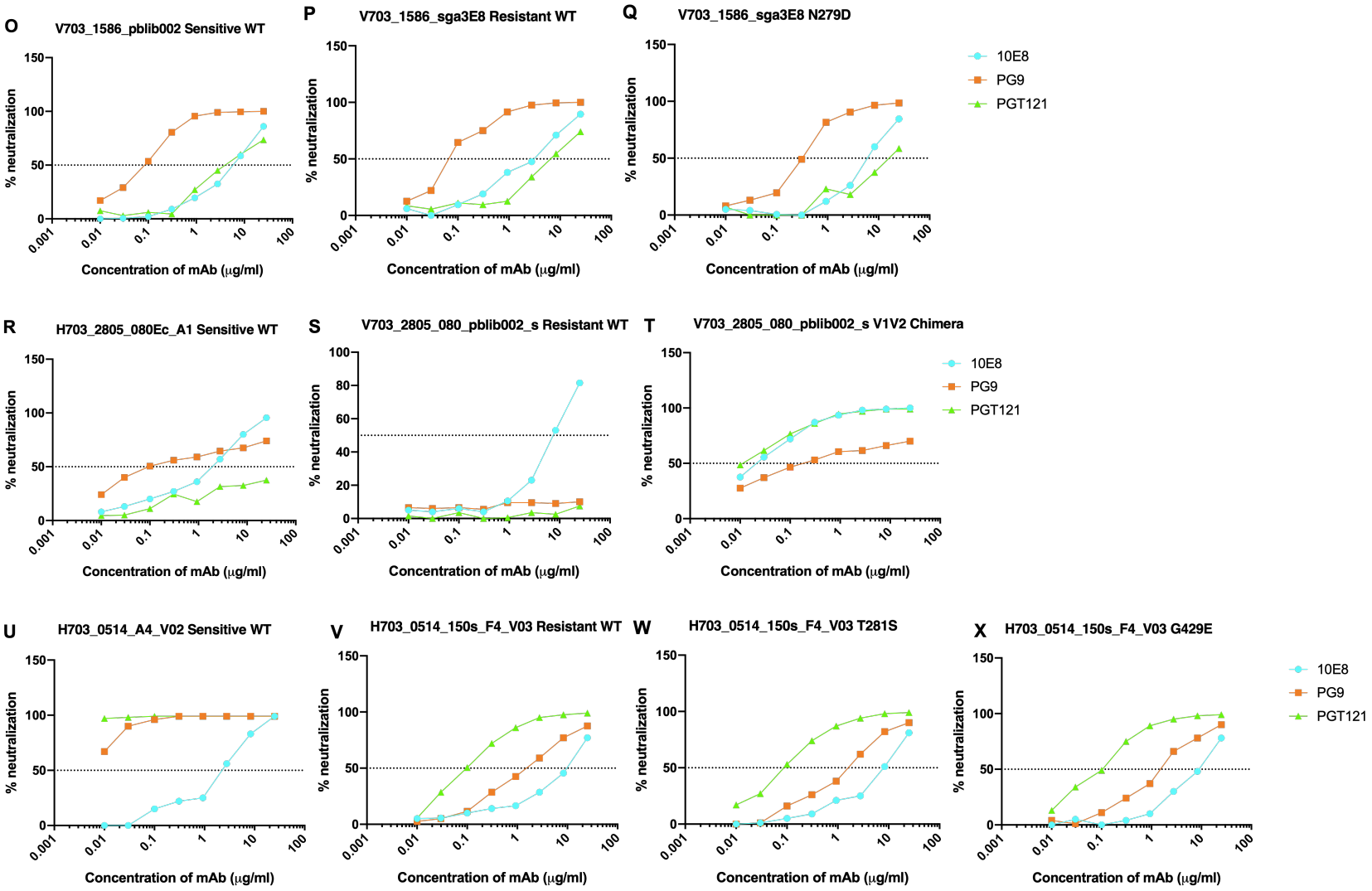

Figure 3.3.2. Overall neutralization curves of mutated viruses. Neutralization curves of (A-E) PTID 703-1714, (F-I) PTID 703-2769, (J-N) PTID 703-0510, (O-Q) PTID 703-1586, (R-T) PTID 703-2805 and (U-X) PTID 703-0514 sensitive and resistant WTs, and their respective mutants against mAbs showing the concentration of antibody needed to neutralize 50% of the virus. 10E8 in cyan, PG9 in orange and PGT121 in green.

3.3. Assessing the neutralization phenotype of mutants against other CD4 binding site mAbs

A key question is whether VRC01 resistance conferred cross resistance to other more broad and potent next generation CD4 binding site mAbs which can be used for current and future passive immunization trials, such as VRC01-class N6, 3BNC117, VRC07 and non-VRC01-class HJ16 and 1-18. We therefore assayed each set of clones against the full set of mABs.

For PTID 703-1714, the overall neutralization patterns did not differ between the sensitive WT, resistant WT and the mutants for each mAb. Although position 459 is a contact site for VRC07-523 LS, neither aspartic acid or glutamic acid had an effect on the sensitivity against VRC07-523 LS. All viruses in the set were sensitive to N6, VRC07-523 LS and 1-18 and resistant to 3BNC117 and HJ16, with IC50s of >25 μg/ml (Figure 3.4.1 and Figure 3.4.1A-E).

PTID 703-2769's viruses were overall sensitive to N6, VRC07-523 LS and 1-18 (Figure 3.4.1 and Figure 3.4.2F-I). Interestingly, HJ16 and 3BNC117 followed the same neutralization pattern as VRC01, where they were both sensitive to the VRC01 sensitive WT and the VRC01 resistant mutant containing the sensitive V5 chimera, and resistant to the VRC01 resistant viruses (Figure 3.4.1 and Figure 3.4.2F-I). Both 3BNC117 and HJ16 have contact sites within the β23 and V5 loop regions. We were unable to distinguish whether a single mutation or the entire chimera caused the change in sensitivity.

Both VRC07-523 LS and 1-18 were able to neutralize the set of PTID 703-0510's WT and mutant viruses (Figure 3.4.1 and Figure 3.4.2J-N). Although the viruses are sensitive to N6, the VRC01 resistant viruses (VRC01 resistant WT and V703_0510_pblib003 I371V) have an IC50 of >1 μg/ml whereas the VRC01 sensitive viruses have IC50s of ~1 μg/ml, therefore suggesting that mutations in the CD4 binding loop affect recognition by N6 (Figure 3.4.1 and Figure 3.4.2J-N). All viruses in this set are resistant to 3BNC117 and HJ16 as position 369 are not contact sites for either antibody and therefore mutations at this position would not confer a change in sensitivity.

Due to the VRC01 resistant and sensitive WTs, of PTID 703-1586, not having any major differences between the two sequences, especially in the regions of interest, the same neutralization

patterns for each virus and antibody are seen (Figure 3.4.1 and Figure 3.4.2O-Q). Although position 279 is a contact site for most of the antibodies tested, the mutation N279D did not alter the sensitivity to the viruses. It is possible that other amino acid mutations, alone or in combination with 279, in loop D play a part in the neutralization activity of the antibodies.
The VRC01 sensitive WT virus of PTID 703-2805 is highly sensitive to antibodies N6, 3BNC117, VRC07-523 LS and 1-18 and resistant to HJ16 (Figure 3.4.1 and Figure 3.4.2R). The VRC01 resistant WT is also sensitive to N6, 3BNC117 and VRC07-523 LS, although less so, with IC50s of >1 μg/ml (Figure 3.4.1 and Figure 3.4.2S). The virus containing the V1V2 region of the VRC01 WT virus was sensitive to N6, VRC07-523 LS and 1-18 (Figure 3.4.1 and Figure 3.4.2T). Following the neutralization pattern of 1-18, it matches the VRC01 pattern where the VRC01 sensitive viruses are sensitive to 1-18 and the VRC01 resistant WT is resistant to 1-18. As mentioned above, the insertion of the chimera may have altered the structure of the virus and this could explain why 3BNC117 becomes resistant to the mutant but is seen to be sensitive to the VRC01 sensitive and resistant WTs.

Finally, PTID 703-0514's viruses were the only viruses seen to be sensitive to HJ16, all with similar IC50s of 0.15 μg/ml (Figure 3.4.1 and Figure 3.4.2U-X). HJ16 contact sites are mainly seen in loop D and around the β23 and V5 loop regions. Antibody 3BNC117 was sensitive to the VRC01 sensitive WT virus and resistant to the VRC01 resistant WT and mutants, suggesting that the mutations had no effect on the neutralization by this antibody, as well as VRC01 (Figure 3.4.1). The remaining viruses were sensitive to antibodies, N6, VRC07-523 LS and 1-18 (Figure 3.4.1).

When analyzing the overall neutralization patterns of each of the CD4 binding site mAbs above, we see that VRC01 resistant variants retain sensitivity to CD4 binding site mAbs, N6, VRC07-523 LS and 1-18 (Figure 3.4.1). The viruses that were resistant to VRC01, with IC80s of >25 μg/ml, retained their sensitivity to N6, VRC07-523 LS and 1-18 with IC50s of <0.1 and 2.97 μg/ml with a standout of 10.08 μg/ml for V703_0510_pblib003 I371V mutant and V703_2805_080_pblib002 resistant WT with IC50 of >25 μg/ml (Figure 3.4.1).

	IC50					
	VRC01	N6	3BNC117	VRC07-523 LS	HJ16	1-18
H703_1714_080s Sensitive WT	0.32	0.03	>25	0.04	>25	0.06
V703_1714_pblib002 Resistant WT	>25	0.02	>25	0.25	>25	0.03
V703_1714_pblib002 D459G	1.89	0.09	>25	0.02	>25	0.07
V703_1714_pblib002 E462D	>25	0.07	>25	0.1	>25	0.07
V703_1714 Resistant D459G E462D	1	0.1	>25	0.06	>25	0.12
H703_1714_080s G459D	>25	0.1	>25	0.06	>25	0.04
H703_1714_080s D462E	0.38	0.6	>25	0.03	>25	0.8
H703_1714_080s G459D D462E	>25	0.02	>25	0.03	>25	0.05
V703_2769_050_RE_pblib002 Sensitive WT	0.14	0.04	0.02	0.01	0.01	0.03
H703_2769_050_RE_p01s Resistant WT	>25	0.49	>25	0.22	>25	0.39
H703_2769_050_RE_p01s R432Q	>25	0.68	>25	0.21	>25	0.5
H703_2769_050_RE_p01s V5 chimera	6.82	0.15	9.72	0.1	0.04	0.21
V703_2769_050_RE_pblib002 Q432R	0.15	0.4	0.03	0.02	0.02	0.07
V703_2769_050_RE_pblib002 V5 chimera	3	0.15	0.12	0.05	>25	0.2
V703_0510_pblib002 Sensitive WT	5.73	0.64	>25	0.05	>25	0.24
V703_0510_pblib003 Resistant WT	>25	2.71	>25	0.21	>25	0.46
V703_0510_pblib003 P369L	1.89	0.09	>25	0.1	>25	0.39
V703_0510_pblib003 I371V	>25	10.08	>25	0.16	>25	0.5
V703_0510_pblib003 P369L I371V	2.67	1.44	>25	0.09	>25	0.49
V703_0510_pblib002 L369P	>25	12.53	>25	0.49	>25	0.9
V703_0510_pblib002 V371I	8.08	0.21	>25	0.06	>25	0.18
V703_0510_pblib002 L369P V371I	>25	4	>25	0.89	>25	0.65
V703_1586_pblib002 Sensitive WT	11.76	0.63	>25	1.33	>25	1.11
V703_1586_sga3E8 Resistant WT	>25	0.63	>25	1.5	>25	0.83
V703_1586_sga3E8 N279D	13.4	1.66	>25	1.74	>25	1
V703_1586_pblib002 D279N	>25	2.26	>25	3.56	>25	2.23
H703_2805_080Ec_A1 Sensitive WT	0.87	<0.01	0.03	<0.01	>25	0.02
V703_2805_080_pblib002 Resistant WT	>25	2.58	6.98	2.4	>25	>25
V703_2805_080_pblib002 V1V2 chimera	3.9	0.19	>25	0.15	>25	0.73
H703_2805_080Ec_A1 V1V2 chimera	0.39	<0.01	0.24	<0.01	>25	0.02
H703_0514_150s_A4_V02_028 Sensitive WT	0.02	<0.01	0.02	<0.01	0.15	<0.01
H703_0514_150s_F4_V03_024 Resistant WT	>25	2.0	>25	2.97	0.15	1.2
H703_0514_150s_F4_V03_024 T281S	>25	2.17	>25	2.74	0.14	0.89
H703_0514_150s_F4_V03_024 G429E	>25	1.28	>25	2.36	0.1	1.03
H703_0514_150s_A4_V02_028 S281T	0.04	<0.01	0.02	<0.01	0.77	<0.01
H703_0514_150s_A4_V02_028 E429G	0.04	<0.01	0.1	<0.01	0.45	<0.01

Figure 3.4.1. Neutralization results of WT and mutant viruses against VRC01, N6, 3BNC117, VRC07-523 LS, HJ16 and 1-18. IC50 profiles in blue represent the viruses most resistant to antibodies (>25 µg/ml), orange (IC50 1-24 µg/ml), and red (<0.1-0.9 µg/ml).

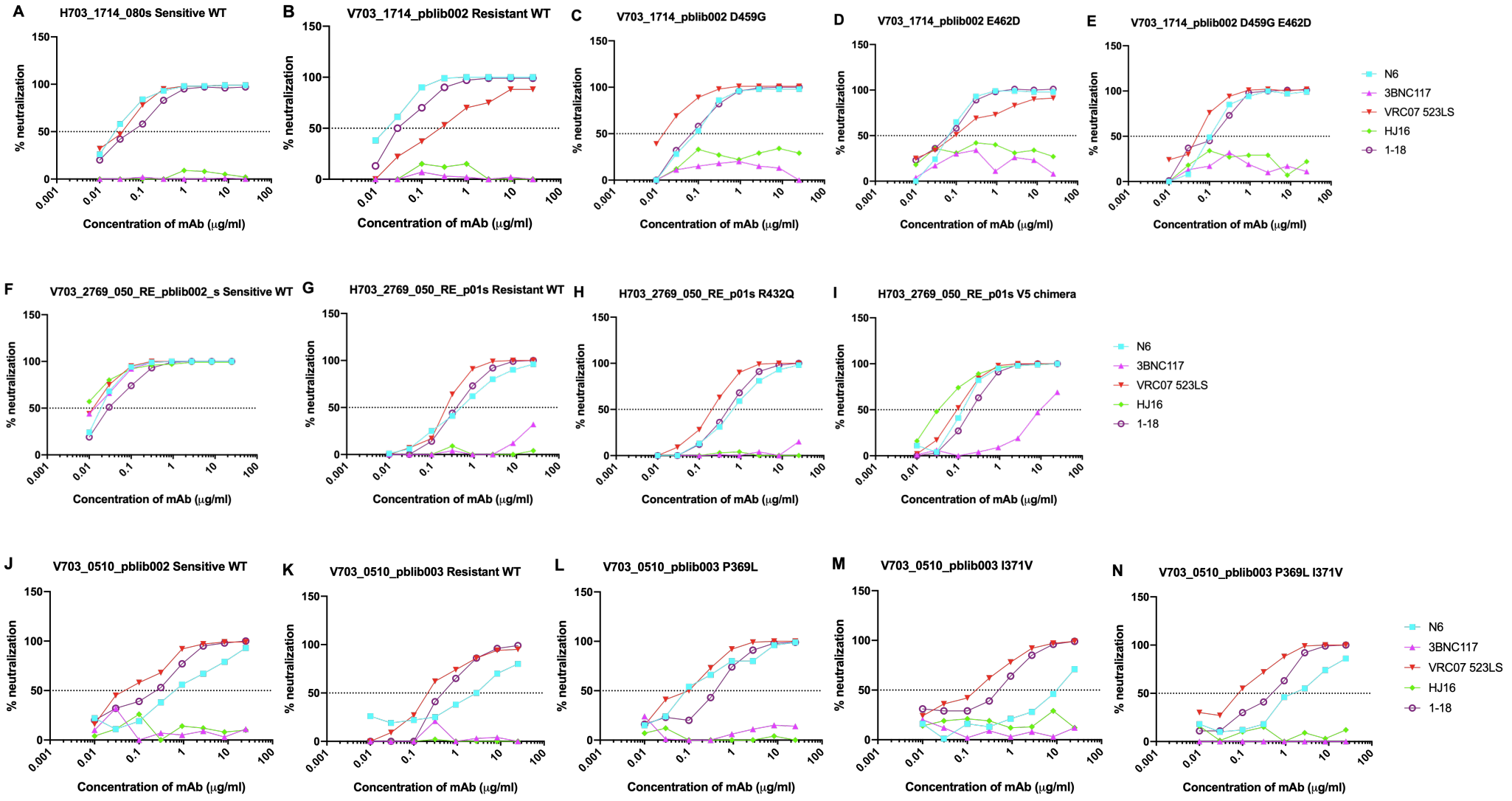
A
H703_1714_080s Sensitive WT
B
V703_1714_pblib002 Resistant WT
C
V703_1714_pblib002 D459G
D
V703_1714_pblib002 E462D
E
V703_1714_pblib002 D459G E462D
F
V703_2769_050_RE_pblib002_s Sensitive WT
G
H703_2769_050_RE_p01s Resistant WT
H
H703_2769_050_RE_p01s R432Q
I
H703_2769_050_RE_p01s V5 chimera
J
V703_0510_pblib002 Sensitive WT
K
V703_0510_pblib003 Resistant WT
L
V703_0510_pblib003 P369L
M
V703_0510_pblib003 I371V
N
V703_0510_pblib003 P369L I371V
% neutralization
Concentration of mAb (μg/ml)
N6
3BNC117
VRC07 523LS
HJ16
1-18

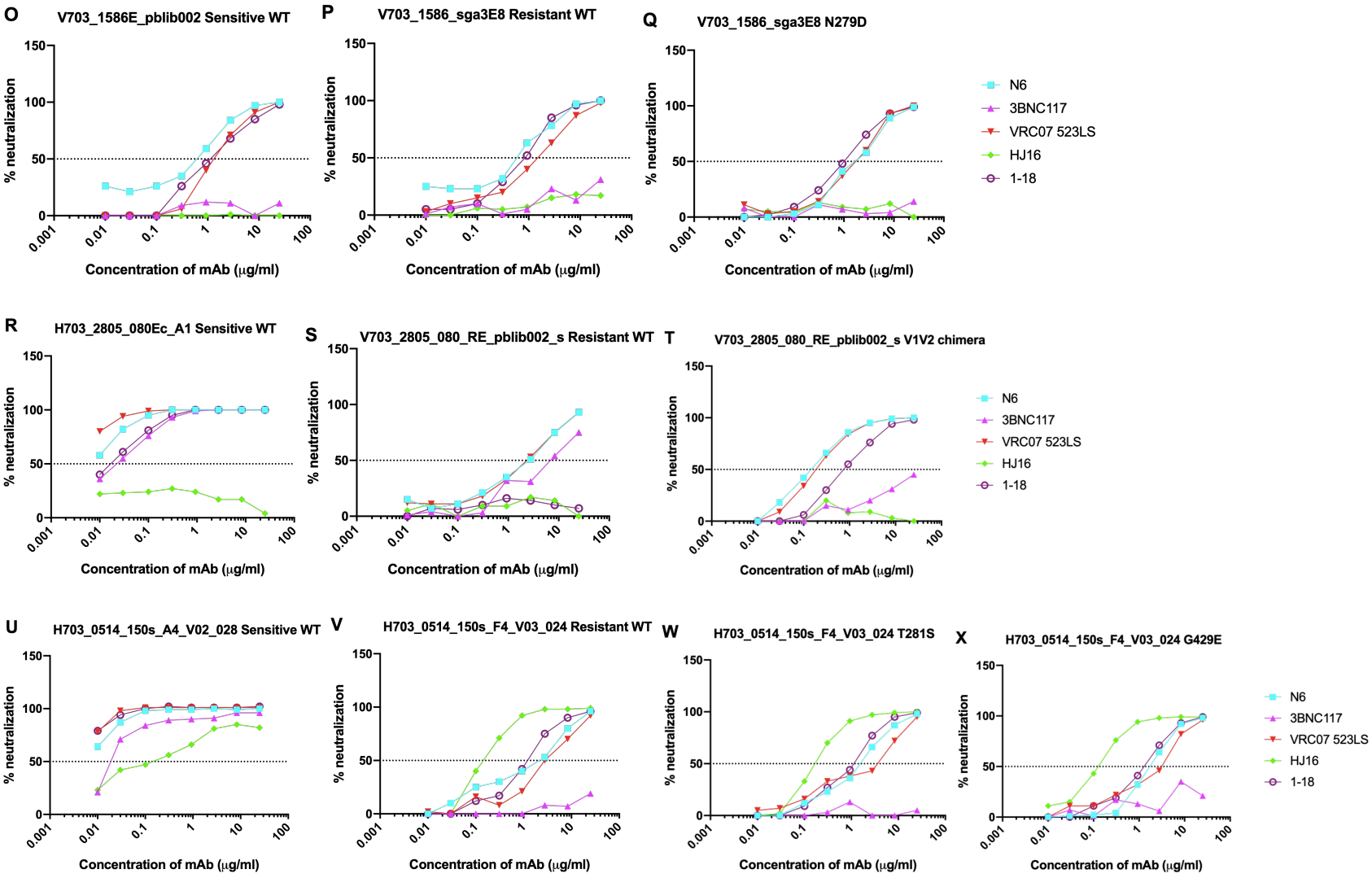

Figure 3.4.2. Neutralization curves of mutated viruses against other CD4 binding site mAbs. Neutralization curves of (A-E) PTID 703-1714, (F-I) PTID 703-2769, (J-N) PTID 703-0510, (O-Q) PTID 703-1586, (R-T) PTID 703-2805 and (U-X) PTID 703-0514 sensitive and resistant WTs, and their respective mutants against mAbs showing the concentration of antibody needed to neutralize 50% of the virus. N6 in cyan, 3BNC117 in magenta, VRC07-523 LS in red, HJ16 in green and 1-18 in purple.

4. Discussion

To date, there has been limited success in the development of a vaccine to prevent the spread of HIV-1. Since the discovery of bNAbs, the field has been able to isolate several mAbs, test how they bind to the various epitopes of the HIV-1 Env glycoprotein and understand their maturation pathways. Despite these leaps in our knowledge, vaccines to elicit bNAbs have proved to be ineffective thus far and there has been no human clinical data to support the focus on bNAbs. Therefore, the AMP trial was carried out to determine whether a passively infused, CD4 binding site bNAb, VRC01, was able to prevent HIV-1 infection. The results showed that, although no overall protection was seen, bNAb prophylaxis can be effective (Corey *et al*., 2021). Furthermore, using the AMP trial data, researchers were able to predict HIV-1 prevention threshold by quantifying the neutralization potency of antibody in the serum of an individual against an HIV-1 isolate, called the PT_{80} biomarker (Gilbert *et al*., 2022). bNAb concentrations 200-fold higher than that needed to reduce infection by 80% in vitro was estimated to be required for prevention efficacy against acquisition of the circulating viruses (Gilbert *et al*., 2022).

The AMP study also provided the field with an opportunity to assess the viral transmission bottleneck. Although older studies, which sequenced the virus at more limited depth, showed that multi-lineage infections were rare, accounting for only about 20% of infections, this dogma has been challenged by data from AMP. A high proportion of multi-lineage infections were identified, accounting for 46% in HVTN 703 and 37% in HVTN 704 (Unpublished data, Williamson, Mullins *et al*). Multi-lineage viruses obviously differed genotypically, but when cloned out and the viruses tested against VRC01, we also identified seven cases where these viruses also differed phenotypically within donors, with differential sensitivity profiles to VRC01. This resistance is likely due to infection with resistant viruses, but VRC01 escape post acquisition may also contribute to observation of discrepant phenotypes.

The implications of higher numbers of multi-lineage viruses are significant and make both passive and active vaccination more complicated, as the diverse infecting viruses need to be neutralized

and may contain mutations that confer resistance to the mAb it has been exposed to. This requires further investigation of how to prevent HIV-1 transmission. Clinical success of bNAb passive immunization strategies will therefore likely require combinations of antibodies to increase the overall breadth and potency against new infection with diverse TF isolates and prevent the emergence of resistance (Walsh and Seaman, 2021). Studies show that three or four bNAbs that target different epitopes, rather than overlapping epitopes, are able to act together and provide better breadth and potency, by simultaneously targeting a given virus (Walsh and Seaman, 2021). A combination currently being tested for efficacy testing contains VRC07-523 LS (CD4 binding site), PGT121.414 LS (V3 glycan) and PGDM1400 LS (V2 glycan), which has been predicted to have 99% neutralization breadth (Gilbert *et al*., 2022). Such combinations of antibodies become even more relevant in the context of higher levels of multi-lineage transmission.

This particular study focused on identifying resistance mutations that distinguish the Envs with discordant phenotypes. Of the seven sets of phenotypically discordant Envs, we found the mutations that conferred sensitivity in six. To confirm our findings, we then reversed the experiment to see if the identified mutations caused resistance when put in sensitive wild types. Unsurprisingly mutations that conferred differential phenotypes were found predominantly in the CD4 binding site. The single mutations were found at 279 and 280 in loop D, 369 in the CD4 binding-loop, 459 between the β23 and the V5 loop. In two cases either the entire V1V2 region or the β23 and V5 loop chimeras of their sensitive clones were transferred into the resistant backbone and conferred VRC01 sensitivity. However, when reversed their respective sensitive WTs did not become resistant. This may be due to lengths of chimeras and PNGS, and shifts in overall Env conformation, rather than specific amino acid mutations within the chimeras. Finally, in one participant, all three resistant clones differed to the sensitive clone by length, approximately 100 amino acids and glycosylation patterns and despite making several mutants and with machine learning results, we failed to find the cause of VRC01 resistance. We therefore see that each set of discordant viruses showed different patterns of mutations that cause

resistance or sensitivity. The data suggests that mutations outside the CD4 binding site and away from the VRC01 binding footprint do not often contribute to resistance towards VRC01.

During this study we set out to identify novel mutations, not previously associated with VRC01 resistance. We only found one mutation that had not been discovered before, at position 369. V703_0510_pblib002 with novel mutation L369P as well as L369P together with V371I are significantly more resistant to VRC01 than the sensitive WT when tested in the TZM-bl neutralization assay. We will then need to validate these novel mutations by determining if they occur in more Envs as well as whether they expand to other subtypes which would be seen in the HVTN 704 trial, which was carried out in the Americas and Switzerland. It is possible that, if we had been able to assess a larger data set, we would have identified other novel mutations.

We also assessed whether there was concordance between the machine learning prediction results and the laboratory results. In five of the six cases of discordant sets, the predictions for the WT resistant sequences had a higher probability of sensitivity to VRC01 and/or a lower IC80 than the WT sensitive sequence. The only discrepancy seen was with PTID 703-1586 where the WT sensitive sequence is seen to have a lower predicted probability of sensitivity to VRC01 and higher IC80 than the WT resistant sequence. However, it was shown that this was not the case when the clones were tested for sensitivity against VRC01. However, as more data of Env sequences with known VRC01 neutralization profiles and new sieve sites are identified as an iterative process, the machine learning tool will be improved. Refinement of the machine learning will be of value in follow-up studies of evolving/waning VRC01 resistance in AMP breakthrough infections as well as in future trials of antibodies, and vaccines that trigger VRC01-like responses (Leggat *et al*., 2022).

Finally, we have shown that VRC01 resistance does not necessarily result in resistance to other CD4 binding site mAbs, either VRC01 class and non-VRC01 class. mAb 1-18 is a non-VRC01 class antibody and therefore does not bind to the virus in the same manner as VRC01-class antibodies, not mimicking the CD4 binding interaction. It approaches the virus at a different angle to VRC01

class antibodies and therefore would not be affected by VRC01 resistance mutations. Although N6 is a VRC01 class antibody, it is able to overcome major mechanisms of resistance as it has a slightly different mode of Env recognition (Ding *et al*., 2021). Both VRC01 and VRC07 were cloned from the same HIV-1 infected individual. However, VRC07 was then engineered to include mutations that enhanced its breadth and potency compared to the parental mAb. Mutations were also introduced to improve the half-life of the antibody, denoted as LS (Walsh and Seaman, 2021). Therefore, although these mAbs target the same epitope as VRC01, they are more potent, can target the virus at slightly different angles and perhaps avoid steric clashes with glycans. These differences in mode of binding and an increased affinity may explain why such antibodies are not affected by VRC01 resistance. This means that in future cure and prevention studies, it will be possible to include mAbs that target the same epitope as the resistance mutations may not confer cross resistance to the other more broad and potent mAbs.

There are several limitations to this study. We were limited in the number of phenotypically discordant envelopes from multi-lineage HIV-1 transmissions from the HVTN 703 AMP trial and therefore were unable to identify more than one novel VRC01 resistance mutation. Furthermore, we did not assess the impact of the identified resistance mutations on replicative capacity, although there is evidence that antibody escape mutations in the Env can affect replication capacity in vivo (Lynch *et al.*, 2015). Future studies will assess whether the VRC01 resistance mutations conferred a fitness cost to the viruses. If resistance is associated with a fitness cost, a less fit virus may reduce disease progression, as the efficiency of viral entry will be decreased, their viral loads will be lower and CD4+ T cell count higher. By doing a longitudinal analysis of the multi-lineage viruses' kinetics over time, we will be able to determine which virus was selected for and what mutations they had at the identified sieve site of interest.

5. Conclusion

The aim of this project was both to identify novel HIV-1 Env mutations that confer resistance to VRC01 as well as define VRC01 resistance mutations in phenotypically discordant Envs from multi-lineage HIV-1 transmissions. Ultra-deep sequencing revealed a higher-than-expected proportion of multi-lineage infections. Multi-lineage infections are genotypically distinct, however they may also be phenotypically different. It is unclear whether discordance occurred at infection or as a result of selection pressure. Identification of novel bNAb resistance mutations will lead to further understanding of how HIV-1 evolves under antibody pressure and will be important when designing bNAb combinations that have a wide range of coverage. A novel mutation was found at position 369 in the CD4 binding loop. We only found one novel mutation in the seven sets of viruses with discordant phenotypes, where the other resistance mutations were previously defined. With more time and further studies, new pathways to resistance will occur and be able to be followed. Overall the machine learning tool was concordant with the laboratory analyses. Further studies will investigate the kinetics of VRC01 resistance mutations as well as focus on whether mutations causing resistance confer a fitness cost to the virus.

6. **References**

Abrahams, M.-R. et al. (2009) 'Quantitating the Multiplicity of Infection with Human Immunodeficiency Virus Type 1 Subtype C Reveals a Non-Poisson Distribution of Transmitted Variants', Journal of Virology, 83(8), pp. 3556–3567. doi: 10.1128/jvi.02132-08.

Ahmed, Y., Tian, M. and Gao, Y. (2017) 'Development of an anti-HIV vaccine eliciting broadly neutralizing antibodies', AIDS Research and Therapy. BioMed Central, 14(1), pp. 1–6. doi: 10.1186/s12981-017-0178-3.

Anklesaria, P. and Russell, N.D. (2023) 'Iterative hypothesis testing in HIV vaccine research: Moving towards success', Journal of the International AIDS Society, 26(5). doi:10.1002/jia2.26102.

Araújo, L. A. L. and Almeida, S. E. M. (2013) 'HIV-1 diversity in the envelope glycoproteins: Implications for viral entry inhibition', Viruses, 5(2), pp. 595–604. doi: 10.3390/v5020595.

Batorsky, R., Sergeev, R. A. and Rouzine, I. M. (2014) 'The Route of HIV Escape from Immune Response Targeting Multiple Sites Is Determined by the Cost-Benefit Tradeoff of Escape Mutations', PLoS Computational Biology, 10(10). doi: 10.1371/journal.pcbi.1003878.

Van Beek, M., Nussenzweig, M. C. and Chakraborty, A. K. (2022) 'Two complementary features of humoral immune memory confer protection against the same or variant antigens.', Proceedings of the National Academy of Sciences of the United States of America, 119(37), p. e2205598119. doi: 10.1073/pnas.2205598119.

Binley, J. M. et al. (2008) 'Profiling the Specificity of Neutralizing Antibodies in a Large Panel of Plasmas from Patients Chronically Infected with Human Immunodeficiency Virus Type 1 Subtypes B and C', Journal of Virology, 82(23), pp. 11651–11668. doi: 10.1128/jvi.01762-08.

Blumenthal, R., Durell, S. and Viard, M. (2012) 'HIV entry and envelope glycoprotein-mediated fusion', Journal of Biological Chemistry, 287(49), pp. 40841–40849. doi: 10.1074/jbc.R112.406272.

Bukenya, D. et al. (2019) 'What causes non-adherence among some individuals on long term antiretroviral therapy? Experiences of individuals with poor viral suppression in Uganda', AIDS Research and Therapy. BioMed Central, 16(1), pp. 1–9. doi: 10.1186/s12981-018-0214-y.

Burton, D.R. and Hangartner, L., 2016. Broadly neutralizing antibodies to HIV and their role in vaccine design. Annual review of immunology, 34, pp.635-659.

Campbell-Yesufu, O.T. and Gandhi, R.T., 2011. Update on human immunodeficiency virus (HIV)-2 infection. Clinical infectious diseases, 52(6), pp.780-787.

Checkley, M. A., Luttge, B. G. and Freed, E. O. (2012) 'Checkley 2011 JMB', 410(4), pp. 582–608. doi: 10.1016/j.jmb.2011.04.042.HIV-1.

Cohen, M. S. et al. (2011) 'Prevention of HIV-1 Infection with Early Antiretroviral Therapy', New England Journal of Medicine. Massachusetts Medical Society, 365(6), pp. 493–505. doi: 10.1056/NEJMoa1105243.

Corey, L. et al. (2021) 'Two Randomized Trials of Neutralizing Antibodies to Prevent HIV-1 Acquisition', New England Journal of Medicine, 384(11), pp. 1003–1014. doi: 10.1056/nejmoa2031738.

Cross, S. a (2011) 'The role of adaptive stress responses in HIV replication and macrophage-mediated neurotoxicity.', Dissertation Abstracts International: Section B: The Sciences and Engineering, p. 3421.

Deshpande, S. et al. (2016) 'HIV-1 clade C escapes broadly neutralizing autologous antibodies with N332 glycan specificity by distinct mechanisms', Retrovirology. BioMed Central, 13(1), pp. 1–9. doi: 10.1186/s12977-016-0297-2.

Ding, C. et al. (2021) 'Employing Broadly Neutralizing Antibodies as a Human Immunodeficiency Virus Prophylactic & Therapeutic Application', Frontiers in Immunology, 12(July), pp. 1–16. doi: 10.3389/fimmu.2021.697683.

Forthal, D.N., 2014. Functions of antibodies. Microbiology spectrum, 2(4), pp.2-4.

Gąciarz, A. and Ruddock, L. W. (2017) 'Complementarity determining regions and frameworks contribute to the disulfide bond independent folding of intrinsically stable scFv', PLoS ONE, 12(12), pp. 1–20. doi: 10.1371/journal.pone.0189964.

Gilbert, P. B. et al. (2022) 'Neutralization titer biomarker for antibody-mediated prevention of HIV-1 acquisition', Nature Medicine. Springer US, 28(9), pp. 1924–1932. doi: 10.1038/s41591-022-01953-6.

Granich, R. et al. (2012) 'Expanding ART for treatment and prevention of HIV in South Africa: Estimated cost and cost-effectiveness 2011-2050', PLoS ONE, 7(2). doi: 10.1371/journal.pone.0030216.

Harris, J., 2003. AIDS vaccine fails to prevent HIV infection. Weekly releases (1997–2007), 7(48), p.2334.

van Heuvel, Y., Schatz, S., Rosengarten, J.F. and Stitz, J., 2022. Infectious RNA: Human Immunodeficiency Virus (HIV) Biology, Therapeutic Intervention, and the Quest for a Vaccine. Toxins, 14(2), p.138.

Huang, J., Ofek, G., Laub, L., Louder, M.K., Doria-Rose, N.A., Longo, N.S., Imamichi, H., Bailer, R.T., Chakrabarti, B., Sharma, S.K. and Alam, S.M., 2012. Broad and potent neutralization of HIV-1 by a gp41-specific human antibody. Nature, 491(7424), pp.406-412.

Huang, J. et al. (2018) 'Identification of a CD4-Binding-Site Antibody to HIV that Evolved Near-Pan Neutralization Breadth', 45(5), pp. 1108–1121. doi: 10.1016/j.immuni.2016.10.027.Identification.

Hurst, S. A., Appelgren, K. E. and Kourtis, A. P. (2015) 'Prevention of mother-to-child transmission of HIV Type 1: The role of neonatal and infant prophylaxis', Expert Review of Anti-Infective Therapy, 13(2), pp. 169–181. doi: 10.1586/14787210.2015.999667.

Janeway Jr, C.A., Travers, P., Walport, M. and Shlomchik, M.J., 2001. The structure of a typical antibody molecule. In Immunobiology: The Immune System in Health and Disease. 5th edition. Garland Science.

Joseph, S.B., Swanstrom, R., Kashuba, A.D. and Cohen, M.S., 2015. Bottlenecks in HIV-1 transmission: insights from the study of founder viruses. Nature Reviews Microbiology, 13(7), pp.414-425.

Julg, B. and Barouch, D. H. (2019) 'Neutralizing antibodies for HIV-1 prevention', Current Opinion in HIV and AIDS, 14(4), pp. 318–324. doi: 10.1097/COH.0000000000000556.

Keele, B. F. et al. (2008) 'Identification and characterization of transmitted and early founder virus envelopes in primary HIV-1 infection'.

Kim, J.H., Excler, J.L. and Michael, N.L., 2015. Lessons from the RV144 Thai phase III HIV-1 vaccine trial and the search for correlates of protection. Annual review of medicine, 66, pp.423-437.

Kwong, P.D. and Mascola, J.R., 2018. HIV-1 vaccines based on antibody identification, B cell ontogeny, and epitope structure. Immunity, 48(5), pp.855-871.

Landais, E. and Moore, P. L. (2018) 'Development of broadly neutralizing antibodies in HIV-1 infected elite neutralizers', Retrovirology. BioMed Central, 15(1), pp. 1–14. doi: 10.1186/s12977-018-0443-0.

Larsson, A. (2014) 'AliView: A fast and lightweight alignment viewer and editor for large datasets', Bioinformatics, 30(22), pp. 3276–3278. doi:10.1093/bioinformatics/btu531.

Lefranc, M. P. and Lefranc, G. (2020) 'Immunoglobulins or antibodies: IMGT® bridging genes, structures and functions', Biomedicines, 8(9), pp. 1–112. doi: 10.3390/biomedicines8090319.

Leggat, D.J., Cohen, K.W., Willis, J.R., Fulp, W.J., deCamp, A.C., Kalyuzhniy, O., Cottrell, C.A., Menis, S., Finak, G., Ballweber-Fleming, L. and Srikanth, A., 2022. Vaccination induces HIV broadly neutralizing antibody precursors in humans. Science, 378(6623), p.eadd6502.

Lynch, R. M. et al. (2015) 'HIV-1 Fitness Cost Associated with Escape from the VRC01 Class of CD4 Binding Site Neutralizing Antibodies', Journal of Virology, 89(8), pp. 4201–4213. doi: 10.1128/jvi.03608-14.

Lundgren, J. and Phillips, A., 2018. Prevention of HIV transmission by antiretroviral therapy. The Lancet HIV, 5(3), pp.e108-e109.

Macharia, G. N. et al. (2020) 'Infection with multiple HIV-1 founder variants is associated with lower viral replicative capacity, faster cd4+ t cell decline and increased immune activation during acute infection', PLoS Pathogens, 16(9), pp. 1–22. doi: 10.1371/journal.ppat.1008853.

Magaret, C. A. et al. (2019) 'Prediction of VRC01 neutralization sensitivity by HIV-1 gp160 sequence features', PLoS Computational Biology, 15(4), pp. 1–35. doi: 10.1371/journal.pcbi.1006952.

Montefiori, D., 2004. Evaluating Neutralizing Antibodies Against HIV, SIV, and SHIV in Luciferase Reporter Gene Assays. Current Protocols in Immunology, 64(1).

Moore, P. L. et al. (2009) 'Limited neutralizing antibody specificities drive neutralization escape in early HIV-1 subtype C infection', PLoS Pathogens, 5(9). doi: 10.1371/journal.ppat.1000598.

Moore, P.L., Williamson, C. and Morris, L., 2015. Virological features associated with the development of broadly neutralizing antibodies to HIV-1. Trends in microbiology, 23(4), pp.204-211.

Morris, L. and Mkhize, N. N. (2017) 'Prospects for passive immunity to prevent HIV infection', PLoS Medicine, 14(11), pp. 1–5. doi: 10.1371/journal.pmed.1002436.

Murin, C. D., Wilson, I. A. and Ward, A. B. (2019) 'Antibody responses to viral infections: a structural perspective across three different enveloped viruses', Nature Microbiology, 4(5), pp. 734–747. doi: 10.1038/s41564-019-0392-y.

Pancera, M. et al. (2010) 'Structure of HIV-1 gp120 with gp41-interactive region reveals layered envelope architecture and basis of conformational mobility', Proceedings of the National Academy of Sciences of the United States of America, 107(3), pp. 1166–1171. doi: 10.1073/pnas.0911004107.

Powell, R. L. R., Kinge, T. and Nyambi, P. N. (2010) 'Infection by Discordant Strains of HIV-1 Markedly Enhances the Neutralizing Antibody Response against Heterologous Virus', Journal of Virology, 84(18), pp. 9415–9426. doi: 10.1128/jvi.02732-09.

Rabiu, M., Willie, R. and Parumasur, N. (2021) Optimal Control Strategies and Sensitivity Analysis of an HIV/AIDS-Resistant Model with Behavior Change, Acta Biotheoretica. Springer Netherlands. doi: 10.1007/s10441-021-09421-3.

Ramjee, G. and Daniels, B. (2013) 'Women and HIV in Sub-Saharan Africa', AIDS Research and Therapy, 10(1), pp. 1–9. doi: 10.1186/1742-6405-10-30.

Raska, M. et al. (2014) 'Differential glycosylation of envelope gp120 is associated with differential recognition of HIV-1 by virus-specific antibodies and cell infection', AIDS Research and Therapy, 11(1), pp. 1–16. doi: 10.1186/1742-6405-11-23.

Reeves, D. B. et al. (2020) 'Mathematical modeling to reveal breakthrough mechanisms in the HIV Antibody Mediated Prevention (AMP) trials', PLoS Computational Biology, 16(2), pp. 1–27. doi: 10.1371/journal.pcbi.1007626.

Rerks-Ngarm, S., Pitisuttithum, P., Excler, J.L., Nitayaphan, S., Kaewkungwal, J., Premsri, N., Kunasol, P., Karasavvas, N., Schuetz, A., Ngauy, V. and Sinangil, F., 2017. Randomized, double-blind evaluation of late boost strategies for HIV-uninfected vaccine recipients in the RV144 HIV vaccine efficacy trial. The Journal of infectious diseases, 215(8), pp.1255-1263.

Richman, D. D. et al. (2003) 'Rapid evolution of the neutralizing antibody response to HIV type 1 infection', Proceedings of the National Academy of Sciences of the United States of America, 100(7), pp. 4144–4149. doi: 10.1073/pnas.0630530100.

Roth, D. B. (2015) 'V(D)J recombination: Mechanism, errors, and fidelity', Mobile DNA III, 2(6), pp. 313–324. doi: 10.1128/9781555819217.ch14.

Saunders, K. O. et al. (2015) 'Sustained Delivery of a Broadly Neutralizing Antibody in Nonhuman Primates Confers Long-Term Protection against Simian/Human Immunodeficiency Virus Infection', Journal of Virology, 89(11), pp. 5895–5903. doi: 10.1128/jvi.00210-15.

Sela-Culang, I., Kunik, V. and Ofran, Y. (2013) 'The structural basis of antibody-antigen recognition', Frontiers in Immunology, 4(OCT), pp. 1–13. doi: 10.3389/fimmu.2013.00302.

Statssa.gov.za. 2022
Available at: <https://www.statssa.gov.za/publications/P0302/P03022021.pdf> [Accessed 31 August 2022].

Taylor, B.S., Sobieszczyk, M.E., McCutchan, F.E. and Hammer, S.M., 2008. The challenge of HIV-1 subtype diversity. New England Journal of Medicine, 358(15), pp.1590-1602.

Tian, J. et al. (2016) 'Effect of Glycosylation on an Immunodominant Region in the V1V2 Variable Domain of the HIV-1 Envelope gp120 Protein', PLoS Computational Biology, 12(10), pp. 1–33. doi: 10.1371/journal.pcbi.1005094.

Vaccari, M. et al. (2010) 'Phase III HIV vaccine trial in Thailand: a step toward a protective vaccine for HIV', 9(9), pp. 997–1005. doi: 10.1586/erv.10.104.Phase.

Walsh, S. R. and Seaman, M. S. (2021) 'Broadly Neutralizing Antibodies for HIV-1 Prevention', Frontiers in Immunology, 12(July), pp. 1–14. doi: 10.3389/fimmu.2021.712122.

World Health Organization (WHO) (2022) HIV
Available at: https://www.who.int/data/gho/data/themes/hiv-aids (Accessed: August 22, 2022).

Wibmer, C. K., Moore, P. L. and Morris, L. (2015) 'HIV broadly neutralizing antibody targets', Curr Opin HIV AIDS, 10(3), pp. 135–143. doi: 10.1097/COH.0000000000000153.HIV.

Yoon, H. et al. (2015) 'CATNAP: A tool to compile, analyze and tally neutralizing antibody panels', Nucleic Acids Research, 43(W1). doi:10.1093/nar/gkv404.

Zhou, P. et al. (2019) 'Broadly resistant HIV-1 against CD4-binding site neutralizing antibodies', PLoS Pathogens, 15(6), pp. 1–24. doi: 10.1371/journal.ppat.1007819.

Zolla-Pazner, S. and Cardozo, T., 2010. Structure–function relationships of HIV-1 envelope sequence-variable regions refocus vaccine design. Nature reviews Immunology, 10(7), pp.527-535.

Zolla-Pazner, S., Michael, N.L. and Kim, J.H. (2021) 'A tale of four studies: HIV vaccine immunogenicity and efficacy in clinical trials', The Lancet HIV, 8(7). doi:10.1016/s2352-3018(21)00073-4.

Appendix A- Sequences of viruses

Table A1. Accession numbers for nucleotide sequences of viruses analysed

Clone name	Accession
HXB2	K03455.1
V703_1714_080_RE_pblib002	ON891052.1
H703_1714_080s	ON891051.1
H703_2769_050_RE_p01s	ON891085.1
V703_2769_050_RE_pblib002_s	ON891086.1
V703_0510_260_RE_pblib001_s	ON890964.1
V703_0510_260_RE_pblib002_s	ON890965.1
V703_0510_260_RE_pblib003_s	ON890966.1
V703_1586_210_RE_sga3E8_s	ON891044.1
V703_1586_210_RE_pblib002_s	ON891043.1
H703_2805_080Ec_A1	ON891088.1
V703_2805_080_RE_pblib002_s	ON891089.1
V703_0514_150_RE_pblib004_s	ON890968.1
H703_0514_150e_6C1	ON890971.1
H703_0514_150s_F4_V03_024	ON890970.1
H703_0514_150s_A4_V02_028	ON890969.1
H703_1945_090s_2F1	ON891072.1
H703_0805_770_RE_e10C9s	ON890995.1
V703_0458_260_RE_sga6H5_s	ON890961.1
H703_1313_040s	ON891026.1
H703_1194_150_RE_cs	ON891014.1
V703_1848_190_RE_pblib002_s	ON891062.1
H703_1453_240_RE_e9B7s	ON891036.1
H703_0993_110_RE_cs	ON891005.1
H703_0472_030s	ON890962.1
V703_0712_250_RE_pblib002_s	ON890989.1

Appendix B- Lists of primers

Table B1. Primers used to mutate Resistant WT plasmids.

Resistant Virus Name	Mutagenesis primers
V703_1714_pblib002 WT Resistant	
V703_1714_pblib002 D459G	F: GAACGTGATGGAG**G**TGCTAATGAAAGTAACACAGAGAC Tm=79.6°C R: GTCTCTGTGTTACTTTCATTAGCA**C**CTCCATCACGTTC Tm=79.6°C
V703_1714_pblib002 E462D	F: GAACGTGATGGAGATGCTAATGA**C**AGTAACACAGAGAC Tm=79.6°C R: GTCTCTGTGTTACT**G**TCATTAGCATCTCCATCACGTTC Tm=79.6°C
V703_1714_pblib002 D459G E462D	F: GAACGTGATGGAG**G**TGCTAATGA**C**AGTAACACAGAGAC Tm=79.6°C R: GTCTCTGTGTTACT**G**TCATTAGCA**C**CTCCATCACGTTC Tm=79.6°C
V703_0510_pblib003 WT Resistant	
V703_0510_pblib003 P369L	F: TCCTCAGGAGGGGATC**T**AGAAATTACAACTCATAGCTTTAAC Tm=79.5°C R: GTTAAAGCTATGAGTTGTAATTTCT**A**GATCCCCTCCTGAGGA Tm=79.5°C
V703_0510_pblib003 I371V	F: TCAGGAGGGGATCCAGAA**G**TTACAACTCATAGCTTTAAC Tm=79.5°C R: GTTAAAGCTATGAGTTGTAA**C**TTCTGGATCCCCTCCTGA Tm=79.5°C
V703_0510_pblib003 P369L I371V	F: TCAGGAGGGGATC**T**AGAA**G**TTACAACTCATAGCTTTAAC Tm=79.5°C R: GTTAAAGCTATGAGTTGTAA**C**TTCT**A**GATCCCCTCCTGA Tm=79.5°C
H703_0514_150s_F4_V03_024 WT Resistant	
H703_0514_150s_F4_V03_024 T281S	F: ATTAGATCTAAAAATCTAACAGACAAT**T**CCAAAATAATAATAGTACATCTTAATCAG Tm=77.33°C R: CTGATTAAGATGTACTATTATTATTTTGG**A**ATTGTCTGTTAGATTTTTAGATCTAAT Tm=77.33°C
H703_0514_150s_F4_V03_024 G429E	F: CAAATCATAAACATGTGGCAAG**A**GGTAGGACGAGCAATG Tm=79.6°C R: CATTGCTCGTCCTACC**T**CTTGCCACATGTTTATGATTTG Tm=79.6°C
H703_0514_150s_F4_V03_024 V5 chimera	F: AAGGAACGAATAGTACAAGTGAGACATTCAGACCTGGAGGA Tm=83°C R: CTATTGACACGTGATGGAGGACAAGGAACGAATAGTACAAG Tm=83°C
H703_0514_150s_F4_V03_024 CD4 chimera	F: CAGGAGGGGACCTAGAAGTTGTTACACATAGTTTCAATTGT Tm=83°C R: AATACAACAACACTAGTATTTGAACCATCTGCAGGAGGGGA Tm=83°C
V703_1586_sga3E8 WT Resistant	
V703_1586_sga3E8 N279D	F: ATGATTAGATCTGAAAATCTGACA**G**ACAATGCCAAAACAATAATAGTACAC Tm=78.19°C R: GTGTACTATTATTGTTTTGGCATTGT**C**TGTCAGATTTTCAGATCTAATCAT Tm=78.19°C
H703_2769_050_RE_p01s WT Resistant	
H703_2769_050_RE_p01s R432Q	F: TGGCAGCAGGTAGGGC**A**AGCAATATATGCCCCT Tm=80.5°C R: AGGGGCATATATTGCT**T**GCCCTACCTGCTGCCA Tm=80.5°C
H703_2769_050_RE_p01s V5 chimera	F: TGAACAACAGCACAGAGACATTCAGACCTGGAGGAGGAGAT Tm=83.89°C R: CTACTGACACGTGATGGAGGAAATGTGAACAACAGCACAGA Tm=85.12°C
V703_2805_080_RE_pblib002_s WT Resistant	
V703_2805_080_RE_pblib002_s Resistant with Sensitive V1V2 chimera	R: CAGAGTGGGGTCAACTTTACACATG Tm=74.18°C F: CTGTCCAAAGGTCTCTTTTGACCCA- For resistant backbone Tm=74.18°C
	F: CATGTGTAAAGTTGACCCCACTCTG Tm=74.18°C R: TGGGTCAAAAGAGACCTTTGGACAG- For sensitive insert Tm=74.18°C
V703_2805_080_RE_pblib002_s V5 chimera	F: ATCCTAACCATACGGAGGTATTCAGACCTGGAGGAGGAGAC Tm=86°C R: ACACGTGATGGAGGAGGTAATAATATGAGCAATCCTAACCA Tm=81°C

Table B2. Primers used to mutate Sensitive WT plasmids.

Sensitive Virus Name	Mutagenesis primers
H703_1714_080s WT Sensitive	
H703_1714_080s G459D	F: CTATTGGAACGTGATGGAG**A**TGCTAATGACAGTAACACA Tm=78.43°C R: TGTGTTACTGTCATTAGCATCTCCATCACGTTCCAATAG Tm=78.43°C
H703_1714_080s D462E	F: CGTGATGGAGGTGCTAATGA**A**AGTAACACAGAGACA Tm=78°C R: TGTCTCTGTGTTACTTTCATTAGCACCTCCATCACG Tm=78°C
H703_1714_080s G459D D462E	F: TTGGAACGTGATGGAG**A**TGCTAATGA**A**AGTAACACAGAGACA Tm=77°C R: TGTCTCTGTGTTACTTTCATTAGCATCTCCATCACGTTCCAA Tm=77°C
V703_0510_pblib002 WT Sensitive	
V703_0510_pblib002 L369P	F: TCCTCAGGAGGGGATC**C**AGAAGTTACAACTCAT Tm=77.69°C R: ATGAGTTGTAACTTCTGGATCCCCTCCTGAGGA Tm=77.69°C
V703_0510_pblib002 V371I	F: TCCTCAGGAGGGGATCTAGAA**A**TTACAACTCATAGCTTT Tm=78.43°C R: AAAGCTATGAGTTGTAATTTCTAGATCCCCTCCTGAGGA Tm=78.43°C
V703_0510_pblib002 L369P V371I	F: CCATCCTCAGGAGGGGATC**C**AGAA**A**TTACAACTCATAGC TTT Tm=78.11°C R: AAAGCTATGAGTTGTAATTTCTGGATCCCCTCCTGAGGATGG Tm=79.11°C
H703_0514_150s_A4_V02_028 WT Sensitive	
H703_0514_150s_A4_V02_028 S281T	F: AGATCTAAAAATCTGACAGAAAATA**C**CAAAATAATAATAGTACATCTTAATAAGACTGTA Tm=78°C R: TACAGTCTTATTAAGATGTACTATTATTATTTTGGTATTTTCTGTCAGATTTTTAGATCT Tm=78°C
H703_0514_150s_A4_V02_028 E429G	F: ATAAACATGTGGCAGG**G**GGTAGGACGAGCAATG Tm=79.33°C R: CATTGCTCGTCCTACCCCCTGCCACATGTTTAT Tm=79.33°C
H703_0514_150s_A4_V02_028 V5 chimera	F: TAAATAATACAAATACAAATGAGACATTCAGACCTGGAGG Tm=81°C R: TTTGTATTTGTATTATTTATTCCTCCATCACGTGTCAATA Tm=81.55°C
H703_0514_150s_A4_V02_028 CD4 chimera	F: TAGGAGGGGACCCAGAAATTGTTACACATAGTTTCAATTGT Tm=83°C R: TTCAATACAACAATAATATTTAAACCACCCGTAGGAGGGGA Tm=81.84°C
V703_1586E_pblib002 WT Sensitive	
V703_1586_210_RE_pblib002_s D279N	F: ATGATTAGATCTGAAAATCTGACA**A**ACAATGCCAAAACAATAATAGTACAC Tm=78.19°C R: GTGTACTATTATTGTTTTGGCATTGTTTGTCAGATTTTCAGATCTAATCAT Tm=78.19°C
V703_2769_050_RE_pblib002_s WT Sensitive	
V703_2769_050_RE_pblib002_s Q432R	F: TGGCAGCAGGTAGGAC**G**AGCAATATATGCCCCT Tm=°C R: AGGGGCATATATTGCTCGTCCTACCTGCTGCCA Tm=°C
V703_2769_050_RE_pblib002_s V5 chimera	F: AATAACAGCACAGAGGAGATATTCTTCAGACCTGGAGGAGGAGAT Tm=°C R: CTACTGACACGTGATGGTGGAGAAACAAATAAGACCAATAACAG Tm=°C
H703_2805_080Ec_A1 WT Sensitive	
H703_2805_080Ec_A1 Sensitive with Resistant V1V2 chimera	F: TGTCCAAAGGTCTCTTTTGACCCA Tm=74.18°C R: AGAGTGGGGTCAACTTTACACATGG- For sensitive backbone Tm=74.18°C
	F: CCATGTGTAAAGTTGACCCCACTCT Tm=74.18°C R: TGGGTCAAAAGAGACCTTTGGACA – For resistant insert Tm=74.18°C
H703_2805_080Ec_A1 V5 chimera	F: CATGCCGATGGAAATGAGACATTCAGACCGGGAGGAGGAGAC Tm=90.32°C R: TTGACACGTGATGGAGGAGGTAGTGACAATGATACCGGTCAT Tm=87.41°C

Table B3. Primers used to sequence plasmids

Primer	Sequence (5'-3')
EnvB	AGA AAG AGC AGA AGA CAG TGG CAA TGA
A589	GTGTAAAGTTAACCCCACTCTG
A589 rev	CAGAGTGGGGTTAACTTTACAC
EnvA	TGCTGCTCCCAAGAACCCAA
E55	GCCCCAGACTGTGAGTTGCAACAGATG
Mf	GGA GGA GAT ATG AGG GAC AAT TGG
Nr	GGT GAG TAT CCC TGC CTA ACT CTA

Appendix C- Important findings

Clone name	Initial IC80	Experimental IC50
V703_1714_080_RE_pblib002 WT resistant	>100	>25
H703_1714_080c WT sensitive	0.89	0.32
V703_1714_080_RE_pblib002 D459G		1.89
H703_1714_080c G459D		>25
H703_2769_050_RE_p01s WT resistant	74.88	>25
V703_2769_050_RE_pblib002 WT sensitive	0.26	0.14
H703_2769_050_RE_p01s V5 chimera		6.82
V703_0510_260_RE_pblib003 WT resistant	>100	>25
V703_0510_260_RE_pblib002 WT sensitive	17.58	5.73
V703_0510_260_RE_pblib003 P369L		1.83
V703_0510_260_RE_pblib002 L369P		>25
V703_1586_210_RE_sga3E8 WT resistant	>100	>25
V703_1586_210_RE_pblib002 WT sensitive	34.03	11.76
V703_1586_210_RE_sga3E8 N279D		13.4
V703_1586_210_RE_pblib002 D279N		>25
V703_2805_080_RE_pblib002 WT resistant	>100	>25
H703_2805_080Es WT sensitive	1.04	0.87
V703_2805_080_RE_pblib002 V1V2 chimera		3.9

Figure C1. Important findings. Initial IC80 results compared to experimental IC50 results. Blue represents resistant viruses, orange represented intermediate viruses and red represents sensitive viruses.

Appendix D- Ethics clearance certificate

UNIVERSITY OF THE WITWATERSRAND, JOHANNESBURG

R14/49 Miss Paula Cohen

HUMAN RESEARCH ETHICS COMMITTEE (MEDICAL)

CLEARANCE CERTIFICATE NO. M210406

NAME: (Principal Investigator)	Miss Paula Cohen
DEPARTMENT:	Virology National Institute for Communicable Diseases
PROJECT TITLE:	Identification of Novel HIV Envelope Mutations that Confer Resistance to VRC01
DATE CONSIDERED:	30/04/2021
DECISION:	Approved unconditionally
CONDITIONS:	
SUPERVISOR:	Prof P. Moore
APPROVED BY:	Dr CB Penny, Chairperson, HREC (Medical)
DATE OF APPROVAL:	09/06/2021

This clearance certificate is valid for 5 years from date of approval. Extension may be applied for.

DECLARATION OF INVESTIGATORS

To be completed in duplicate and **ONE COPY** returned to the Research Office Secretary on the Third Floor, Faculty of Health Sciences, Phillip Tobias Building, 29 Princess of Wales Terrace, Parktown, 2193, University of the Witwatersrand. I/we fully understand the conditions under which I am/we are authorized to carry out the above-mentioned research and I/we undertake to ensure compliance with these conditions.Should any departure be contemplated, from the research protocol as approved, I/we undertake to resubmit the application to the Committee. **I agree to submit a yearly progress report.** The date for annual re-certification will be one year after the date of convened meeting where the study was initially reviewed. In this case, the study was initially reviewed in **April** and will therefore be due in the month of **April** each year. Unreported changes to the application may invalidate the clearance given by the HREC (Medical).

Principal Investigator Signature

29/04/2022
Date

PLEASE QUOTE THE PROTOCOL NUMBER IN ALL ENQUIRIES

Appendix E- Turnitin report

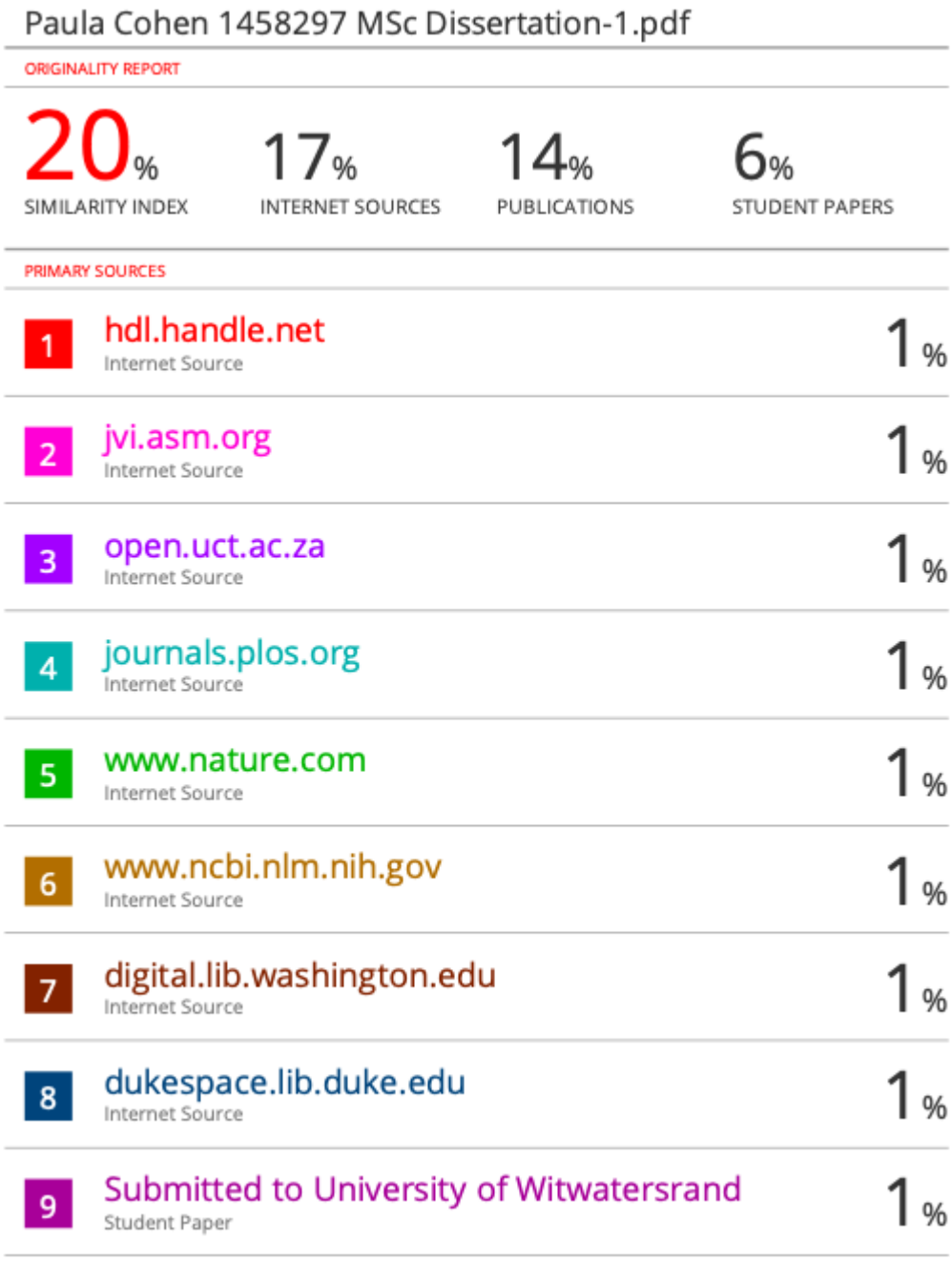

Paula Cohen 1458297 MSc Dissertation-1.pdf

ORIGINALITY REPORT

20%	17%	14%	6%
SIMILARITY INDEX	INTERNET SOURCES	PUBLICATIONS	STUDENT PAPERS

PRIMARY SOURCES

1	hdl.handle.net Internet Source	1%
2	jvi.asm.org Internet Source	1%
3	open.uct.ac.za Internet Source	1%
4	journals.plos.org Internet Source	1%
5	www.nature.com Internet Source	1%
6	www.ncbi.nlm.nih.gov Internet Source	1%
7	digital.lib.washington.edu Internet Source	1%
8	dukespace.lib.duke.edu Internet Source	1%
9	Submitted to University of Witwatersrand Student Paper	1%